平成 10 年度　学位請求論文

Study on Distributed Feedback Quantum Wire Semiconductor Lasers Using V-Grooved Substrates

V溝基板を用いた 分布帰還型量子細線 半導体レーザ に関する研究

1998 年 12 月 18 日提出

指導教官　中野義昭　助教授

Department of Electronic Engineering
University of Tokyo
東京大学　大学院　工学系研究科
電子工学専攻
学籍番号　67134

TODA Tomoaki
戸田知朗

運命によって「諦め」を得た「媚態」が
「意気地」の自由に生きるのが「いき」である。

——九鬼周造

CONTENTS

■ Chapter 1

Introduction

1-1 Introductory remark

Semiconductor lasers are an important device as an ideal light source in optical communication systems. They are a fundamental component of optoelectronics and photonics together with optical fibers and detectors. Lasers produce a pure light, it propagates in fibers without losses for a long distance, and detectors receive it. Any of them should not be omitted in this simple scheme. Their roles are comparable with the entrance gate, road, and exit of highway. If even one of them were lacked, the system would be incomplete. Though it still can be displayed as an object of modern arts, it is no more what engineers seek.

As good a property as possible is naturally demanded for these indispensable components. The engineers have responded to such a request for the last few decade. Those remarkable progresses actually made the importance of optoelectronics and photonics decisive. The properties of above key devices are reaching the level of practical use. It even makes us feel that the motivation of studying is now concentrated in a productive side rather than a fundamental research. Based on commercially available devices, many applications to a system are stimulated, and some of them will be utilized in a telecommunication system.

These days the integration of lasers with other functional components like modulators and passive taper waveguides is a hot topic in this field in relation with coming FTTH (fiber to the home) concept. Its integration scale is just that numerable at a glance, but is expected to be so increased as LSI (large scale integrated) circuit in electronics in the near future for the achievement of further sophisticated functions in the informatic processing. It is impossible to compare it with the electrical one due to the different properties between photons and electrons. But such a challenge in optoelectronics is useful to develop complimentary LSI circuits using both merits to the most.

As is mentioned in the above paragraphs, The importance of semiconductor lasers is growing and growing as well as optical fibers and detectors. Further improvements in their structure design and processing are not only significant for the improvement of a device itself but also very effective for the development of the entire optoelectronics because their contribution is direct. In fact, there are still quite lots of things left to do in lasers comparing with the other 2 components whose properties have already been close

to a theoretical limit or an ideal one. Even if the lasers supplied by today's technology is enough for a present application, it is undoubtedly inadequate for a future one. It is always very significant to seek a new technology to replace present one with it. And it is in lasers, too.

1-2 Brief overview on semiconductor lasers

The least but enough knowledge shall be given in this section to smoothly construct the discussion to validate the subject of this thesis.

1-2-1 Semiconductors as laser materials

Semiconductor lasers are literally the name of lasers made of semiconductor materials. Among various types of lasers which have been known since 1960, it has peculiar features such as a small size (a few hundred micron), high emission efficiency, low cost and so on. In Figure1, the representative compound materials known in semiconductor lasers are shown with their bandgaps and lattice constants. It is also notable that nitride materials have recently been lighted up in the region of higher bandgap materials. The success of blue light lasers has impressed their potentiality strongly since a few years ago.

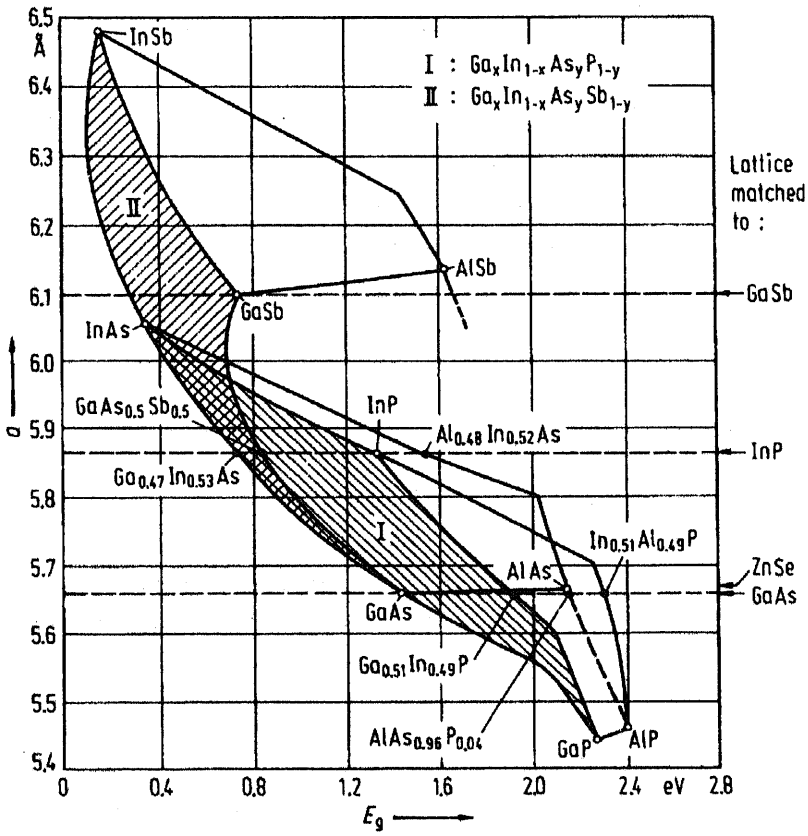

Figure 1-1 Lattice constants and bandgap energies of III-V laser materials[1].

In Figure 1-1, 2 groups of materials are important in this thesis. One is the group based on GaAs substrate, and another is based on InP substrate. The former has long been studied as laser materials, and its laser is actually used in the pick-up system of CD (compact disc) known as a record medium of audio systems and computers. The wavelength corresponding to its band gap energy ranges from 630 to 880[nm], what we call, short wavelength. On the other hand, InP based materials are relatively new, and is important as a light source for telecommunications using silica optical fiber with its lowest loss at 1.55[μm] and zero dispersion at 1.3[μm]. It is called as long wavelength comparing with the previous one. In this thesis, both materials are treated.

GaAs offers good materials for the fundamental research because heterostructure is achievable without any growth problems coming from lattice mismatch. InP is for aiming at the practical use in telecommunications. As far as we concern the impact of studying, the latter is more exciting. This thesis is constituted of a fundamental part (preliminary in one sense) using GaAs substrate and a more advanced part on InP.

1-2-2 Structures of semiconductor lasers[2]

All the lasers can be classified by their cavity. Fabry-Perot type is the most popular because of its simplicity and facility of a fabrication. It is constituted of 2 mirrors which front to each other. Because 2 mirrors can be made easily by cleaving a substrate in semiconductor lasers, it is more favored for the fundamental research. It is a standard type which has been used from the beginning of studying about semiconductor lasers.

It has many modes in the longitudinal direction of the cavity, which are simply determined by

$$\frac{1}{\lambda} = \frac{m\pi}{L} \tag{1}$$

, where λ is a lasing wavelength , L is a length of cavity and m is an integer. The lasing mode is selected by the overlapping with a gain profile determined by the material and structure of an active layer. But a mode separation is in general so small that the mode stability is usually bad and that it often causes mode hopping that leads to the non-linearity of laser operation. This instability is sometimes understood positively when it is applied to a tuning of lasing wavelength by combining with additional mode selective structures[3], but is normally considered to be unfavorable.

A good candidate to solve this problem is the incorporation of DFB (distributed feedback) cavity. It has a periodically modulated structure in it to induce a variation of refractive index and gain along the cavity. In this cavity, the reflection of lightwave of which wavelength (Bragg wavelength) is related with the periodicity of a structure by the equation of (11) in chapter 2 is selectively so high that the feedback of that lightwave is more effective than the other wavelength. It results that the lasing occurs from around Bragg wavelength. Precisely saying, lasing from Bragg wavelength is permitted in the DFB cavity in which only the gain modulation or a $\lambda/4$ shift at the center of cavity exists (see chapter 2). In the normal DFB cavity where the uniform index modulation is introduced and dominant, the lasing wavelength is detuned from Bragg wavelength due to index coupling of forward and backward propagating light. But the selectivity of a single lasing mode is still a consistent property in this type of cavity as far as gain coupling effect is valid. SMSR (side mode suppression ratio) is reported to be more than 40[dB] in various type of such DFB lasers ever reported[4,5,6], while that of FP cavity is at most

20[dB]. The dynamic mode stability is one of the most impressed and useful characteristics of DFB cavity.

Another possible structure is the combination of FP and DFB cavity. Either side of FP cavity is connected to a periodically modulated cavity. Such a structure is called DBR (distributed Bragg reflector). But here the current injection for lasing is limited in the region of FP cavity. And thus, the gain is given by the FP part. The electrode on DBR part is isolated electrically from the others, and normally is used independently from the others on the FP region. An interesting example where this structure is applied is VICSEL (vertically integrated cavity surface emitting laser). As an edge emitting laser, the tunable wavelength laser is well-known with various type of grating structure for tuning mechanisms[7,8]. This type of lasers is normally made for a particular purpose, and its structure is specialized for each purpose by making the most use of DBR effect. Nevertheless, it holds the mode selective property coming from periodical structures.

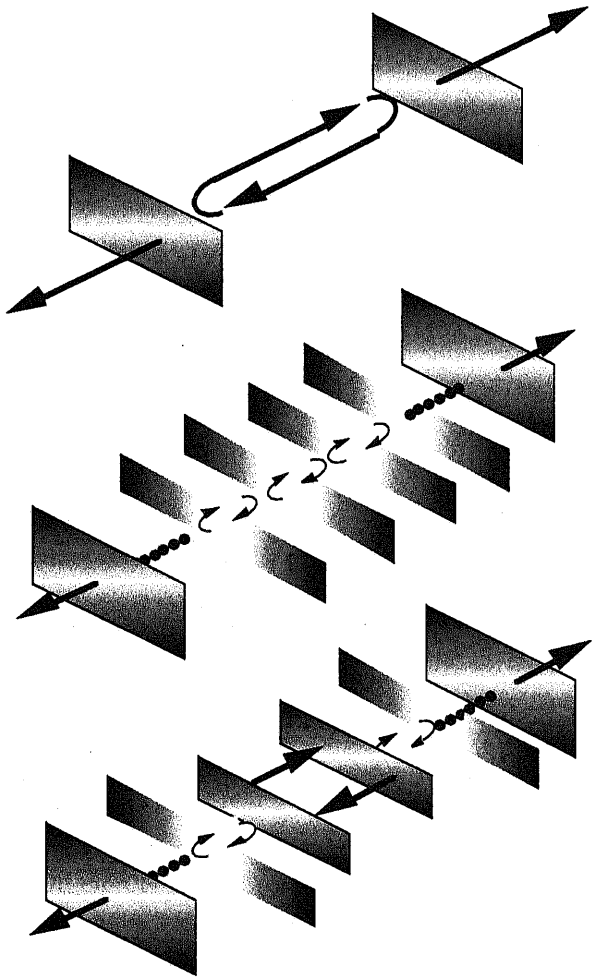

Figure 1-2 Various cavities in semiconductor lasers. FP, DFB and DBR type respectively from above.

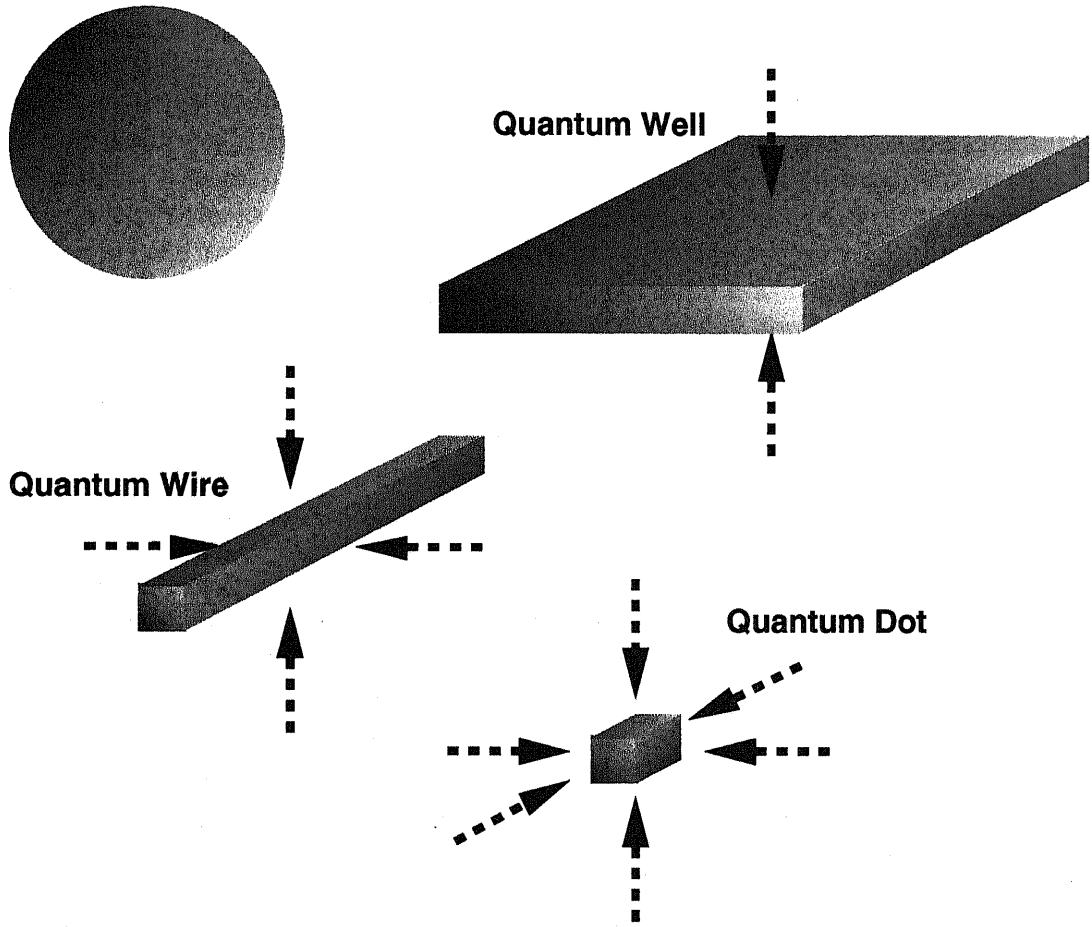

Figure 1-3 Quantum confined structures as an active part of semiconductor lasers. They are called quantum well, quantum wire, and quantum dot.

The active region in semiconductor lasers is a face of people, and decides almost all the dynamic properties of lasers. And thus, it is also possible to classify lasers by the variety of active part structures.

The simplest one is a bulky type. Almost no practical use is found now other than for cost-down issues or for fundamental researches on waveguides because next quantum well (QWL) is more popular and is grown as easily as a bulky one nowadays. The use of a bulk layer is swept away by the remarkable development of growth technology and the success of use of quantum effects in device engineering[9]. As thin a layer as is expected to induce quantum effects was very difficult to obtain in LPE (liquid phase epitaxy) method. However, today it is available for everyone by MBE (molecular beam epitaxy) and MOVPE (metal organic vapor phase epitaxy) method. Even more complicated structures composed of multiple thin layers are also feasible for specific applications.

QWL structure brings the modification of carrier density states in active part. Since the gain changes discretely at the energy determined by the confined states, the higher differential gain is realized. It means that the lower carrier density is needed for obtaining a constant gain. Hence, if the sum of the gain of QWLs is high enough to compensate the loss of the cavity, a lower threshold current is achievable. The most of lasers fabricated

today have a QWL structure in them due to this splendid result. Moreover, it becomes easier to design and modify laser properties by adding strains, doping and so on because their effect reflects sensibly on laser characteristics even if they change is small. The merits to use QWLs as an active part have been reported from the various aspects[9], and it is now a common sense to use a QWL structure in the design of semiconductor lasers.

Naturally there exists the idea to use further quantum effects such as a 2D confined or 3D confined carrier states, what we call, QWR (quantum wire) or QD (quantum dot). But no experimental result which proves theoretical predictions reported on lasers has ever been done. Incompleteness of processing to realize such a low dimensional structure is the biggest problem that we have to get over. The driving force to enhance the use of QWL structure was the development of planar growth technology to stack a layer in parallel at each step. The control of growth in the plane is necessary for the formation of QWR and QD, and it needs a special treatment of a substrate before or after the growth. Almost all the challenges to make QWR and QD have been carried out based on such an idea[10-15]. Although self-formation technology of QWR and QD without any annoying pre- or post-processes are paid more attention in journals[16,17], their properties are also still far away from the expected one. Especially QWRs formed by self-formation look like wrinkles rather than wire and its quality on the uniformity is out of discussion.

The application of these low dimensional structures is still on the way of development. A new epoch-making idea is needed for a break-through in the limit of fabrication technique in this domain. Moreover, such an idea must be what enables us to obtain uniform and controlable QWRs in both geometry and optical property.

At the last of this section we just refer the name of quantum cascade laser[18]. Its active part is peculiar because it is designed for the mono-carrier light emission mechanism between the energy states of electrons. Its active part is multiple QWLs, but it should be classified apart from normal QWL lasers because its emission mechanism is completely different from ordinary one. Though the application is now limited owing to the lack of suitable combination of materials with high band offset on electron side to realize a wider energy state separation, it is interesting in the point that it shows a new style of semiconductor lasers in the future.

1-3 Semiconductor lasers in optoelectronics

What makes optoelectronics in the engineering as it is today is undoubtedly the appearance of semiconductor lasers and optical fibers. The former enabled us to use a pure light more conveniently and cheaply, and the latter opened the way to telecommunications using a lightwave as a carrier. But those are just a starting point. The drive force to conduct researches in optoelectronics is given in another form.

The explosive increase of demands on the capacity of information network certainly accelerated the progress in optoelectronics. The rapid popularization of computers at home gave a chance to people to utilize a new communication tool in addition to a conventional simple telephone and fax. Sales of useful products handling images such as a portable video camera or a digital camera augmented a data size of personal use in the computer and more seriously in the network. It leads to the necessity of introducing much larger capacity and high speed of network where all kinds of data including text, sounds, and images are free to be sent and received quickly.

B-ISDN (broadband integrated service digital network) is believed to be an alternative to respond this request[24]. It is constituted of optical fiber network with WDM (wavelength division multiplexing) system. In WDM system, multiple wavelengths of lightwave serves as a carrier of information. And thus, the smaller the separation of each wavelength is, the higher capacity of network is achievable. In such a system, lasers with their lasing wavelength precisely controlled are needed because its precision directly influences on a capability of the system. It means that the single mode laser with its lasing wavelength stable and its linewidth narrow are demanded for such a system in the future. The most possible candidate for this purpose is apparently DFB lasers. It was stated in the last section that they had favorable features satisfying above requirements. Therefore, several optical switching devices like a wavelength multiplexer, demultiplexer and converter for the WDM system are now studied under the condition to use DFB lasers as a light source.

Taking these situations into considerations, it is clear that the improvement of DFB laser characteristics is very important and useful. It doesn't mean only the amelioration of a light source, but also the reduction of severe requirements demanded for the other devices. It also contributes to the acceleration of development in WDM systems and further sophisticated systems.

1-4 What improvement is needed in DFB lasers?

The improvement of DFB lasers is meaningful. In due course, it is worth while to resume the problems of DFB lasers with regard to suitability to a WDM system. It is also discussed what solution is possible against those problems and how effective it is for the amelioration of DFB laser properties.

1-4-1 Problems to be solved for ideal DFB lasers

DFB lasers are considered to be a relatively mature device among the optical components needed in a WDM system. Considering that about 30 years have been devoted for the development of DFB lasers, it is not surprising. The productive aspects such as the establishment of a stable fabrication process is a trend of studying about DFB lasers[20,21]. The motivation for a introduction of phase shifts in grating or gain coupling can also be said to be partly started from such a demand. But this situation never comes from the fact that there is nothing left for the innovation of DFB laser characteristics. They are not still necessarily better than FP type lasers. One of the reasons is obviously indispensable defects caused from the more complicated fabrication process of DFB lasers. Though it is possible to approach to this problem from the viewpoint of processing quality as has often been done, it is quite difficult to expect a great progress to improve all the defects in DFB lasers. It would be more hopeful to introduce a new structure without additional difficulties in processing for the dramatic innovation.

As was partly mentioned in the previous sections, the positive features of DFB lasers could be summarized like bellow[4-6,22-24].

- stable single mode oscillation
- high stability of lasing wavelength
- small linewidth enhancement factor
- immunity against the external reflection

All these are the properties superior to FP lasers. Furthermore, the design of lasing wavelength by Bragg wavelength ease difficulty of fabrication process needed for a laser array in a WDM system. It is impossible to select a lasing wavelength of FP lasers as precisely as DFB lasers because the operation of FP lasers is often seriously influenced not only by a device structure, but also by uncertain elements such as a carrier injection, temperature, and cavity length. Consequently FP lasers are not for WDM systems, where it is said that a wavelength separation of 0.8[nm] is desired for a future system.

The representative disadvantages of DFB lasers are shown in the followings.

- complexity of fabrication process
- lower limit in high-speed modulation
- higher threshold current density

These are in contrary the properties inferior to FP lasers reported experimentally on DFB lasers. Note that they are never potentially worse than FP lasers

The complexity of fabrication process is inevitable for the incorporation of index or/and gain modulation in a cavity. Hence it must be accepted to a certain extent. But the other 2 terms are not originally essential in DFB lasers and are brought about unintentionally through the incompleteness of processing. The most serious problem held in DFB laser processing is the regrowth which often spoils a crystal quality by various defects. Though these 2 problems also belong to "fabrication process" in that sense, it would rather be related specifically with the quality of grating used in a DFB cavity than the complexity. Therefore, the improvement of DFB laser characteristics depends on how grating is introduced in DFB lasers. One may say that laser properties are more effectively innovated by a different method like band engineering in laser active layer. But it is evidently not a definitive solution for the amelioration of DFB laser characteristics since the same method is also applicable to FP lasers and above problems lying between DFB and FP lasers remains untouched. Then DFB lasers are always inferior to FP lasers in the points mentioned above. After all, while it is important to reduce negative factors in processing of DFB lasers, we need a more drastic way to decide the superiority of DFB lasers to FP lasers.

1-4-2 DFB lasers and QWR array

To overcome demerits of DFB lasers in the previous section, it is interesting to pay attention to the resemblance of a QWR array to a grating in DFB lasers (Figure 1-4). Normally the cross-sectional size of a grating teeth used in DFB lasers is on the order of 100[nm], while QWR size is a few tens [nm] at most. If we scale down the cross-sectional size of grating, it is structurally quite similar to a QWR array. Hence, the DFB laser is potentially a QWR laser and it is especially operable as a DFB laser whose grating works as an active part, too.

QWR has been known as a promising structure for further improvements in laser properties and been expected to be used as an active part of lasers (see section 1-2-2). Among the important favorable effects of QWR lasers predicted in a number of articles[25-28] are

- low threshold current density
- small linewidth enhancement factor
- high characteristic temperature

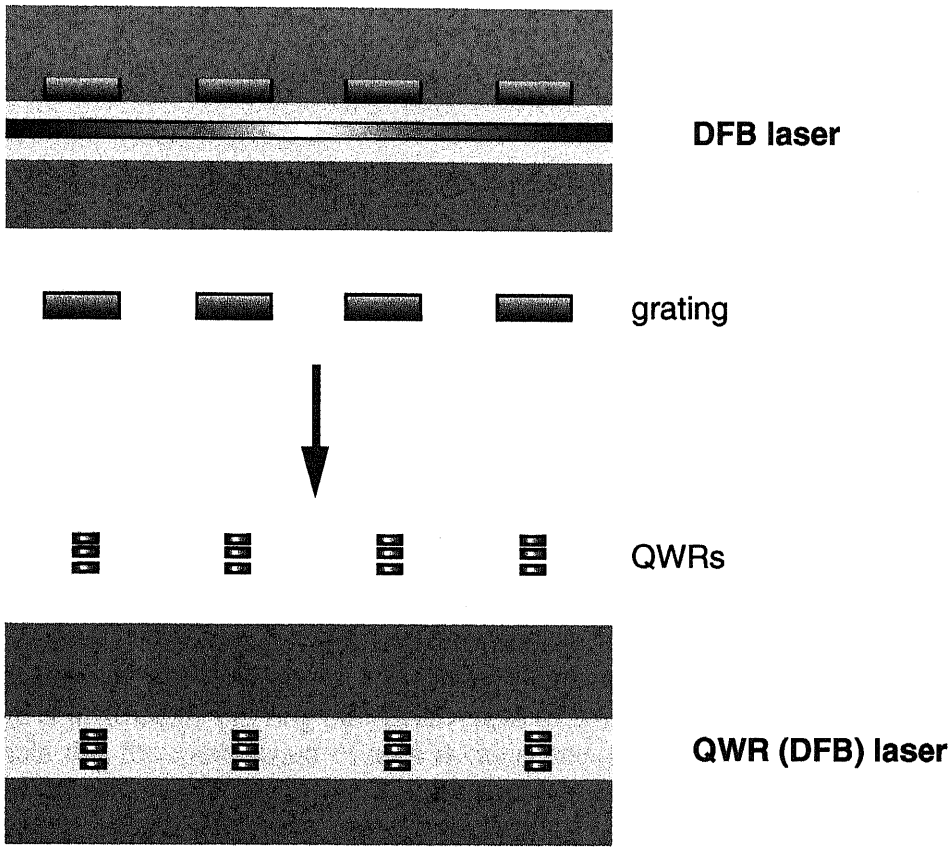

Figure 1-4 Similarlity of QWR array to grating in DFB lasers.

- high differential gain

Neither of them is still not realized sufficiently. But those are exactly coincided with what was demanded for DFB lasers to compete with FP lasers in the above section. And thus, theoretical predictions suggest attractive resulsts in DFB lasers with QWR array as an active part. We should not miss another essential effect of QWR array in DFB lasers, too. Because above QWR properties are also applicable to FP lasers and in this sense there is no meaning to specilaize this idea to DFB lasers.

We remember that what makes the characteristics of DFB lasers worse in some aspects is processing to form a grating structure in a DFB cavity. And the incorporation of a QWR array in DFB lasers and FP lasers concludes that this disadvantageous condition is now even for both types of lasers. As a result, unfavorable defects attributed only to DFB lasers are cancelled. Because it is, for instance, known from theoretical studying that DFB lasers are essentially better than FP lasers in threshold current density if all the conditions for both are the same except for the existence of a grating, we can expect better characteristics in DFB lasers than FP lasers using a QWR array.

Then, all we have to do is to prove advantages of QWR lasers over conventional one experimentally, and the possibility of fabrication of DFB lasers using QWRs as an active grating. The first issue is needed to keep advantages to use QWRs in semiconductor lasers. It is achieved by showing above predicted merits in real QWR lasers. As for the second one, almost no reports on DFB lasers based on QWRs have been reported before[29]. It is even unknown whether such a laser operable at room temperature is feasible or not.

It is finally concluded that the realization of new lasers with a QWR array as an active grating in a DFB cavity is valuable in the following meanings.

- It is the invention of a new DFB laser for more advanced optoelectronic technology better than conventional one.
- The DFB laser's characteristics over a conventional FP laser are very useful for the achievement of an ideal semiconductor laser.
- It also means the realization of QWR lasers with the aid of several advantages of a DFB cavity.
- The introduction of a new type of active part in DFB lasers is helpful for the integration technology.

1-5 Contents of this thesis

This thesis is attempted to contribute to the improvement of DFB laser properties. It is challenged by introducing QWR array structure as an active grating. It is essentially a practical way to achieve higher performances of a DFB laser than conventional one. And it is also useful to compensate DFB laser characteristics inferior to FP laser ones. Though the realization of QWR lasers is still difficult technologically even in a FP type, its challenge is justified by proving the effectiveness of using a DFB cavity in QWR lasers. It can be said that the combination of a DFB cavity and a QWR array is suitable to show a good performance of QWR lasers. But the stress is especially laid to improve the DFB laser characteristics in this thesis, rather than those of QWR lasers.

In the 2nd chapter, fundamental properties of DFB lasers are explained analytically. There, some important facts are mentioned with respect to lasing wavelength and stopband of DFB lasers. They are important concerning with later experimental results. The discussion is based on the traditional coupled mode equations.

There are so many varieties of a QWR ever reported in publications. The most appropriate one must be chosen as the active part of DFB lasers for a practical use, that is, for practical QWR devices operable at room temperature. Almost all of them ever proposed are not efficient from the viewpoint of device applications. The fabrication techniques are still developing and each has its own problems to be overcome somehow. the 3rd chapter is devoted to resume properties of each QWR, and it is discussed what type of a QWR should be incorporated with regard to DFB lasers.

Subsequently, the fabrication of DFB lasers using the conventional QWR array on GaAs V-grooved substrates are stated. A strained InGaAs QWR array is used as an active part and grating. Its luminescence peak is designed in the short wavelength region for the ease of laser fabrication. It is actually a good experiment to clarify the feasibility of DFB QWR lasers and to investigate difficulties preventing us from achieving their realization. Those useful experimental results are summarized to refine the conditions needed for a new method to make QWRs and be applied to DFB lasers.

New technology for the formation of QWRs on InP V-grooved substrates, which covers the long wavelength domain known in the telecommunications, is proposed based on the discussions in the 4th chapter. It is experimentally examined using the MOVPE system. The use of InP substrates is more valuable considering the usefulness of QWR applications in telecommunications. The characteristics of new QWRs are evaluated by microscopic and optical methods. The validity of this method from the point of view of

applicability to DFB lasers, especially for the long wavelength DFB lasers are proved in both quality and controllability of processing. This is chapter 5.

The introduction of new QWRs in DFB lasers is the subject of the 6th chapter. Several types of a laser structure are designed so that the quality of regrowth process and, of course, the possibility of laser operation are optimized. The key factor is the regrowth on a non-planar substrate with grating on it. The best condition is sought to satisfy these requirements. Fabricated DFB lasers are operated under the pulsed current injection at room temperature. Lasing is successfully reported from those lasers.

The 7th chapter is for the conclusion of this thesis.

Reference

[1]Otfried Madelung (ed.), "Semiconductors-Basic Data", Springer-Verlag Berlin Heidelberg New York, 1996.

[2]K.Iga (ed.), "Semiconductor Lasers", Ohm, 1994 (in Japanese).

[3]J.B.D.Soole, K.Poguntke, A.Scherer, H.P.LeBlanc, C.Chang-Hasnain, J.R.Hayes, C.Caneau, R.Bhat, and M.A.Koza, "multistripe array grating integrated cavity (magic) laser; a new semiconductor laser for WDM applications, Electron.Lett., vol.28, 1805, 1992.

[4]Y.Luo, Y.Nakano, K.Tada, T.Inoue, H.Hosomatsu, and H.Iwaoka, "fabrication and characterization of gain-coupled distributed feedback semiconductor lasers with a corrugated active layer", IEEE J.Quantum Electron., vol.27, 1724, 1991.

[5]B.Borchert, K.David, B.Stegmuller, R.Gessner, M.Beschorner, D.Sacher, and G.Franz, "1.55μm gain-coupled quantum-well distributed feedback lasers with high single-mode yield and narrow linewidth", IEEE Photon.Technol.Lett., vol.3, 955, 1991.

[6]W.T.Tsang, F.S.Choa, M.C.Wu, Y.K.Chen, R.A.Logan, A.M.Sergent, and C.A.Burrus, "long-wavelngth InGaAsP/InP distributed feedback lasers incorporating gain-coupled mechanism", IEEE Photon.Technol.Lett., vol.4, 212, 1992.

[7]Y.Kotaki, M.Matsuda, H.Ishikawa, and H.Imai, "tunable DBR lasers with wide tuning range", Elctron.Lett., vol.24, 503, 1988.

[8]Y.Tohmori, Y.Yoshikuni, T.Tamamura, H.Ishii, Y.Kondo, and M.Yamamoto, "broad range wavelength tuning in DBR lasers with super structure grating (SSG)", IEEE Photon.Technol.Lett., vol.5, 126, 1993.

[9]P.S.Zory,Jr. (ed.), "Quantum Well Lasers", Academic Press, 1993.

[10]M.Notomi, S.Nojima, M.Okamoto, H.Iwamura, and T.Tamamura, "size dependence of lateral quantum-confinement effects of the optical response in $InGa_{0.53}As_{0.43}$ quantum wires", Physical Rev.B, vol.52, 11073, 1995.

[11]H.Akiyama, T.Someya, M.Yoshita, T.Sasaki, and H.Skaki, "photoluminescence study of lateral confinement energy in T-shaped $In_xGa_{1-x}As$ quantum wires", Physical Rev.B, vol.57, 3765, 1998.

[12]H.Ando, H.Saito, A.Chavez-Pirson, H.Gotoh, and N.Kobayashi, "excitonic optical properties in fractional-layer-superlattice wire structures in the intermediate confinement regimebetween two dimensions and one dimension", Physical Rev.B, vol.55, 2429, 1997.

[13]F.Vouilloz, D.Y.Oberli, M.-A.Dupertuis, A.Gustafsson, F.Reinhardt, and E.Kapon, "effect of lateral confinement on valence band mixing and polarization anisotropy in quantum wires", vol.57, 12378, 1998.

[14]S.Ishida, and Y.Arakawa, "seeded self-assembled GaAs quantum dots grown in two-dimentional V-grooves by selective metal-organic chemical vapor deposition", ApplPhys.Lett, vol.72, 800, 1998.

[15]A.Hartmann, L.Loubies, F.Reinhardt, and E.Kapon, "self-limiting growth of quaantum dot heterostructures on nonplanar {111}B substrates", vol.71, 1314, 1997.

[16]A.C.Chen, A.M.Moy, P.J.Pearah, K.C.Hsieh, and K.Y.Cheng, "$Ga_xIn_{1-x}P$ multiple-quantum-wire heterostructures prepared by the strain induced lateral layer ordering process", ApplPhys.Lett., vol.62, 1359, 1993.

[17]S.Raymond, S.Fasard, P.J.Poole, A.Wojs, P.Hawrylak, C.Gould, A.Schrajda, S.Charbonneau, D.Leonard, R.Leon, P.M.Petroff, and J.L.Merz, "state-filling and magneto-photpluminescence of excited states in InGaAs/GaAs self-assembled dots", Superlattices and Microstructures, vol.21, 542, 1997.

[18]C.Gmachl, F.Capasso, J.Faist, A.L.Hutchinson, A.Tredicucci, D.L.Sivco, J.N.Baillargeon, S.N.G.Chu, and A.Y.Cho, "continuous-wave and high-power pulsed operation of index-coupled distributed feedback quantum cascade laser at $\lambda \approx 8.5\mu m$", ApplPhys.Lett., vol.72, 1430, 1998.

[19]J.E.Midwinter (ed.), "Photonics in Swithing volume I", Academic Press, 1993.

[20]T.W.Johaness, A.Rast, W.Harth, and J.Rieger, "gain-coupled DFB lasers with a titanium surface Bragg grating", Electron.Lett., vol.31, 370, 1995.

[21]Y.Watanabe, N.Cheng, K.Takei, K.Chikuma, N.Futakuchi, and Y.Nakano, "laterally coupled strained MQW ridge waveguide ditributed-feedback laser diode fabricated by wet-dry hybrid etching process", IEEE Photon.Technol.Lett., vol.10, 1688, 1998.

[22]K.Kudo, J.I.Shim, K.Komori, and S.Arai, "reduction of effective linewidth enhancement factor α_{eff} of DFB lasers with complex coupling coefficients", IEEE Photon.Technol.Lett., vol.4, 531, 1992.

[23]S.Ogita, M.Yano, H.Imai, "theoretical calculation of the linewidth enhancement factor of DFB lasers", Electron.Lett., vol.22, 580, 1986.

[24]Y.Nakano, Y.Deguchi, K.Ikeda, Y.Luo, K.Tada, "reduction of excess intensity noise induced by external reflection in a gain-coupled distributed feedback semiconductor laser", IEEE J.Quantum Electron., vol.27, 99, 1991.

[25]Y.Arakawa, K.Vahara and A.Yariv, "quantum noise and dynamics in quantum well and quantum wire lasers", ApplPhys.Lett., vol.45, 950, 1984.

[26]Y. Arakawa, A.Yariv, "quantum well lasers-gain, spectra, dynamics", IEEE J.Quantum Electron. vol.22, 1887, 1986.

[27]M. Asada, Y. Miyamoto, and Y. Suematsu, "theoretical gain of quantum well-wire lasers", Japan J.Appl.Phys., vol.24, 95, 1985.

[28]A.Yariv, "scaling lows and minimum threshold currents for quantum-confined semiconductor lasers", Appl.Phys.Lett., vol.53, 1033, 1988.

[29]M.Walther, E. Kapon, C. Caneau, D.M. Hwang, and L.M. Schiavone, "InGaAs/GaAs strained quantum wire lasers grown by organometallic chemical vapor deposition on nonplanar substrates", Appl.Phys.Lett., vol.62, 2170, 1993.

■ Chapter 2

Fundamentals of DFB lasers

2-1 Introduction

The simplest model for an analysis of DFB lasers is the coupled mode theory. Since it was applied to DFB lasers by H.Kogelnik and C.V.Shank in 1971 [1], it has often been used to understand the operation of DFB lasers. Though several numerical methods [2-4] were proposed to compensate the precision which is omitted as much as possible in the coupled mode theory for the simplification, many of the experimental results on DFB lasers are comprehensive qualitatively by this simple model. It offers a good way to learn the behavior of DFB lasers. In this chapter, we review several properties of DFB lasers based on a set of coupled mode equations.

2-2 Coupled mode equations

Assume that a laser cavity with a narrow waveguide in the transverse direction enough to exclude the other modes than the first TE mode. It is true in most semiconductor lasers. For such TE-like modes, the next well-known Helmholz equation is utilized for the calculation of modes in the cavity.

$$\nabla^2 E + k_0{}^2 n^2 E = 0 \tag{1}$$

We take z axis along the cavity and assume the next form of solution.

$$E(x,y,z) = A_{lm}(x,y;z)B(z) \tag{2}$$

l and m is the number of mode in the lateral and transverse direction. Because we are interested in only the lowest mode with l=0, m=0, we replace A_{00} with A. Then function A is a normalized solution for the next equation.

$$\frac{\partial^2 A}{\partial x^2} + \frac{\partial^2 A}{\partial y^2} + k_0{}^2\left(n^2 - n_{eff}{}^2\right)A = 0 \tag{3}$$

Here, although A is dependent on z, its dependency is supposed to be very small. This assumption is true when a grating layer thickness is much smaller than that of a

waveguide. Hence, above equation of (3) can be derived from (1) by ignoring the differential A on z. n_{eff} is the effective reflective index in the longitudinal direction and is determined by the boundary conditions in the plane normal to the longitudinal direction. Therefore, the simplified equation for z axis follows.

$$\frac{\partial^2 B}{\partial z^2} + k_0{}^2 n_{eff}{}^2 B = 0 \tag{4}$$

Note that n_{eff} defined in above style is dependent on z when the original reflective index n is a function of z. In the case of a uniform grating n_{eff} has the same periodicity as a grating.

This is the basic equation to consider a 1 dimensional in-plane lasers. To induce coupled mode equations from (4), all we have to do is to accept the assumptions shown in below.

- 2nd order differential of envelope function is negligible.
- a feedback loop of an identified wavelength concerning to a multiple reflection is not taken into a consideration.
- Absolute value of refractive index is much larger than that of gain.

$$\mathrm{Re}(n) >> \mathrm{Im}(n) \tag{5}$$

- Lasing wavelength does not deviate from Bragg wavelength so much.

$$k_0 n_{eff,0} \cong \frac{2\pi}{\Lambda_m} \tag{6}$$

Then the following set of equations called coupled wave equations are obtained.

$$-\frac{dR}{dz} + \left\{ g_{eff,0} - i\left(k_0 n_{eff,0} - \frac{2\pi}{\Lambda_m} \right) \right\} R = i\kappa_m S \tag{7}$$

$$\frac{dS}{dz} + \left\{ g_{eff,0} - i\left(k_0 n_{eff,0} - \frac{2\pi}{\Lambda_m} \right) \right\} S = i\kappa'_m R \tag{8}$$

$$n_{eff} = \sum_{m=-\infty}^{\infty} \left(n_{eff,m} + i g_{eff,m} \right) e^{i\frac{2m\pi}{l} z} \tag{9}$$

n_0 and g_0 is the average of refractive index and gain respectively. R and S are incorporated from B by the following equations.

$$B(z) = R(z) e^{-i\frac{2\pi}{\Lambda_m}} + S(z) e^{i\frac{2\pi}{\Lambda_m}} \tag{10}$$

R and S are a sort of envelope function of electric fields in the periodically modulated cavity. R corresponds to a forward propagating lightwave and S does to a backward propagating one.

$$\Lambda_m = \frac{2l}{m} \tag{11}$$

$$\kappa_m = k_0 n_{eff,-m} + i g_{eff,-m} \quad \kappa'_m = k_0 n_{eff,m} + i g_{eff,m} \tag{12}$$

Λ_m is so called mth Bragg wavelength of a grating. Coupling coefficients κ are constituted of mth (or -mth) element of Fourier expansion of n_{eff}. We omitted the higher order products on these Fourier coefficients in κ because it is expected to be small comparing with the average n_0 and g_0. They are an important parameter to describe the interaction caused by a grating, and express the peculiar behaviors of DFB lasers. Counterpropagating lightwaves R and S are coupled to each other through these parameters. When we neglect the variation of function A(x,y;z) on z, κ can be expressed as below using the structural parameter n in a grating layer.

$$\kappa_m = \Gamma(k_0 n_{-m} + i g_{-m}) \; \kappa'_m = \Gamma(k_0 n_m + i g_m) \tag{13}$$

$$n = \sum_{m=-\infty}^{\infty} (n_m + i g_m) e^{i\frac{2m\pi}{l}z} \tag{14}$$

Γ is an optical confinement factor of a grating layer.

2-3 Solution of coupled mode equations

The analytical solution of a set of equations (7) and (8) is found easily in the next form. The first integration is obtained by calculating $(7)\times\nabla S + (8)\times\nabla R$, and integrate both sides on z.

$$(g_{eff,0} - i\delta)RS + C_1 = i\frac{1}{2}\kappa_m S^2 + i\frac{1}{2}\kappa'_m R^2 \tag{15}$$

$$\delta = k_0 n_{eff,0} - \frac{2\pi}{\Lambda_m} \tag{16}$$

δ is a detuning from Bragg wavelength. C_1 is an integral constant.
The second integration is given by $(7)\times S + (8)\times R$.

$$-S\frac{dR}{dz} + R\frac{dS}{dz} + (g_{eff,0} - i\delta)RS = i\kappa_m S^2 + i\kappa'_m R^2 \tag{17}$$

It is transformed into the differential equation on function R/S.

$$\frac{d(S/R)}{dz} - i\kappa_m\left(\frac{S}{R}\right)^2 + 2(g_{eff,0} - i\delta)\frac{S}{R} - i\kappa'_m = 0 \tag{18}$$

Because it is a simple differential equation in the form of a variable separation, it is analytically solvable on R/S. At first, we define 2 solutions of the next equation as α and β.

$$i\kappa_m X^2 - 2(g_{eff,0} - i\delta)X + i\kappa'_m = 0 \tag{19}$$

Using α and β the solution for (17) is given as

$$\frac{1}{i\kappa_m(\alpha-\beta)}\ln\left(\frac{S/R-\alpha}{S/R-\beta}\right) = z + C_2 \tag{20}$$

C2 is naturally an integral constant. (15) and (20) are the solution of coupled mode equations.

2-4 Determination of integral constants and eigenvalues

The determination of integral constants, and eigenvalues of a boundary problem as threshold gain and lasing wavelength is needed to accomplish the whole work in this chapter. C_1 in (15) remains undetermined because the intensity of electric field is free in coupled mode equations. The question is how to determine C_2 in (20). In fact it is very easy in this case because the boundary conditions of 1 dimensional laser cavity is given by the reflection at both facets, that is,

$$\left.\frac{S}{R}\right|_{z=L} = R_r \qquad \left.\frac{R}{S}\right|_{z=0} = R_l \tag{21}$$

The facet is located at z=L and z=0 in above conditions. L is the length of a cavity. R_r and R_l is the reflection at each facet. They are in general complex numbers.

Substituting 2 conditions of (21) into (20) and diminishing C_2 from resulted 2 equations conclude the next equation on threshold gain and lasing wavelength.

$$\frac{1}{i\kappa_m(\alpha-\beta)}\ln\left(\frac{R_r-\alpha}{R_r-\beta}\cdot\frac{1-\beta R_l}{1-\alpha R_l}\right) = L \tag{22}$$

This is the eigenvalue equation for coupled mode equations in the general form. Threshold gain and lasing wavelength for DFB lasers are determined from this complex equation.

The treatment in the existence of finite reflections makes a story complicated and must depend on the numerical calculations for a simple explanation. Anti-reflection at the both facets is assumed for the clearance of discussion.

$$R_r = 0\ ,\ R_l = 0 \tag{23}$$

From(22), the next simpler equation is obtained.

$$\frac{1}{i\kappa_m(\alpha-\beta)}\ln\left(\frac{\alpha}{\beta}\right) = \frac{\ln\left(\dfrac{(g_{eff,0}-i\delta)+\sqrt{(g_{eff,0}-i\delta)^2+\kappa_m\kappa'_m}}{(g_{eff,0}-i\delta)-\sqrt{(g_{eff,0}-i\delta)^2+\kappa_m\kappa'_m}}\right)}{2\sqrt{(g_{eff,0}-i\delta)^2+\kappa_m\kappa'_m}} = L \tag{24}$$

When the absolute value of coupling constants is very small, the threshold current become very large because no lasing is possible in FP laser with no reflection at the facets. The small coupling constant means that the properties of DFB lasers resemble to FP lasers.

$$\left|\frac{\kappa_m}{g_{eff,0}-i\delta}\right| << 1 \tag{25}$$

Using this relation, (24) is approximated as (26).

$$\ln\left(-\frac{4\left(g_{eff,0}-i\delta\right)^2}{\kappa_m\kappa_{-m}}\right)=2\left(g_{eff,0}-i\delta\right) \tag{26}$$

It is divided into next 2 equations in a real space.

$$\ln\left(\frac{2G}{K}\right)=GL\cos(\varphi) \tag{27}$$

$$\pm\frac{1}{2}\pi+2p\pi+\varphi-\vartheta=GL\sin(\varphi),\quad p=0,\pm1,\pm2,\pm3,... \tag{28}$$

Above equations are obtained by replacing the terms in (26) with following new ones, and comparing the both sides to separate a real part and an imaginary part.

$$g_{eff,0}-i\delta=Ge^{i\varphi},\ \kappa_m\kappa_m'=K^2e^{i2\vartheta},\ G>0,K>0\in\Re \tag{29}$$

When φ satisfies (27) and (28), φ+2π is also their solution. Therefore it is enough only to consider the case of p=0. At first we take (28) to understand how the solution behaves when we change the coupling constants. In (28), the phase of coupling constants can influence on the property of gain and lasing wavelength. The second equation of (29) contains the products of 2 coupling constants where the phase of index and gain coupling are conjugate. It means that θ is simply determined by the relation of index and gain coupling, not depends on the facet phase. We don't mind that index and gain coupling is a real number in this case and θ is expressed as

$$\theta=\arctan\left(\frac{g_m'}{k_0n_m'}\right),\quad \kappa_m=\left(k_0n_m'+ig_m'\right)e^{i\phi},\kappa_{-m}'=\left(k_0n_m'+ig_m'\right)e^{-i\phi},\quad n_m',g_m'\in\Re \tag{30}$$

κ_m and κ_{-m} are the coupling constants shown in (12) or in (13). Each coupling constant corresponds to θ summarized in the table below.

index coupling	$\vartheta=0$
in-phase (gain coupling)	$0<\vartheta<\frac{\pi}{2}$
anti-phase (gain coupling)	$-\frac{\pi}{2}<\vartheta<0$
pure gain coupling	$\vartheta=\pm\frac{\pi}{2}$

Table 2-1 phase of coupling constants

We don't care about the problem on the existence of a solution. We suppose that the set of equations (28) and (29) has a solution which satisfies the assumption (25). Note that φ in (29) is symmetry against the origin when index coupling is incorporated. It means that $\pm\varphi_0$ ($\varphi_0>0$) is a solution at the same time. It coincides with the fact that index coupling has 2 lasing modes which appears symmetrically on Bragg wavelength.

$$g_{eff,0} = G\cos\varphi\ ,\quad \delta = -G\sin\varphi \tag{31}$$

From (31) they actually have the same threshold current and different lasing wavelengths. Then it is more interesting to know what happens when an infinitesimal gain coupling is added to a laser structure. The variation of $g_{eff,0}$ and δ are calculated by differentiating (27) and (28) on θ. The selectivity of lasing wavelength is observed as a difference in threshold current. Its differential is

$$\frac{dg_{eff,0}}{d\vartheta} = \frac{-G\sin\varphi}{(1-GL\cos\varphi)^2 + G^2L^2\sin^2\varphi} \tag{32}$$

The denominator of (32) is apparently positive, and not zero unless GL does not equal to 1. The numerator of (32) is exactly δ in (31). Therefore, the variation of $g_{eff,0}$ is proportional to the products of detuning from Bragg wavelength and phase variation of coupling constant.

$$dg_{eff,0} = C\delta\cdot d\vartheta,\quad C>0 \tag{33}$$

When the gain coupling is in-phase, dθ is positive(see Table 2-1). It concludes that the threshold gain is lower for the wavelength with negative δ. Negative δ corresponds to φ_0 among the 2 modes of index coupling lasers. The other one apparently gives positive δ. The mode whose detuning is negative is the one on the long wavelength side of Bragg wavelength, and the laser operation is achieved at that wavelength as the in-phase of coupling constant is introduced in DFB lasers. The degenerate modes in index coupling is now dissolved.

Anti-phase offers negative θ in (33) to the contrary of the previous case, and the wavelength on the short wavelength side of Bragg wavelength is chosen as a lasing mode. Hence, the introduction of gain coupling is proved to be helpful to dissolve the degeneracy in index coupling and choose the lasing mode which we want.

The incorporation of gain coupling is accompanied with a shift of lasing wavelength, and the symmetry of lasing spectrum on Bragg wavelength in index coupling is lost. The counterpart of (32) for δ is

$$\frac{d\delta}{d\vartheta} = \frac{G(GL-\cos\varphi)}{(1-GL\cos\varphi)^2 + G^2L^2\sin^2\varphi} \tag{34}$$

GL should be much larger than 1 in this case because of anti-reflection on the facets and a small coupling constant. It means that the right hand side of (34) is always positive. If we discuss each case of coupling constant as is done on the threshold current, the result is summarized simply like following. A shift of the lasing wavelength occurs so as to make it close to Bragg wavelength. Here, the lasing wavelength is a long wavelength side for in-phase and a short wavelength side for anti-phase. The introduction of higher gain coupling enables us to achieve the lasing at a closer position to Bragg wavelength.

Actually in pure gain coupling $\varphi=0$ is a possible solution. Its mode is related with either $\pm\varphi_0$ ($\varphi_0>0$) in index coupling as a result of above lasing wavelength shift. When the pure gain coupling is considered as a limitation of in-phase, the mode corresponding to + sign (long wavelength side) is lased at Bragg wavelength in DFB laser. On the hand, in the case of anti-phase, lasing mode at Bragg wavelength comes from one with - sign (short wavelength side). $\varphi=0$ means no detuning from Bragg wavelength (see (31)). DFB laser is operated precisely at a Bragg wavelength in pure gain coupling.

2-5 Conclusion

Based on coupled mode equations, several fundamental features of DFB laser are discussed. Every phenomenological results stated in this chapter are proved analytically under the assumption of existence of a solution of coupled mode equations, a small coupling constant, and no reflection at facets. Especially we lay the stress on the properties related with the phase of complex coupling, where index and gain coupling coexist. Those results are useful to analyze a spectrum of DFB lasers because most available DFB lasers belong to a complex coupling type. Though the more precise discussion must be constructed from the numerical calculations, these features clarified through the simplification is certainly valid for the general case, too. Many experiments carried out in the past proves the effectiveness of coupled mode equations by comparing both numerical and experimental results. Hence all the results obtained in this chapter are true in the real DFB lasers. The facts proved in this chapter are quoted in the later chapter.

Reference

[1]H.Kogelnik and C.V.Shank, "Coupled-wave theory of distributed feedback lasers", J.ApplPhys., vol.43, 2327, 1972.

[2]P.Vankwikelberge, G.Morthier, and R.Baets, "CLADISS-A longitudinal multimode model for the analysis of the static, dynamic, and stochastic behavior of diode lasers with distributed feedback", IEEE J.Quantum Electron., vol.26, 1728, 1990.

[3]T.Makino, "Transfer matrix formulation of spontaneous emission noise of DFB semiconductor lasers", J.Lightwave Technol., vol.9, 84, 1991.

[4]A.Lowery and D.Novak, "Performance comparison of gain coupled and index-coupled DFB semiconductor lasers", IEEE J.Quantum Electron., vol.30, 2051, 1994.

■ Chapter 3

Fabrication method of QWRs and its suitability to DFB lasers

3-1 Introduction

It has already been stated in chapter 1 that what kept so dramatic a development in optoelectronics was the remarkable progress in growth technology of semiconductor materials with which the band engineering of compound materials were available for the first time. An employment of QWL (quantum well) in laser structures can be counted among the most fruitful results of those technology. It impressed in our mind the effectiveness to make the best use of low dimensional structures in device physics. Further studying to seek QWR (quantum wire) and QD (quantum dot) followed at once. But their quality level is not yet high enough to attract attentions to practical devices using them. Unfortunately they are just used for the exploration in material physics to study particular characteristics of 2D or 3D confined electrons, and no more progress in devices has ever been reported recently except for lasers based on self-organized QDs.

It is no doubt that the fabrication of 2D or 3D confined structure is much more difficult than 1D structure represented by QWLs. Because ever developed growth technology is essentially for 1D, and no functional apparatus for 2D or 3D control of growth directions is equipped. Hence, a specific additional process to induce 2D or 3D confinement in grown layers was inevitably contained in all the idea ever reported. We should learn at first from those experiments of predecessors. It is important to resume what methods have been applied for such a purpose and what disadvantages were incidental to each method. It will give us a useful information to judge which to take and to drop off when we actually apply QWRs to DFB lasers. The objective of this chapter is to investigate the best way for the fabrication of QWR DFB lasers.

3-2 Various QWRs and their formation

It is interesting to mention about the analogy of formation of QWRs and QDs. We can always found the counterpart of one in the others. Whether we make QWRs or QDs, what

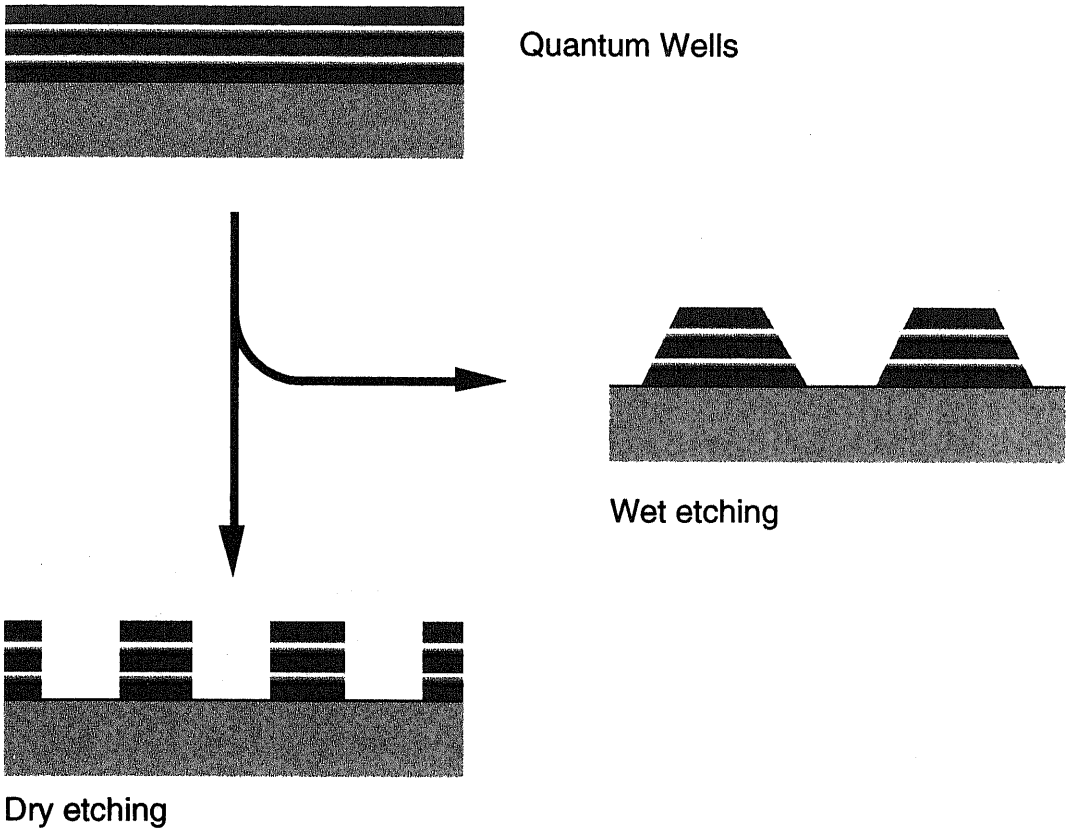

Figure 3-1 QWRs formed by etching multiple QWLs (right: trapezoidal type made by wet etching, lower: rectangular type by dry etching). Each QWL in the mesa structures works as a QWR.

is necessary for that purpose is the growth controllability in the plane of a substrate. Because requirements are the same for any direction in the plane without an orientation dependency of substrate, once QWRs are fabricated, it is easier to enhance its technology to QDs. And thus, almost all the methods used for QWRs are also applicable to QDs.

In this section, because our interest is in QWRs, only QWR's case is picked up for further discussions.

3-2-1 How to make QWRs

The proposal to use QWRs in semiconductor lasers appeared in the beginning of 1980's[1]. But it took more than 5 years until its fabrication started. In fact, this 5 years corresponds to the period when the remarkable development of growth technology was achieved being pressed by the popularization of QWLs. The fabrication of QWRs is relatively a new subject in the optoelectronics and photonics.

Method I: Patterning of QWL (Figure 3-1)

The first one is a direct method to pattern a substrate with QWLs so that ridge stripes with QWLs in it are left by an etching process. The width of QWR is controlled by the etching process. Patterns are made through a series of photolithography processing. EB

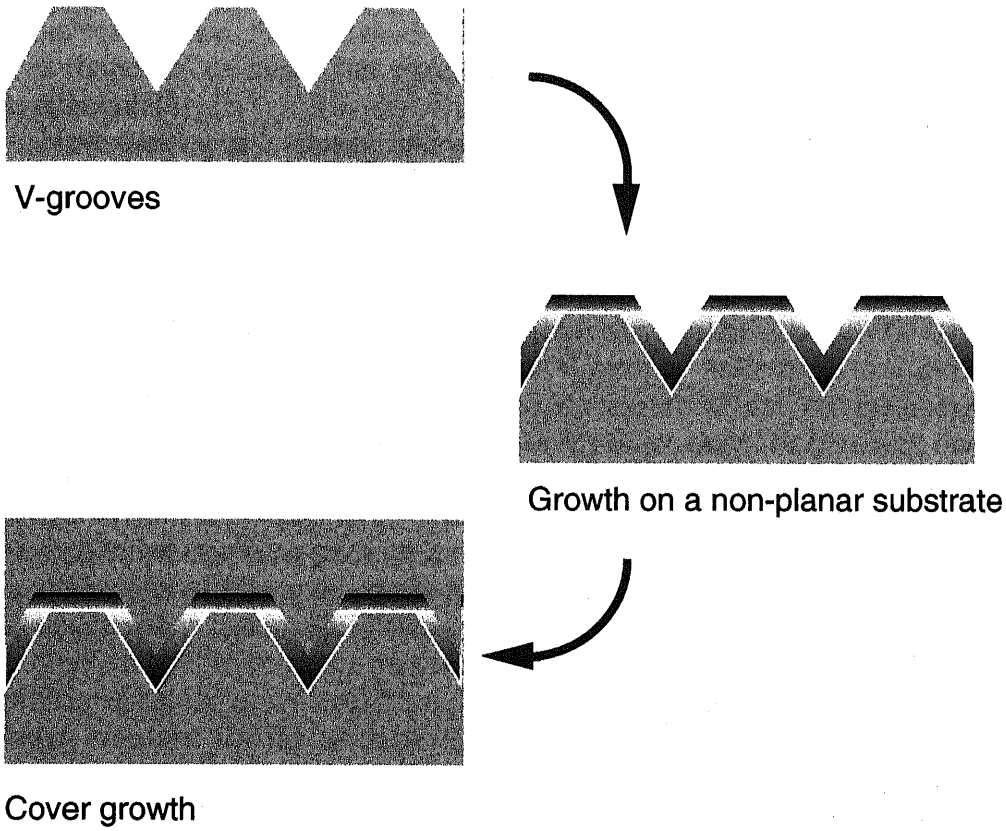

Figure 3-2 QWRs made by growth on a V-grooved substrate. QWRs are placed at the bottom of V-grooves. QWLs are also formed on the ridges and the shoulders of V-grooves.

(Electron Beam) patterning is often used for this purpose. As the etching method, both wet and dry process are possible. QWRs are cut out from QWLs with the depicted resist pattern as a mask. Then QWRs are capped by the regrowth so as to form a heterostructure.

This method is so simple that it is often used when QWRs are needed in experiments. No demand for the special growth technique except for a regrowth on nonplanar substrate is considered as another merit. Because QWR is formed by the patterning, the controllability of QWR's position is also good. The QWR array needed for DFB lasers is producible by this method. The lateral size of QWR was more than 10nm in the case of GaAs materials[2]. But the smallest one applied to a laser cavity was 25[nm][3]. The easiness of stacking the same size of QWR is attractive for the application to semiconductor lasers, too.

But the quality of QWRs highly depends on the etching process. The orientation dependency in wet etching process using chemicals often prevents us from obtaining a rectangular mesa structure. It results a non-uniformity of stacked QWRs, which leads to unfavorable broadening in emission spectrum of QWRs. Dry etching process is less influenced in this point. Another serious fault of this method is to introduce defects in the area close to or the interface of QWRs because 2 etched sides surrounding a QWR remain exposed without any protections in the successive device processing, and defects incorporated in such a way are said to serve as carrier capturing center, or carrier loss in devices. It evidently spoils the quality of QWRs, especially at as high a temperature as

room temperature. Since those defects work as a center of non-irradiative recombination, it is hopeless to expect an excellent behavior as optical devices operable at room temperature[3].

Nevertheless, it is almost impossible to avoid completely the incorporation of such defects in the etching process. In this sense, QWRs made by this method is not proper for the realization of practical optical devices. Its use should be apecilized for material sciences like many papers ever published unless this problem is not solved.

Method II: Growth on nonplanar substrate(Figure 3-2)
The most well-known process is to use V-grooves made by a wet etching of (100) substrate[4]. This method was tried for GaAs materials at first, and the lasing operation of a semiconductor laser with GaAs/AlGaAs QWR as an active part was demonstrated at room temperature. Though it is still questionable whether it owes its lasing property to QWRs or not, it successfully shows a good quality of QWRs fabricated in this way at least. Another one is to grow on a ridge structures. It uses the formation of surface with an orientation of high index number (311)A during the growth, and ridges become sharp as the growth is continued. QWRs are finally formed on top of it[5].

Though both is known to produce a good optical quality of QWRs, the former is more promising as far as we see the recent results. No challenges to make a semiconductor lasers are done for the latter method. Hence, we take a growth on V-grooves in this section.

V-grooves are prepared in $(0\bar{1}1)$ direction of (100) substrate by wet etching. Because QWR size is controlled by the growth on V-grooves, the patterning size (V-groove size) is independent from it. Note that this condition is different from that of etched QWLs (Method I). A critical resolution of photolithography is not necessary in this method. Only the sharpness and smoothness of V-grooves are demanded in this process. Because QWR position is precisely controlled by that of V-groove, a uniform QWR array is producible and is, off course, applicable to DFB lasers. Regrowth follows after the formation of V-grooves. Since QWR is fabricated by the epitaxial growth, its quality is expected to be better and free from defects contrary to the previous case. Although, owing to the regrowth process on a patterned substrate, the treatment of samples before regrowth must be careful, its interface can be improved by several growth techniques. Stacking of QWR is also established for GaAs materials. As it is achieved only by the growth conditions, the precise copy of the first QWR can be piled repetitively for any sizes of QWR. The achieved lateral QWR size by this method was about 10[nm]. Its cross-section normally offers a triangular shape coming from the geometry of V-grooves. As an unusual case, rectangular one has also been reported recently[6].

A representative defect of this method is the coexistence of parasitic structures. Especially QWLs are so prominent in the optical characteristics among given nanostructures on V-grooves that it can even conceal the QWR characteristics in the experiment. Therefore, a special care is needed to utilize this method in devices or the characterization of QWRs. In most cases, such a disadvantage has been overcome by removing QWLs by additional lithography processes. But this inconvenient procedure apparently disturbs and limits the application of this method in spite of lots of proofs to show a good quality of QWRs. In relation with these QWLs, the weak lateral confinement of carriers in QWR is criticized because QWR connects to parasitic QWLs on both sides at the bottom of V-grooves. The weak modulation of a layer thickness on V-grooves is only

a main contribution to a confinement of carriers in the lateral direction. Another demerit is that this method is dependent on the material properties because it needs V-grooves with its sharpness kept during the entire growth process. It works very well in GaAs materials for short wavelength, but almost no successful report has been found in InP materials for long wavelength.

Method III: Application of selective area growth (Figure 3-3)
It is considered to be a complement method of II. The substrate is covered by deposited materials such as SiO_2 or Si_3N_4 used in SAG (selective area growth)[7]. The stripe pattern is made by photolithography in the orientation of (011) and the same successive process as SAG is done for it. The mesa structure with (111)B surface is self-formed on the substrate until its top of triangular cross-section become sharp enough to have a small domain to grow a QWR on it. Lateral QWR size is determined by the width of this small linear area. It is very important how small area is obtained through SAG process in this method. In this point, it resembles to the latter one introduced in the last section, where the (311)A facet is used instead of (111)B.

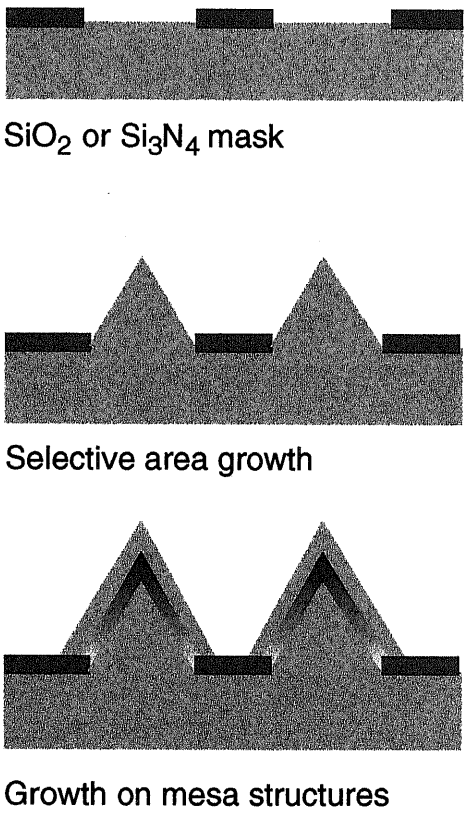

Figure 3-3 QWRs fabricated by applying selective area growth. QWRs are at the top of mesa structures. QWLs are on the side walls.

This method has a problem of parasitic structures similarly to a growth on nonplanar substrates, and undoubtedly its complicated structures disturb applying this method to a device fabrication. It is not always effective for every materials, either. And the QWRs prepared by this method is disadvantageous for the fabrication of DFB lasers as follows. QWR array is producible by using the stripe pattern, but regrowth quality needed for burying QWRs might be worse because the used dielectric mask is embedded together in the regrown layer unless it is not removed after the formation of QWRs. Such a growth on a irregular material usually produces dislocations and defects. And the removal process increases the regrowth time. It is a common sense that the repetition of regrowth is unfavorable in device fabrications.

Method IV: Growth on a cleaved facet (Figure 3-4)
A sample with multiple QWLs on it is previously prepared and is cleaved in the vacuum to keep its facet clean. And then another QWL is grown on the facet. It produces T-shaped junctions of QWLs and each one works as a QWR. The structure is simple and its 2D confinement is well investigated among QWRs ever reported. Its quality is proved to be good, and applicable to lasers by contriving carrier injection[8]. Because the position of QWR is controlled by the first grown QWLs, the fabrication of small QWR array is possible. In addition to that, the density of QWRs is easily controllable. But the large QWR array needed in a fabrication of DFB lasers is not realistic. The coexistence of QWLs are also a serious problem like in the Method II.

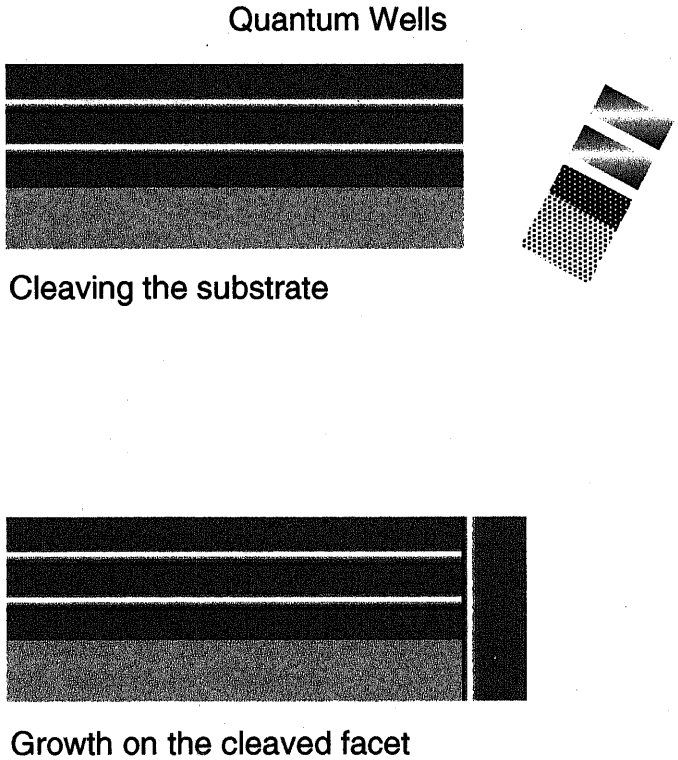

Figure 3-4 T-shaped QWRs formed on the facet containing QWLs. QWRs are at the junctions of horizontal and perpendicular QWLs.

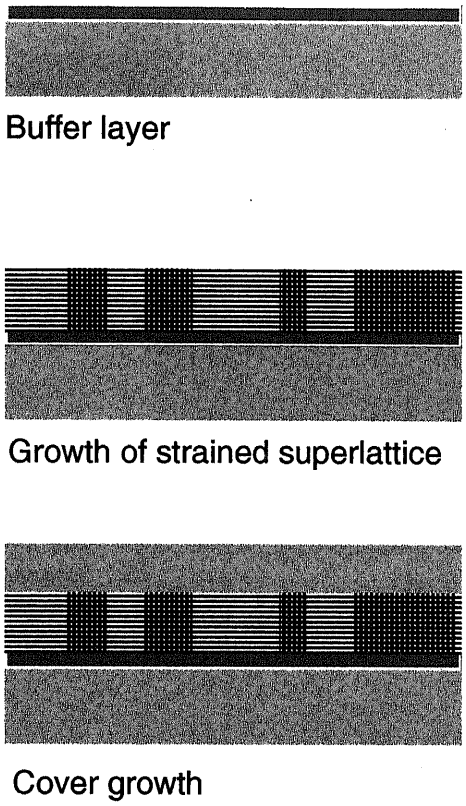

Figure 3-5 Self-ordered QWRs. QWRs are formed in the strained superlattice. Their position, width and length are rondom and not controllable. QWRs are expressed as check patterns in the above figure.

There is a variation in this type of growth. It uses the above facet of multiple QWLs to grow a material selectively. Because it offers the stripe pattern like in the Method III, QWRs are made on top of it[9].

Though a good result on the fabrication of FP lasers was reported in the firsr case[8], no application is found in the latter case.

Method V: Self-formation of QWRs (Figure 3-5)

The most favorite way should not be accomapanied with such a pre-process as is mentioned in the previous sections (Figure 3-1~3-4). For this purpose, QWR must be ordered spontaneously on a substrate. In this method, the strains distributed in layers is used as a source to induce lateral ordering. Such a strain is prepared during a series of growth of buffer layers, and QWRs with the width of several [nm] is formed on it as a result of modulation in the composition of compound materials[10].

But the QWRs obtained by this method are quite different from the image of array or grating. Although the density of QWRs is very high because they are self- ordered and cover the entire surface without any room, QWRs irregularly wind like a river, and their width and length is non-uniform. This poor uniformity of QWRs is one of the biggest problems to be solved in this method. Naturally such QWRs cannot be applied to a grating in DFB lasers. Furthermore, because the material contrast of such a self-formed QWR is known to be very weak, it is still questionable whether it works as a QWR or not under thermally activated conditions near room temperature. As far as this non-

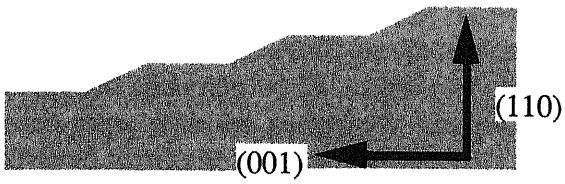

Off-substrate

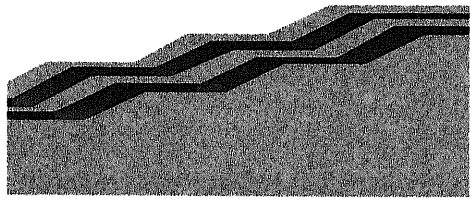

Growth of superlattice

Figure 3-6 QWRs on a vicinal substrate. QWRs are fabricated at each steps as a thickness modulation of growth layers.

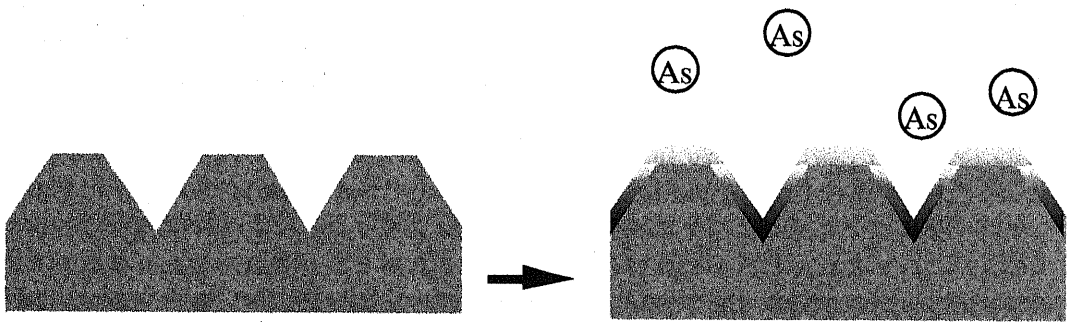

V-grooves (InP)

P and As replacement

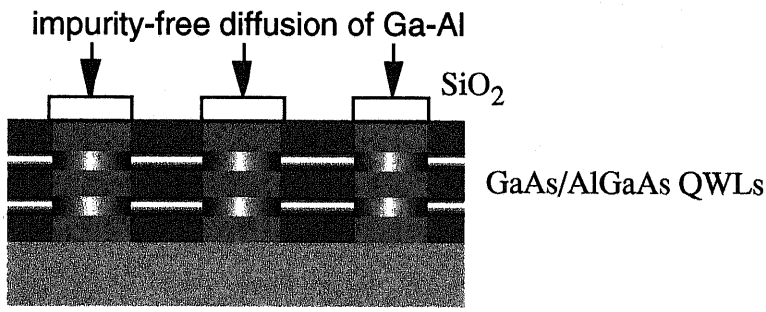

Intermixing of quantum wells

Figure 3-7 Fabrication of QWRs by the surface replacement of group V atoms (above) and the intermixing of QWLs (below). QWRs are located at the bottom of V-grooves (above) and the outside part of intermixed regions in QWLs(below).

uniformity in QWRs are not improved, no excellent features predicted in QWRs are expected even if they are applied to devices.

Method VI: Using the vicinal substrate (Figure 3-6)

Another way to avoid pre-processes is to use a vicinal substrate. It serves as a patterned substrate by its monolayer steps on the surface[11]. QWRs can be formed at each steps with the periodicity determined by the interval of steps. Because QWRs are arrayed regularly, it is possible to apply this method to DFB lasers. The density of QWRs is relatively higher than the Method I, II and III. But the material contrast of QWRs is reported to be weak, and carriers confined in QWRs are considered to be between 1D and 2D even at low temperature[12]. And thus, it is still difficult to use this method for a QWR device fabrication.

Method VII: Other methods (Figure 3-7)

Above mentioned methods have been practiced for the fundamental research of QWRs. Those have been understood to show 1D carrier properties to certain extent. There still are other methods to form QWRs though its property is still poor or doubtful. Most of them are less promising as a candidate for future application to devices, but it is worth while to introduce some of them here. They might give us a hint to invent a new promising methods.

The formation of QWRs on V-grooves has already been stated as Method II. InP was a difficult material to be applied this method as it was [13]. To solve this problem, the replacement of group V atoms (P and As) on the surface in MOVPE reactor was utilized. The efficiency of replacement is dependent on the surface orientation and is faster on (100) surface. Hence, when we make a V-grooves on the substrate, the replacement is effective at the bottom and slow on the sides. This difference cab produce QWRs at the bottom of V-grooves. But the QWR size is on the order of monolayer and off course can be fluctuated along the wire due to the non-uniformity of As and V exchange. The fact that QWLs coexist does not change in this case, too. Above all, luminescence efficiency is extremely low due to its small size, and probably its quality. It is unfortunately never useful from the practical point of view.

Another one is to use intermixing of QWLs to achieve a lateral confinement in QWLs[14]. This idea resembles to that of etching QWLs (Method I), but is different in the viewpoint that the QWRs are not exposed directly to the air during its process. But the defects brought from intermixing itself is not little enough to permit the fabrication of active devices like lasers and amplifiers. The accuracy of intermixing process is also a problem because the controllability of atomic diffusion determines it. It is usually worse than the need for QWRs. The bad contrast at interface in QWRs is not negligible, too.

3-3 Conclusion

All the properties of QWRs mentioned in this chapter are summarized in Table I with regard to applicability to lasers, especially to DFB lasers.

From this investigation, it is now clear that the promising methods for a fabrication of DFB lasers are few. Self-formation method (Method V) is out of discussion. Although using of vicinal substrate (Method VI) or the growth on cleaved facets (Method IV)are possible by principle, they are never a practical way. Because one needs the off-substrate whose steps on the surface is precisely tuned for Bragg wavelength of DFB lasers and the

other a thousand set of QWLs. Considering the disadvantages of regrowth in the selective area growth method (Method III), there are only 2 methods left.

Fabrication process	Applicability to an active part of FP lasers	Applicability to an active grating in DFB lasers
1.Etching of QWLs	possible	possible but no report
2.Growth on nonplanar sub.	possible	possible
3.Selective area growth	possible but no report	impossible
4.Overgrowth on cleaved facet	possible	impossible
5.Self-formation induced by strain	possible	impossible
6.Growth on a vicinal sub.	possible but no report	impossible

Table 3-1 Applicability to an active grating in DFB lasers.

Lasing operation seems to be easier when we use etching of QWLs (Method I) to make QWRs because higher gain is available by stacked QWLs. However, this method is critical to the quality of a mask pattern used in etching process, and the regrowth quality is not reliable. If those conditions are not cleared, the quality of QWRs as the active part itself is questionable. Good performances of QWRs at room temperature is very suspicious due to the defects introduced during the fabrication process. Such a claim must be essentially excluded as possible as we can when we want to discuss the possibility of QWR DFB lasers. Therefore, it would rather be a wise judgment to choose the regrowth on non-planar substrate (Method II) for DFB lasers. The quality as QWRs in this method has been well established and the preparation process is not so difficult as above one. Moreover, there have been some reports on lasing at room temperature in FP QWR lasers. Though it is said that a careful discussion is needed to call them as QWR lasers, it evidently shows good quality of samples employing QWRs fabricated by Method II. Considering that no sufficient results is not still obtained at room temperature by Method I, Method II is more appropriate to the challenge of DFB QWR lasers, again.

Based on this conclusion, we will clarify how QWRs made by the growth on V-grooved substrates works in the fabrication of QWR DFB lasers in the next chapter.

Reference

[1]Y.Arakawa and H.Sakaki, "multidimentional quantum-well laser and temperature dependence of its threshold current", ApplPhys.Lett., vol.40, 939, 1982.

[2]M.Notomi, S.Nojima, M.Okamoto, H.Iwamura, and T.Tamamura, "size dependence of lateral quantum-confinement effects of the optical response in $InGa_{0.53}As_{0.43}$ quantum wires", Physical Rev.B, vol.52, 11073, 1995.

[3]T.Kojima, H.Nakaya, S.Tanaka, S.Tamura, and S.Arai, "evaluation of internal efficiency and waveguide loss of 50nm-period GaInAsP/InP quantum-wire lasers", Proc.10th Int. Conf. on Indium Phosphide and Related Materials, 365, 1998.

[4]E.Kapon, S.Simhony, R.Bhat, and D.M.Hwang, "single quantum wire semiconductor lasers", ApplPhys.Lett., vol.55, 2715, 1989.

[5]S.Watanabe, S.Koshiba, M.Yoshita, H.Sakaki, M.Baba, H.Akiyama, "stimulated emission in ridge quantum wire laser structures measured with optical pumping and microscopic imaging methods", ApplPhys.Lett., vol.73, 511, 1998.

[6]T.Sogawa, S.Ando, and H.Kanbe, "photoluminescence properties of 13×13 nm GaAs quantum wires buried in trench structures reduced by growing GaAs/AlAs superlattice layers", ApplPhys.Lett., 1087, 1995.

[7]S.Tsukamoto, Y.Nagamune, M.Nishioka, Y.Arakawa, "fabrication of GaAs arrowhead-shaped quantum wires by metalorganic chemcal vapor depostion selective growth", ApplPhys.Lett., vol.62, 49, 1993.

[8]W.Wegscheider,L.Pfeiffer,and K.west, "current injection GaAs/AlGaAs quantum wire lasers fabricated by cleaved edge overgrowth", ApplPhys.Lett., 65, 2510 ,1994.

[9]T.Arakawa, H.Watanabe, Y.Nagamune, and Y.Arakawa, "fabrication and microscopic photoluminescence imaging of ridge-type InGaAs quantum wires grown on a (100) cleaved plane of AlGaAs/GaAs superlattice", ApplPhys.Lett., vol.69, 1294, 1996.

[10] S.T.Chou,K.Y.Cheng,L.J.Chou,and K.C.Hsieh, " $Ga_xIn_{1-x}As$ multiple-quantum-wire lasers grown by the strain-induced lateral-layer ordering process", ApplPhys.Lett., 66, 2220 1995.

[11]T,Kato, T.Takeuchi, Y.Inoue, S.Hasegawa, K.Inoue, and H.Nakashima, "stacked GaAs multi-quantum wires grown on vicinal GaAs(110) surfaces by molecular beam epitaxy", ApplPhys.Lett., vol.72, 465, 1998.

[12]H.Ando, H.Saito, A.Chavez-Pirson, H.Gotoh, and N.Kobayashi, "excitonic optical properties in fractional-layer-superlattice wire structures in the intermediate confinement regimebetween two dimensions and one dimension", Physical Rev.B, vol.55, 2429, 1997.

[13]M.Kappelt, V.Turck, and D.Bimberg, "$In_xAs_{1-x}P$ V-groove quantum wires", Proc.10th Int. Conf. on Indium Phosphide and Related Materials, 587, 1998.

[14]A.Pepin, C.Vieu, M.Schneider, R.Planel, J.Bloch, G.Ben Assayag, H.Launois, J.Y.Marzin, and Y.Nissim, "GaAs/AlGaAs quantum wires fabricated by SiO_2 capping-induced intermixing", ApplPhys.Lett., vol.69, 61, 1996.

■ Chapter 4

Fabrication and characterization of InGaAs QWR DFB lasers

4-1 Introduction

The growth on V-grooved substrates was considered to be the best way to make QWRs for the active grating in DFB lasers in chapter 3. It is because V-groove methods has been studied well in fundamental researches and also been applied to FP lasers. As far as we refer to ever published reports, it can offer the highest quality of QWR array suitable for DFB lasers at the same cost of equipments and diffuculty of processing. But almost no experimental results has ever been obtained for DFB lasers even with this method except for the challenge by S.Simhony et al.[1]. In chapter 4, it will be clarified what prevented us from applying QWRs to DFB lasers through the fabrication of QWR DFB lasers. The effectiveness to combine DFB cavity with QWRs for the realization of QWR lasers will also be shown experimentally.

4-2 About QWR DFB lasers

The term "QWR DFB laser" remained in vague without a specific definition in the preceding chapters. When we talk about a QWR laser with a DFB cavity, 3 types are imaginable as is shown in Figure 4-1. One has only QWRs in its cavity (structure (a)), and another has one more grating apart from QWRs. The last one (structure (c)) is a mixed type of (a) and (b). In the structure (a), QWRs must work as a grating as well as a gain region, and in the (b), it serves only as a gain region and not as a grating. The distributed feedback in (b) is given by another grating in the cavity. In the structure (c), though both gratings exist in its cavity like (b), both contribute to a distributed feedback. All of them are undoutedly a QWR laser because their active part is a QWR array. But the types but (b) are more innovative and unique in the following point. Their active part and grating to induce a distributed feedback is identical. It is one of the reasons why the QWR laser structue is considered to be more suitable for DFB lasers than FP lasers. Therefore, we define DFB QWR lasers so as to mean the structure(a) and (c).

In this section, the problems which will be fronted in the process of its realization are reviewed based on possible DFB QWR structures using a V-grooved substrate.

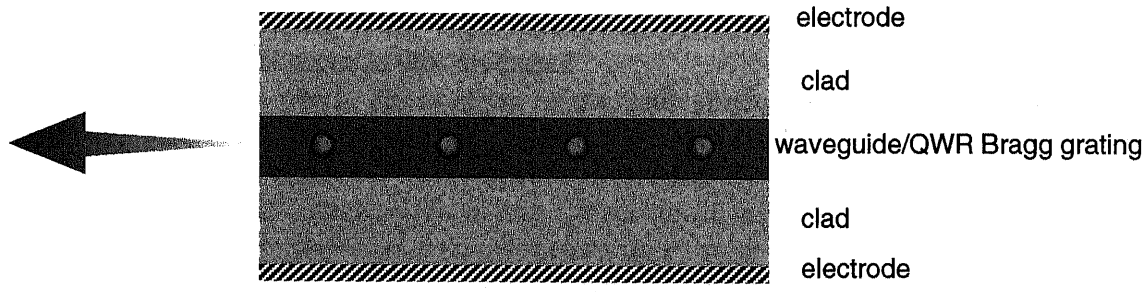

structure (a)

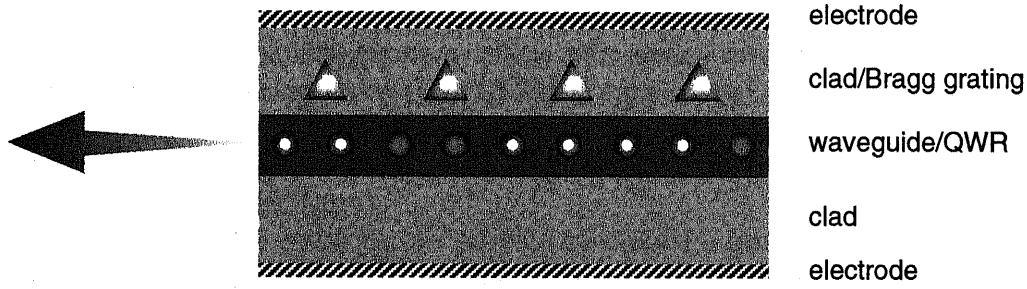

structure (b)

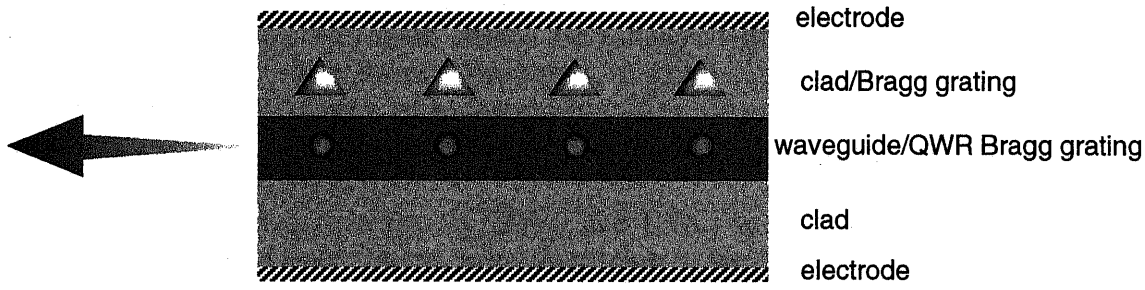

structure (c)

Figure 4-1 Possible QWR DFB laser structures. (a) and (c) are essentially new because their distributed feedback and gain originate from an active grating of QWRs. (b) is the type where the active layer is just replaced with QWRs in conventional DFB lasers.

Our laser structure is simple. The QWR array is sandwitched by the barrier material which works as a waveguide as well as the separate confinement heterostructure introduced in QWL lasers. The waveguide is surrounded by cladding layers with a larger bandgap than the barrier material. Arrayed QWRs serve as the active grating in the cavity which makes DFB laser operation possible. Following the conclusion of the last chapter,

the QWR array fabricated by the V-groove method are incorporated. The question is what kind of problems can occur in this structure?

The most serious one is the existence of parasitic structures called respectively as top QWL and side QWL (Figure 4-2)[2]. Sometimes (311) QWR is included. These are the particular structures observed in QWR structures made by the V-groove method. Due to these structures, the emission from the QWRs must compete with them to reach a threshold gain first in the laser cavity. It causes an extra consumption of injected carriers in the resonator, and it can be happened that none of them can not contribute to lasing. To make it matters worse, the luminescence intensty of QWRs is normally weaker than any others (for example, as is seen in photoluminescence (PL) signal) because of their small volume. As far as we concern lasing from QWRs, we can use a large V-groove arrayed with a periodicity of 1[μm], or 3[μm] without considering Bragg wavelength in DFB lasers. The cavity direction is parallel to a V-groove to be FP lasers. And then, processing to remove parasitic structures become much easier because those structural scale is within the precision of photolithography available with an ordinary apparatus. The predecessors succeeded in achieveing lasing from QWRs in such a way[3]. However we now need the periodicity of a few hundreds [nm] for a DFB cavity, which is apparently beyond the patterning limit with an available mask-aligner. And thus, it is difficult to apply the above method to QWR DFB laasers.

To overcome this problem, we propose to make the most use of properties of a DFB cavity. Because it works as a filter with a very sharp selectivity near the Bragg wavelength, only the emission from QWRs is amplified by designing Bragg wavelength precisely, and it leads to lasing from QWRs. In those lasers, the threshold current is still high at the cost of emssions from other parasitic stuructures because DFB filter cannot suppress completely the amplified spontaneous emission from QWLs. It makes a lasing operation at higher temperature difficult. The unnecessary emission is partly suppressed by fitting the stopband of a DFB filter at those emissions. Though the disadvantage coming from parasitic structures should be eliminated definitively by removing them somehow to benefit several good properties of QWRs, it is useful to investigate the effectiveness of a DFB cavity where the cavity loss is reduced sufficiently so that lasing is achieved. Therefore, we take aim at realizing this selectivity in QWRs and suppression in QWLs of the DFB cavity at first.

The overlapped luminescence of QWRs and QWLs are the next problem owing to parasitic structures. Generally, the larger separation in the emission profile of QWRs and QWLs is desirable to distinguish both emissions and to design Bragg wavelength so that it supports the amplification of QWR emission and the suppression of QWL emission. But in case of the V-groove method, its separation is not very large because it is given by the thickness modulation on V-grooves and is cancelled by the additional confinement energy in QWRs (see Figure 4-3). It is so difficult to control each thickness of QWRs and QWLs independently that a dramatic enhancement of the peak separation is hopeless. At low temperature, at low excitation, the 2 peaks of QWR and QWL on the spectrum look quite clear though the margin of each luminescence is ambiguous. But the separation is gradually lost at higher temperature and the weak one from QWRs is concealed behind the other from QWLs due to the brodening of spectra. It is no more certain whether lasing would occur from QWRs or QWLs at such a temperature. These situation is really unconvenient to comprehend a phenomenon occurring in QWR lasers. To avoid this

obscurity as possible as we can, it would be better to start a challenge for QWR DFB lasers at low temperature.

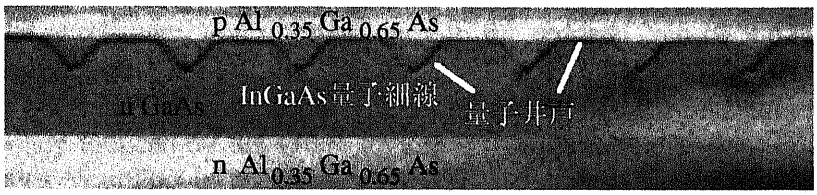

An example of shallow V-grooves

Structure

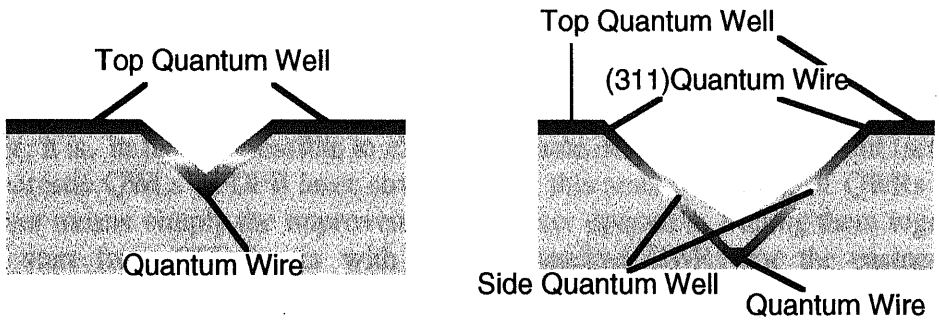

Photoluminescence spectrum

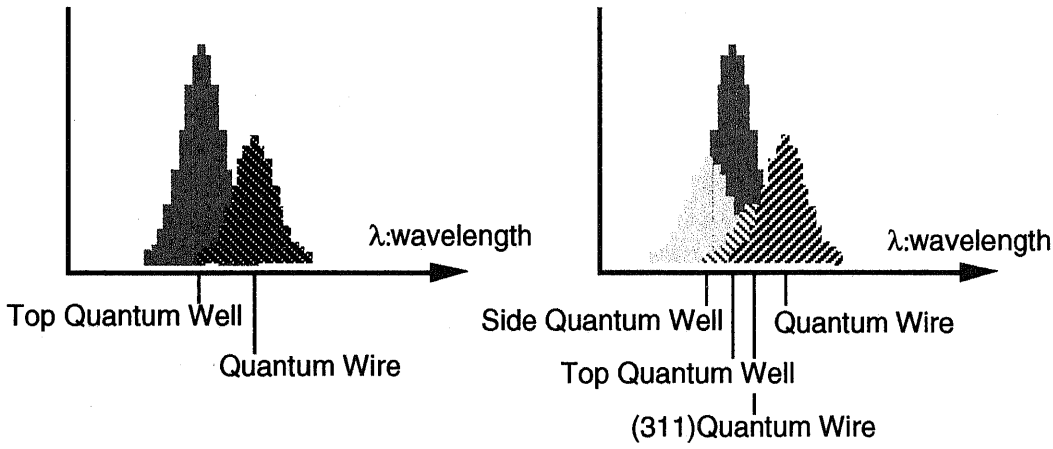

Shallow V-groove **Deep V-groove**

Figure 4-2 QWR array fabricated by the V-groove method. TEM cross-sectional image of QWRs on V-grooves (above: a case of shallow V-grooves). Deep V-grooves usually give more complicated structures than the shallow ones. The possible PL spectrum for each case is also shown in below.

We must consider the smaller optical confinement factor of QWRs, too, due to their small volume. It is an essential problem to be solved in the application of low dimentional structures to devices. Apart from the problem of parasitic structures, it also obstructs the achievement of lasing in QWR lasers by increasing a threshold current. Because QWR's gain is saturated at relatively low injection current, the reduced gain by the inappropreate design of a laser structure can disturb lasing. Hence, the optimization of the confinement factor in QWR lasers is absolutely necessary. Confinement factor is also important for the coupling efficiency induced by the QWR grating. From this point of view, it is helpful to incorporate index coupling in a cavity by using V-grooves on the substrate so as to support the effect of a DFB cavity. Such a structure corresponds to the structure (c) in Figure 4-1.

Because an addtional complicated or non-practical processing in the fabrication of a QWR array should be avoided, the integration of QWRs is limited in the growth direction. But in case of the V-groove method, the stacked number of QWRs is limited by the depth of V-grooves. The integration in plane of the substrate is automatically determined by the Bragg wavelength when we make DFB lasers by the distributed feedback of QWR grating. And Thus, the maximum confinement factor must be designed within these conditions.

However, it is, in fact, impossible to expect tha same order of a confinement factor of QWRs as parastic QWLs in DFB laser structures. In this sense, stacking of QWRs in V-grooves never means simply the improvement of a laser operation. Putting them together, we should start from DFB lasers with a single stacked QWRs for the easiness of fabrication.

As a summary, through the above discussion, we understood that the following terms are the key elements for the achievement of QWR DFB lasers by way of the regrowth on a V-grooved substrate.

1.The use of DFB effect for the suppression of parasitic structure's influence on the emission spectrum of QWR DFB lasers.
2.The experiments at a low temperature for the easiness to analyze experimental results.
3.The optimized design of a waveguide to make the best use of DFB effect. (confinement factor and coupling constant)

4-3 Fundamentals on low-pressure metal organic vapor phase epitaxy on V-grooves [4][5]

2 useful techniques has been known for the reproducible regrowth of QWRs on nonplanar substrates. Both are very important in the V-groove method. And especially one is indispensable to fabricate DFB QWR lasers. The other is used mainly for the improvement of regrowth quality.

In general, prepared non-planar or V-grooved substrates do not exactly have the same geometry. One is different from another because they are highly dependent on the patterning process of V-grooves. It is needless to say that the stability of processing is critical to the conditions to keep the quality of a patterned mask in such a small periodical pattern as a grating of DFB lasers. Suppose that we use a holographic method to obtain stripe mask patterns on substrates. The pattern's quality is influenced by many parameters

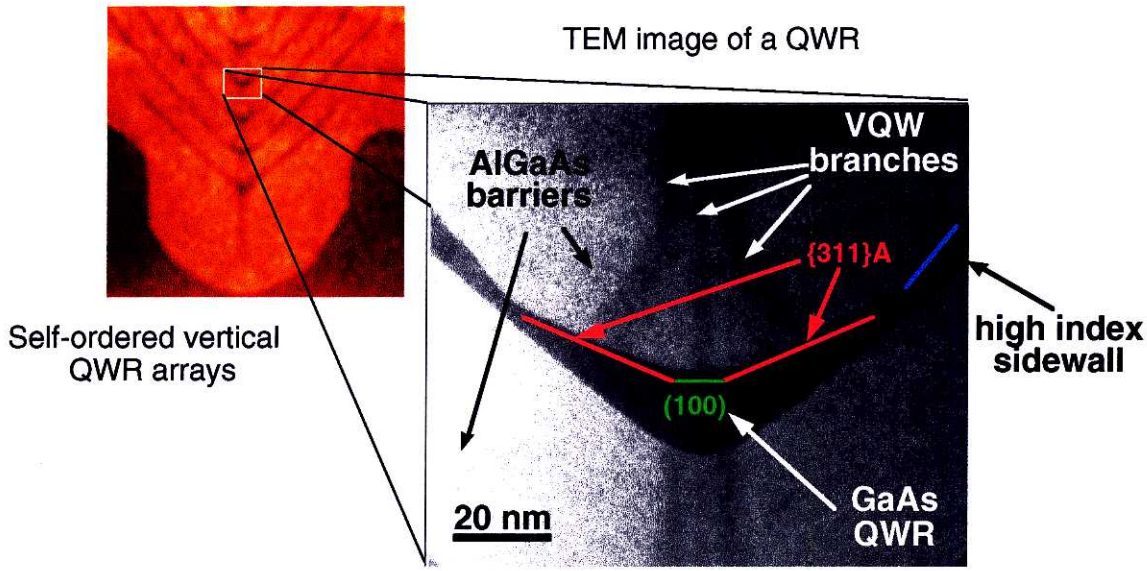

Figure 4-3 QWRs on a GaAs substrate. A typical self-ordering growth is shown in the AFM image on the left side. The TEM image shows a detailed structure of the QWR made by the V-groove method. This is the case where the V-groove is deep. The sharp bottom is reformed by the self-ordering process. (By courtesy of Dr. G.Biasiol in EPFL.)

such as a laser power, a property of resist, dry and wet etching condition and so on. EB (Electron Beam) lithography seems better in viewpoint of the stability for forming a mask, but it is disadvantageous for obtaining large patterns of a QWR array which are useful for a device fabrication. Productivity is also a parameter to be taken into account. Normally, due to fluctuations of those process parameters, V-groove's cross-sectional shape (depth, sharpness at bottoms, roughness of etched surfaces) varies every time processing is repeated. And thus, the regrown layers on V-grooves and resulted QWR's shape are also different at each time. Eventually it leads to the problem of reproducibility in QWRs, whose optical properties are demanded to be unchanged under the same growth condition for the device application. When we make DFB QWR lasers, matching of Bragg wavelength to a QWR gain profile is known to be very significant. And thus, it is naturally unfavorable that the gain profile peak falctuates so much every time we make QWRs. The same sharpness of V-grooves must somehow be supplied before the growth of QWRs in spite of uncertainity of supplied non-planar substrate's quality.

For this purpose, self-ordering process is effective (Figure 4-3). After the growth of GaAs or AlGaAs of a certain thickness, the bottom structure of V-grooves is automatically sharpen. In this process, the particular shape determined by a growth temperature and a material is obtained. We know that a composition of materials and growth temperature is controlled precisely in MOVPE system. This growth uses the orientation dependency of growth rate. If the growth speed of side walls of V-grooves is faster than the other oriented surface and their difference are large sufficiently, the sharpness of V-grooves is always restored at the bottom.

It is remarkable that this method is effective for the various non-planar structures (see AFM image in Figure 4-3). Only the buffer layer thickness needed for the self-ordering phenomenon is influenced by an initial structure. In Figure 4-3, because the first structure

is very different from the V-groove, it necessitates a thicker layer to recover a sharp V-groove on it. But the successive formation of QWRs needs a thinner buffer layer. In the actual formation of QWRs, The fluctuation of an initial V-groove's shape caused by the processing is normally not so large that it does not make a substantial difference in the self-ordering condition. Therefore, the conditions for a self-ordering growth is relatively stable.

Because controlling of the self-ordering growth is not so difficult as trying to copy the V-grooves only by the etching process, it is useful to apply it to innovate the quality of QWRs. Whatever V-grooes are prepared in the preceeding process, the same sharpness of V-grooves are always produced by using this self-ordering process. As a result of the stable formation of a uniform quality of QWRs, the design of Bragg wavelength accurately tuned at the expected wavelength of QWR luminescence become possible for the first time. It enables us to optimize the DFB effect in QWR lasers.

It is also applicable to stack multiple QWRs on V-grooves as is shown in Figure 4-3. Because the same V-grooves are repetitively formed after the growth of a QWR, multiple QWRs with the same optical characteristics can be piled by the simple repeat of one growth recipe. The maximum number of QWRs which can be stacked in one V-groove depends on its depth and the barrier layer thickness for self-ordering. It is known empirically that 3 or 4 QWRs can be formed in V-grooves for DFB lasers with a period of a few hundreds [nm]. As the improvement of optical confinement factor is significant in QWR lasers, its effect is not negligible for the application to devices even if its contribution is small.

The other notable technique is a planarization of V-grooves (Figure 4-4). It is achieved by a similar way to the self-ordering growth, but more easily than it. V-grooves depth is shallower every time we repeat a self-ordering growth. It means that V-grooves are filled and planarized as we grow materials on it. It is apparently more difficult to grow materials on non-planar substrates than planar ones. Hence, it is necessary to planarize the substrate in device structures before the growth of cladding layer and so on. It is also difficult to control the composition of compound materials with more than 3 elements on nonplanar substrates. When the lattice constant drastically varies by the composition materials, it causes a serious damage in the regrowth quality.

As for DFB lasers, it is useful to control index coupling in DFB lasers, too. If we planarize a waveguide by the same material as a waveguide after the formation of QWRs, index coupling is suppressed most effectively. On the contrary, we can actively introduce high index coupling by filling V-grooves with a different material. But the latter is basically difficult to practice other than in the GaAs/AlGaAs case where the lattice mismatch problem is negligible.

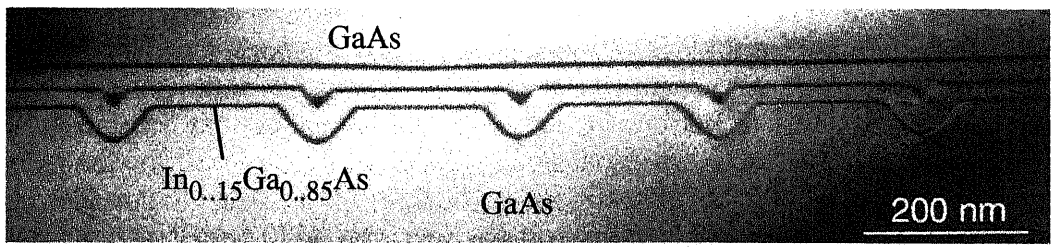

Figure 4-4 Planarization of V-grooves. The TEM image shows its process with InGaAs thin layers as markers in GaAs. Planarization is completed after the 3 setsof GaAs growth.

4-4 Formation of V-groove patterns

Though the V-groove quality is improved by the growth technique shown in 4-3, it is no doubt that the preparation of a high quality of V-grooves is also important. It makes it easier to fabricate QWRs and enables us to stack more QWRs in a V-groove. Several methods are available for the formation of grating with a period of a few hundreds [nm]. One is to use EB lithography and write directly patternes on a substrate. Although a drawn pattern is precise in detail, the patterned area is not large as is mentioned above. The counterpart of this method is a holographic method. It is disadvantageous in the uniformity and varieties of depicted patterns, but is frequently used to obtain a stripe pattern for the grating. Because it is a simple system, the stability and producibility is good. The pattern size drawn by one exposure depends on the optical components and laser properties used in the holography. But more than 1[cm^2] is easily achieved without losing uniformity. It is suitable for a massproduction.

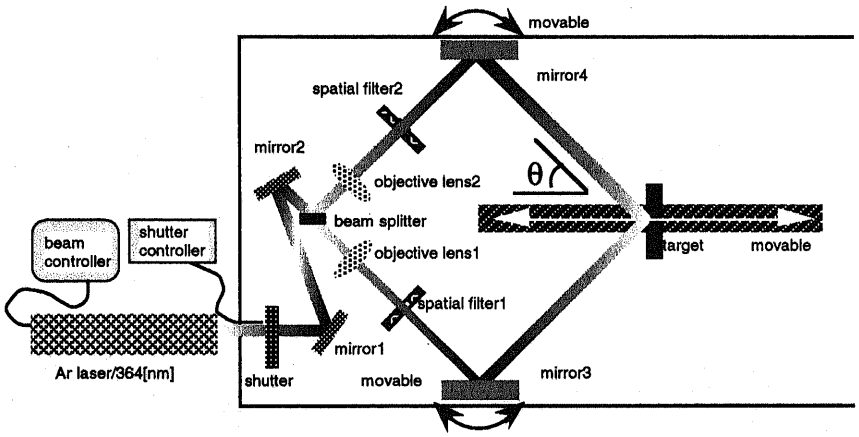

Figure 4-5 Holography system used for the formation of grating.

We use this holographic method for the formation of grating. The set-up is shown in Figure 4-5 (Ar laser 364[nm]; Spectra Physics 2065+Beamlok). This is so called 2 beam interference method which is said to be appropriate to obtain a large uniform patterns on a substrate because its structure is symmetric with regard to the target. The relation between grating pitch Λ and angle of incident lightwave θ is given as follows.

$$\Lambda = \frac{\lambda_{laser}}{2\sin\theta} \qquad (1)$$

The whole process to form a grating is summarized in Figure 4-6. Si_3N_4 is for the anti-reflection to avoid a standing wave effect in exposure and for the improvement of a mask pattern adhesion to the substrate. In this process the resist (AZ photoresist 5214) mask is used to transfer the grating pattern made by holography to Si_3N_4 layer. Because an opening ratio of the resist pattern is likely to be large, the resist pattern is reversed for the better adhesion of pattern to the nitride after the exposure by flooding of ultraviolet ray.

The cross-sectional SEM (scanning electron microscope) photo of a grating obtained by this method is shown in Figure 4-6. The grating was made on a GaAs substrate in $(0\,\bar{1}\,1)$ direction. The grating pitch was about 265[nm]. In our process a quarter of 2 inch wafer was used for one exposure. The quality of the grating was good enough to continue

a regrowth process for it. Next the cleaning process was another problem after clearing the stable formation of V-grooves. The etched surface of V-grooves observed by AFM (atomic force microscope) had many dots on it, which were left on the side walls and even on the bottoms (Figure 6-7). Those particles are said to be an oxidized GaAs originated from the wet etching process, but are still uncertain. Our solution for the wet etching was the mixture of surfaric acid, hydrogen peroxide, and DI water with the ratio of 1:8:80. The observation by AFM revealed that the density of these paticles decreased as we cleaned samples for a longer time in BHF (buffered HF). But it sometimes causes a destruction of surface when the sample contains AlGaAs layer near the surface. The density of particles left on the surface depended on wet etching conditions such as the proportion of mixture and the temperature of solution, too. In general, heating process in a MOVPE reactor has often been used to remove such an oxidized GaAs on the surface. But, in fact, it is even uncertain whether those particles are really harmful to the regrowth process or not.

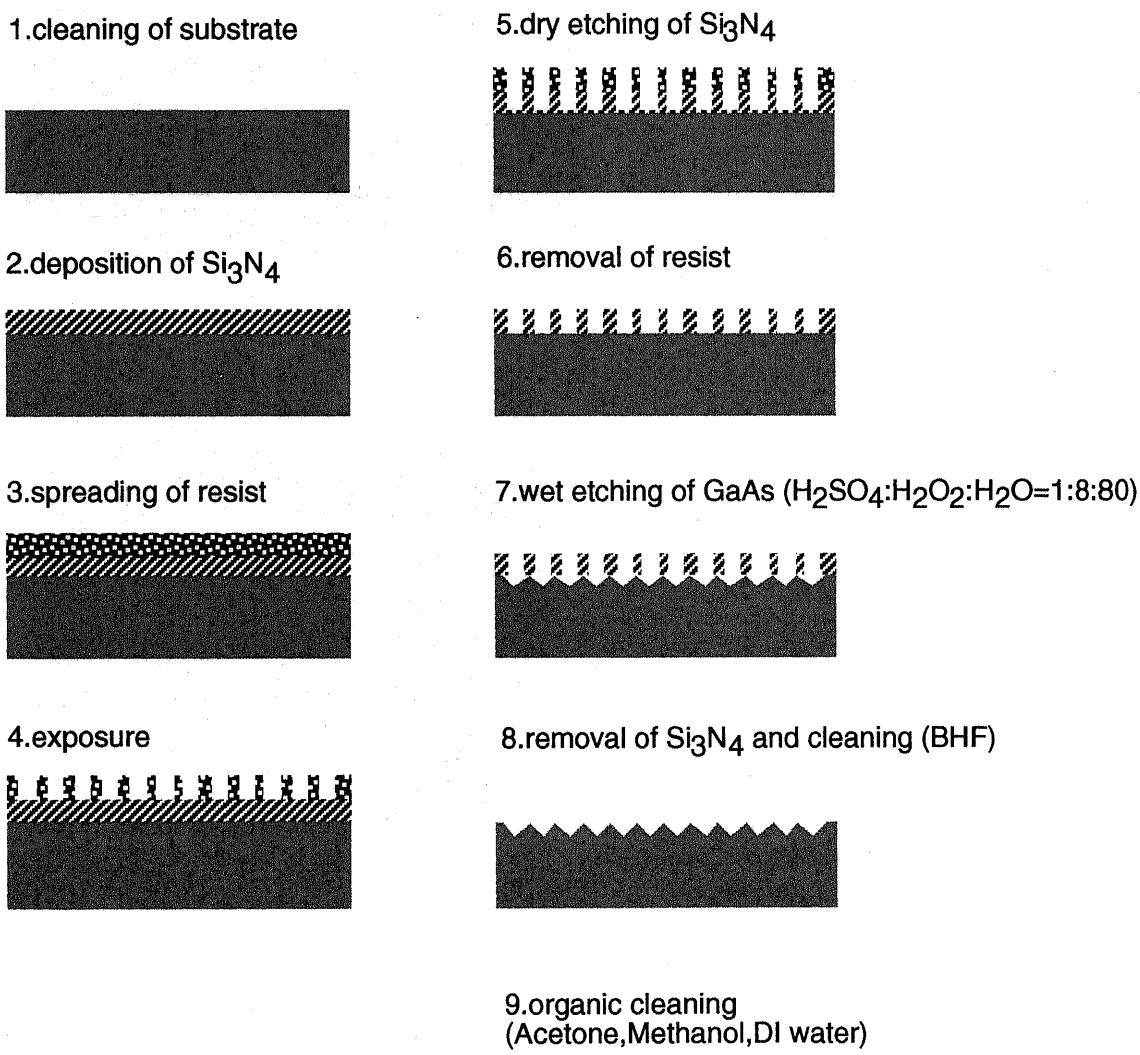

Figure 4-6 Patterning process of V-grooves on GaAs substrates.

Our V-groove had no flat part on top of it. It means that the mask tolerance against the solution was not so good as we had expected. Side etching by the solution was not suppressed effectively by using Si_3N_4 as a mask material. It was considered rather due to the poor quality of our Si_3N_4 used in the process. The non-uniformity of the grating is unfortunately enhanced in such a situation. And the top of V-grooves is also rough. The damage in a nitride mask after the dry etching process was also a possible cause in this result. However, we could regrow QWRs and the successive laser structures on those V-grooves with the help of self-ordering process.

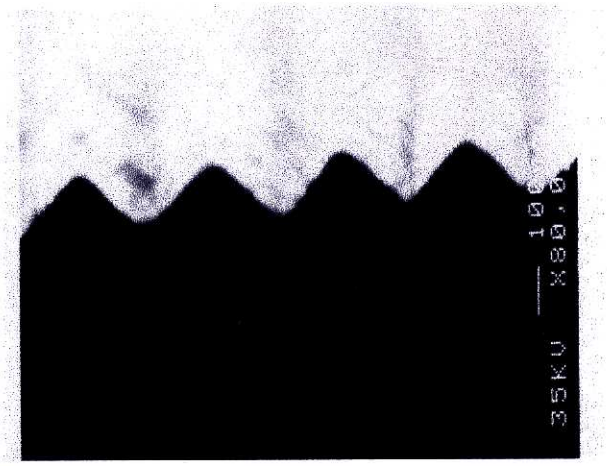

Figure 4-7 V-groove structures fabricated by the process shown in Figure 4-6. The grating pitch was about 265 [nm]. Etched in sulfuric acid solution for 16 [sec].

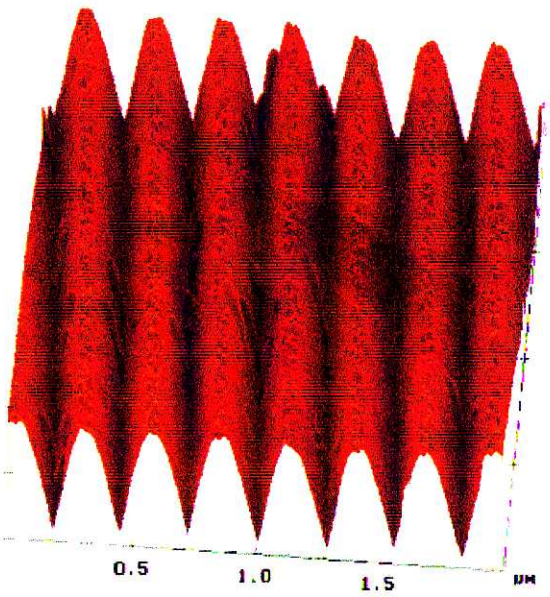

Figure 4-8 AFM image on the V-grooved substrate. The ridge of V-grooves were rough due to overetching. The particle-like roughness was also found on the side wallsof V-grooves.

4-5 Design of DFB lasers

A matching of Bragg wavelength to QWR's gain profile is the most significant in the design of QWR DFB lasers. It is not only because it is related with the achievement of DFB mode lasing from QWRs, but also because laser properties such as a linewidth

enhancement factor is also affected by the relative position of Bragg wavelength in the emission profile. But now we take only the former into consideration.

Especially at low temperature the emission profile is so narrow and sharp that the design of Bragg wavelength is very critical with respect to the precise control of a grating fabrication. We must definitively adjust the grating pitch by refering to a stopband of DFB cavity experimentally. Because structural parameters like an effective index is needed to estimate Bragg wavelength, experimental correction is indispensable. To know the position of stopband it is necessary to make lasers with its Bragg wavelength overlapped with emission profile of QWRs or QWLs in our case. Either is enough to know where to find Bragg wavelength. Therefore, we design our laser at first for an approximate tuning of Bragg wavelength to the emission profile of QWRs and QWLs.

The effective reflective index of the first TE mode in a waveguide was evaluated to determine a grating pitch. The lower Al concentration (50%) of AlGaAs was assumed as a material of a cladding layer because of the easiness of regrowth on a non-planar substrate. The higher Al concentration of AlGaAs was still difficult to be grown at that time. From the point of view on the confinement factor, it would be better to use a symmetric structure. Figure 4-9 is the effective reflactive index which is calculated assuming a simplified symmetric structure composed of 3 layers. The waving active layer in a waveguide was so thin that its contribution was judged to be negligible.

A waveguide as thin as 200[nm] is desirable for a high confinement factor. But the waveguide as thick as twice a depth of V-grooves is needed at least for the formation of V-grooves. The additional thickness by a self-ordered growth and a planarization must also be taken into account. And making V-grooves too close to AlGaAs layer causes the problem of cleaning in BHF stated in the last section. Considering these reasons, we cannot use as thin a waveguide as we want. Our first sample structure is shown in Figure 4 -10.

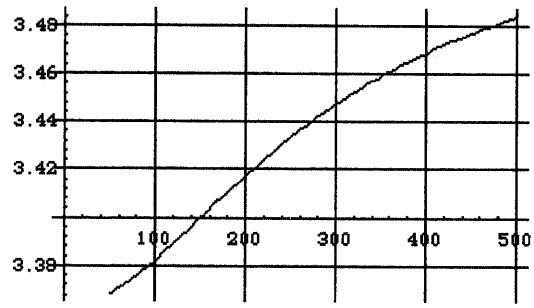

(a)

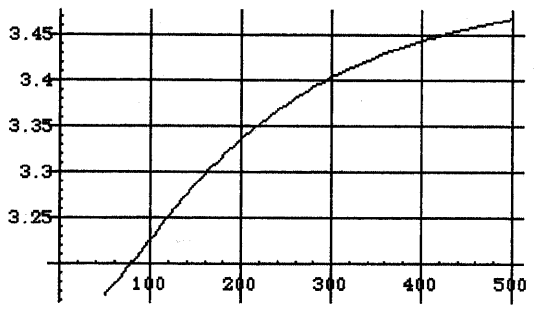

(b)

Figure 4-9 Expected effective reflactive index of a laser waveguide. (a) GaAs with infinite AlGaAs of Al=53% cladding layers on both sides and (b)Al=70%.

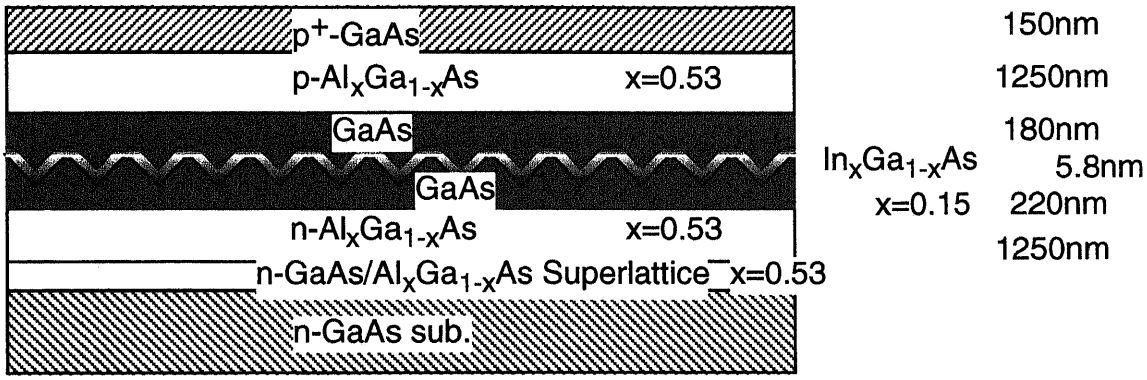

Figure 4-10 Longitudinal layer structure with QWRs. Its Bragg wavelength was detuned from the gainof both parastic QWLs and QWRs. Grating pitch was set at 265[nm].

The first growth on a substrate is done until the 3rd layer. The 3rd layer's thickness is 300[nm] and serves as a lower part of the waveguide. And then after making the V-grooves of 100[nm] depth, we grow the upper laser structure constituted of InGaAs QWRs, a waveguide, a cladding layer, and a capping layer. The values shown in Figure 4-10 are the nominal thickness which is measured on the reference sample. The reference sample is just a planar substrate which is grown together with laser samples. Though the waveguide thickness is thinner than the simple summation of each layer, this lasers's wavegide is evidently thicker than 200[nm]. But we can place QWRs in the center of waveguide instead of that and it is difficult to say simply that it is a disadvantageous condition.

The thickness of a waveguide is necessary for the determination of effective reflactive index. But it cannot help but being ambiguous because it is grown on a nonplanar substrate. Therefore, considering an error of this ambiguity, we assume that the waveguide thickness is about 400[nm]. By using Figure 4-9, the Bragg wavelength was estimated as 919[nm] supposing that the grating pitch is 265[nm]. And 936[nm] for 270[nm] of grating pitch. We compare this value with the experimental data on PL peak wavelength accumulated about the InGaAs QWRs grown on GaAs V-grooved substrate (Figure 4-11). Most data were measured on samples which has QWRs sandwitched by undoped GaAs. It also contains the data obtained from EL (electricluminescence) and PL (photoluminescence) spectrum of samples with a laser structure. Its laser structure is what is designed in Figure 4-10. The points filled with color are the data measured on PL spectrum. QWR luminsecnce at 935~945[nm] for 6[nm] thickness of growth layer is shown in this figure. As for QWL, 912[nm] is given. Therefore, above first grating pitch is supposed to be matched to QWLs, and the second to QWRs. It concludes that 270[nm] is needed for matching of Bragg wavelength to the QWR gain. It also tells that a grating pitch must be controlled within the precision of 5[nm] in our lasers. It is not easy to achieve such a control without calibrations.

At first, it is interesting to check whether lasing happens from QWLs or not when stopband of DFB cavity (or Bragg wavelength) is completely detuned from gain profiles of both QWL and QWR. Another meaning to carry out an experiment by using such a sample is to know how QWL and QWR gain behaves under the current injection.The layer structure influences so much on the luminescence characteristics. It is valuable to investgate differences between optical excitation (like PL) and carrier excitation (like EL). Actually what is more important for making QWR lasers is the latter characteristics.

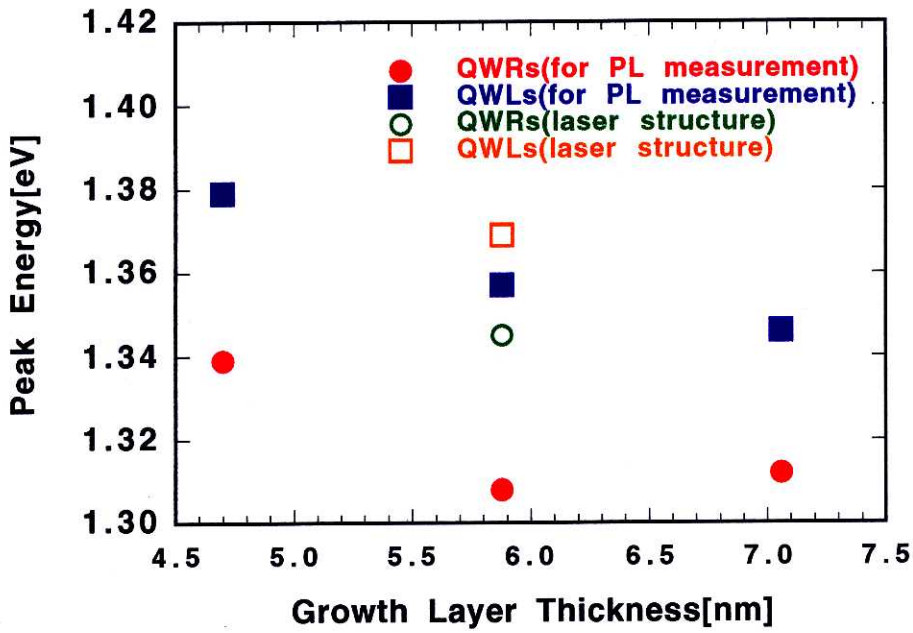

Figure 4-11 PL & EL luminescence peak wavelength of strained InGaAs QWR array with 0.25 μm grating pitch. Horizontal axis means a layer thickness measured on a planar reference substrate grown under the same condition.

One thing to be mentioned about the laser structure in Figure 4-10 is that the PL wavelength of QWR is blue-shifted comparing with other samples. It is explained by a thermally induced intermixing during the successive growth of a cladding and capping layer. Though this phenomenon is observed in both QWL and QWR luminescence, the shift of QWR is much larger because of its sensibility coming from its smaller volume. These different shifts of QWL and QWR leads to a decrease of separation of QWL and QWR gain peaks. Hence, we must remember that the precision demanded for Bragg wavelength design is more critical in actual laser structures.

4-6 Fabrication of QWR lasers on nonplanar substrate

Broad area lasers (stripe width 100[μm]) with its cavity vertical and parallel to QWR array were fabricated. In this section, we call them simply vertical type and parallel type respectively. The structure is shown in Figure 4-10. Bragg wavelength was much shorter than 900[nm] so that it worked as a FP cavity even in vertical type. QWRs were grown under the condition of 5.8[nm] in Figure 4-11.

The cross-sectional TEM photo of this sample is Figure 4-12. The formation of QWRs with 25[nm] lateral width and 10[nm] thickness is observed. Because the waveguide was insufficiently planarized after the growth of QWRs, a modulation of composition in AlGaAs layer is observed as a contrast in the cladding layer. It is so called vertical QWL. It is formed as a result of the difference of migration property of Ga and Al on V-grooves.

Because Al moves slower than Ga into the bottom of V-grooves, less Al concentrated AlGaAs appears vertically from the bottom of V-grooves. The waveguide thickness was about 230[nm] which reduces effective index so as to shift Bragg wavelength to a shorter wavelength. This modification is due to the unexpected stop of growth of above waveguide. The insufficient planarization was also a result of this accident. But an increase of confinement factor may be expected in this structure instead of that thanks to a narrower waveguide.

PL spectrum at 8[K] shows that the laser structure really contains QWRs and parasitic QWLs in it as is shown in Figure 4-11. It is plotted as Figure 4-13. Points indicating 'laser structure' in Figure 4-11 correspond to this sample. QWL's peak was found at 905[nm] and QWR's found at 922[nm]. Their separation was only 17[nm].

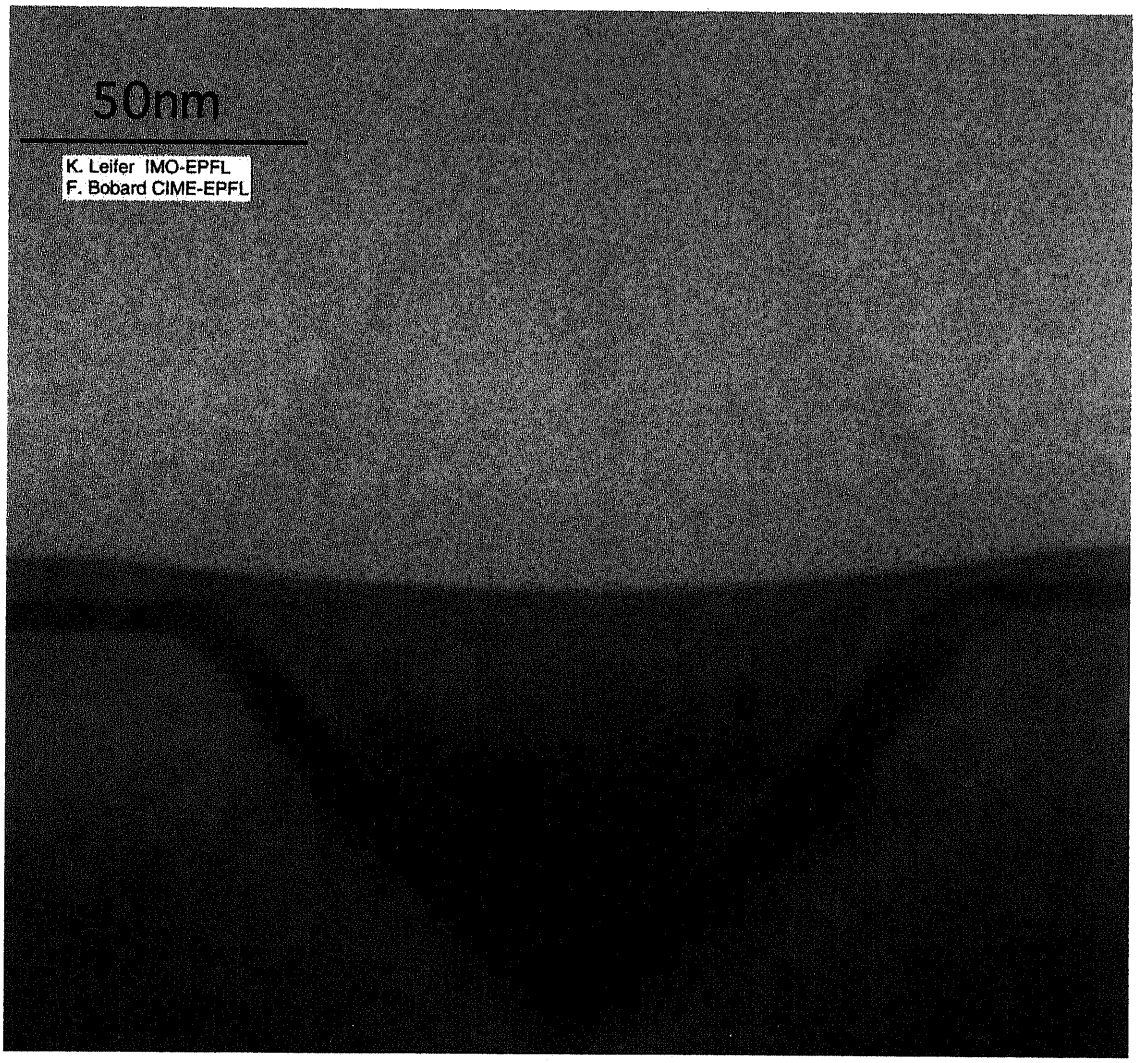

Figure 4-12 Cross-sectional TEM image of a strained InGaAs QWR array made for the lasers in Figure 4-10. The V-groove was not planarized completely and the weak contrast of vertical QWLs was observed in the AlGaAs layer. The shadow in GaAs was due to the strain.

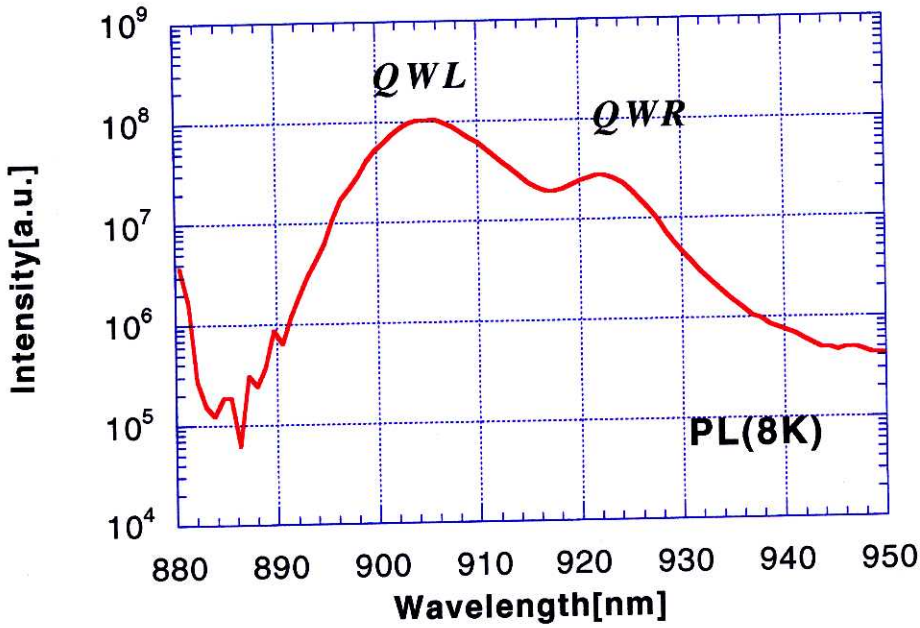

Figure 4-13 PL spectrum of the InGaAs QWR array shown in Figure 4-12 (at 8K). The left peak is QWL, and the right peak is QWR. The luminescence appearing below 880[nm] comes from GaAs of the waveguide.

EL spectra were measured on both vertical and parallel type of lasers with about 500[μm] cavity length. Pulsed current of 1[kHz] and 1[μs] was injected. At low injection current, we can distinguish 2 peaks which evidently comes from QWL and QWR (Figure 4-14). Each peak was easily identified by comparing it with that of PL spectrum in Figure 4-13. Both are in good agreement with each other. Figure 4-14 shows spectra below threshold. No DFB effect can be seen, off course.

Though both are FP type lasers, anisotropy of EL spectrum between vertical type and parallel type was observed. it is clear by comparing the relative intensity of QWR luminescence against QWL at the same injection current. Because QWL is known to have no orientation dependency in its plane, we can make it as a standard to compare the QWR luminescence in both types. The QWR's intensity is stronger in vertical type than in parallel type. It is in accordance with the predicted anisotropy trend on the QWR gain. The modes whose electric field is parallel to QWR axis is amplified more effectively than the other direction. In our laser cavity, a permitted mode in the transverse direction is only the lowest TE mode. The TE mode in the vertical type corresponds to one parallel to QWRs. On the other hand, the TE mode in the parallel type is perpendicular to QWRs. And thus, ASE (amplified spontaneous emission) was stronger in vertical type. To make it clear quantitatively, the intensity of QWL and QWR luminescence and the peak wavelength of both in each spectrum were extracted by fitting a gausssian spectrum to them. The dependence of relative intensity (QWR intensity normalized by QWL intensity) and peak wavelength are shown in Figure 4-15 for both type of lasers. Intensity ratio in Figure 4-15 was defined as the proportion of relative intensity for vertical type and parallel type. We comment here that the results of this figure were consistent in all the measured samples.

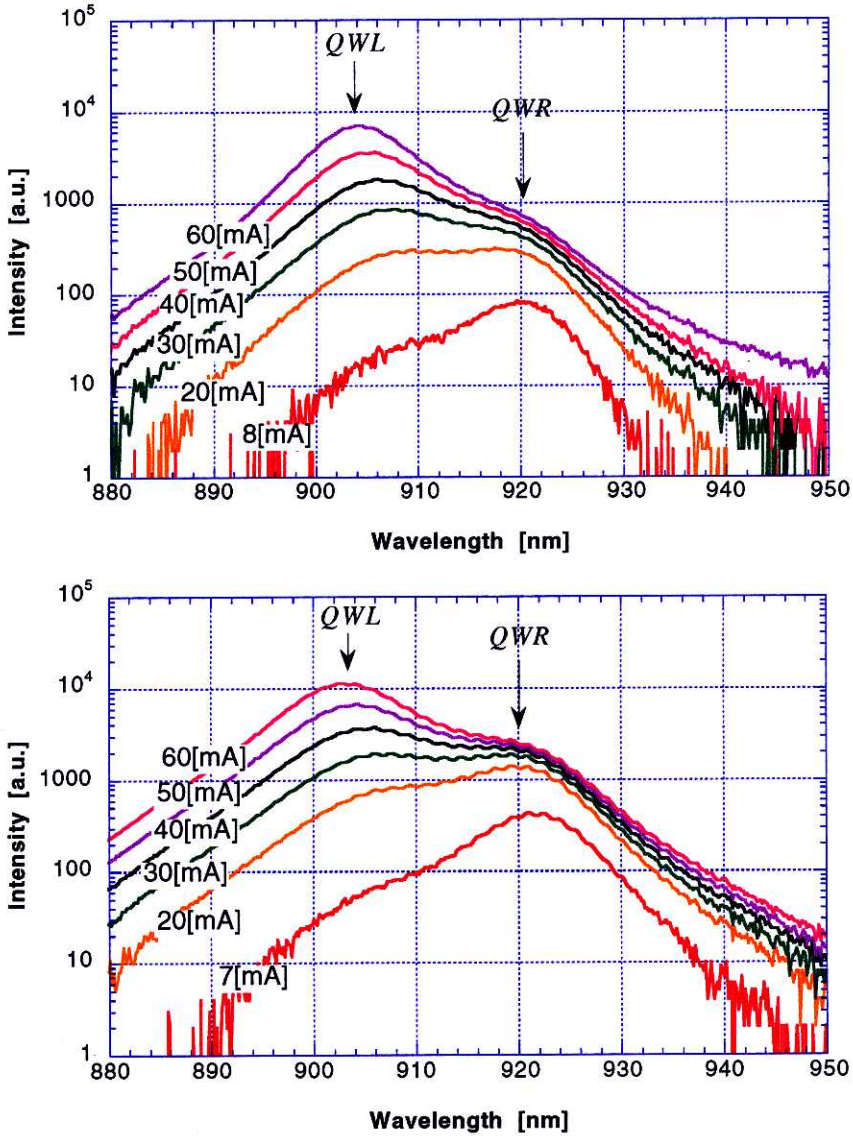

Figure 4-14 EL spectrum of the sample in Figure 4-12 below threshold current (at 70K)(above: parallel type, below: vertical type). Note that each peak position is in good agreement with that of PL spectrum. At low injection current QWR emission was dominant in both cases.

Points at low injection current for QWL in Figure 4-15 are not very correct because QWL intensity was weak and curve fittings precision were ambiguous for them. Pea wavelength shows a good agreement between 2 types of lasers though it is natural because they were made from the same substrate with their orientation of stripe different. Relative intensity of QWR quantitatively shows the anisotropy of QWR emissions in those samples. We assumed that QWL has no orientation dependence in its plane as is reported in many papers on the QWL properties, and thus we normalized QWR intensity by QWL intenity to avoid the diversity of particular smaples. Anisotropy appeared as a stronger intensity in vertical type in this figure, too. And its intensity ratio varied from 2 to 1.6 by changing the injection current. QWR's gain saturation occurred at relatively low injection current (around at 15[mA]). The change in anisotropy is probably due to this

saturation in QWRs and as a result of more contributions from the higher states filled along with the saturation leads to the dissipation of QWR properties.

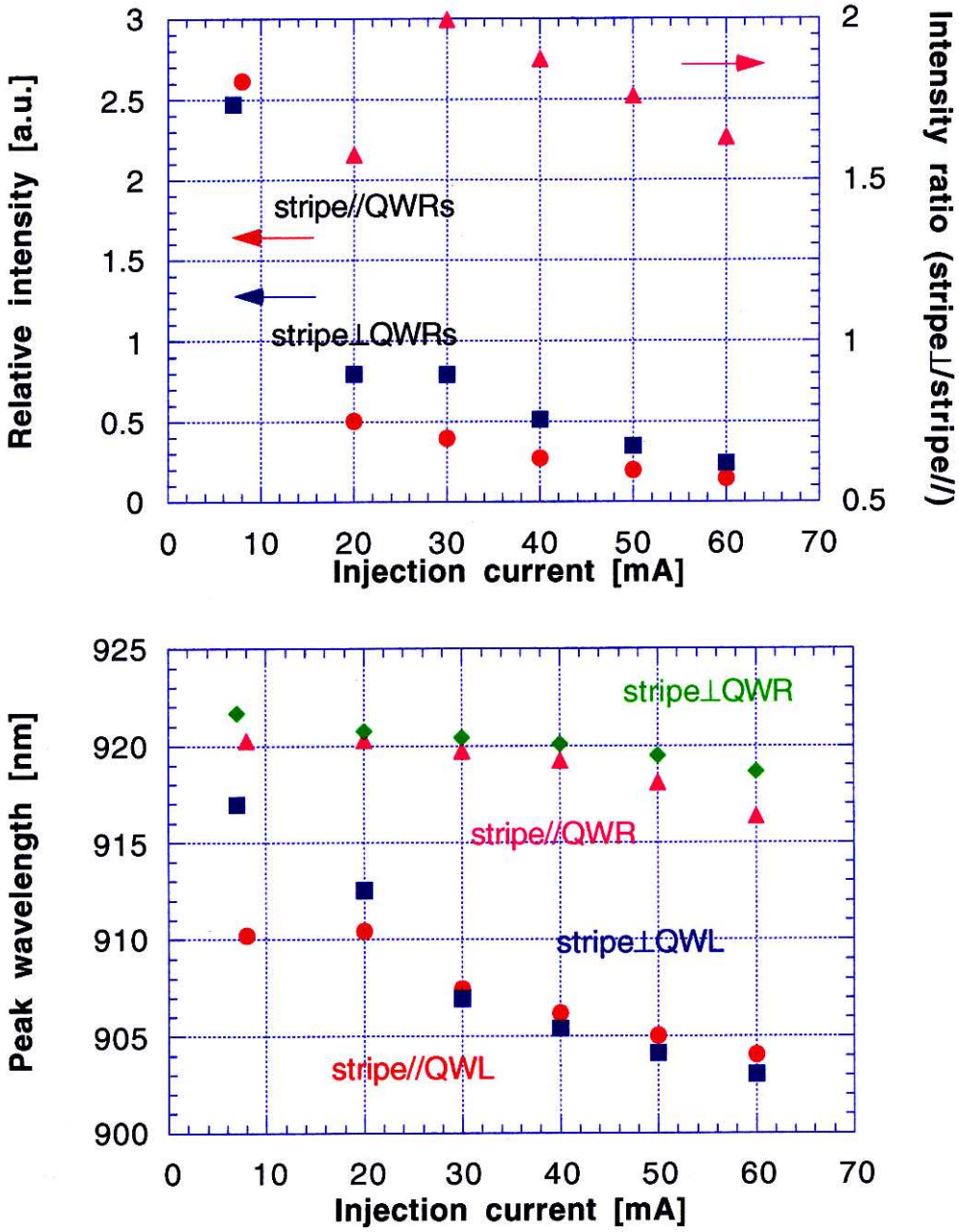

Figure 4-15 Anisotropy of QWR emission, and peak wavelength variation by injected current which is deducted from the EL spectrum (Figure 4-14) of vertical and parallel typesof QWL lasers containing QWRs. Relative intensity is a normalized QWR intensity by that of QWL. Intensity ratio is a relative intensity of vertical type divided by that of parallel type. The points at low injection current are beyond precision except for its sign because of QWL's too small intensity .

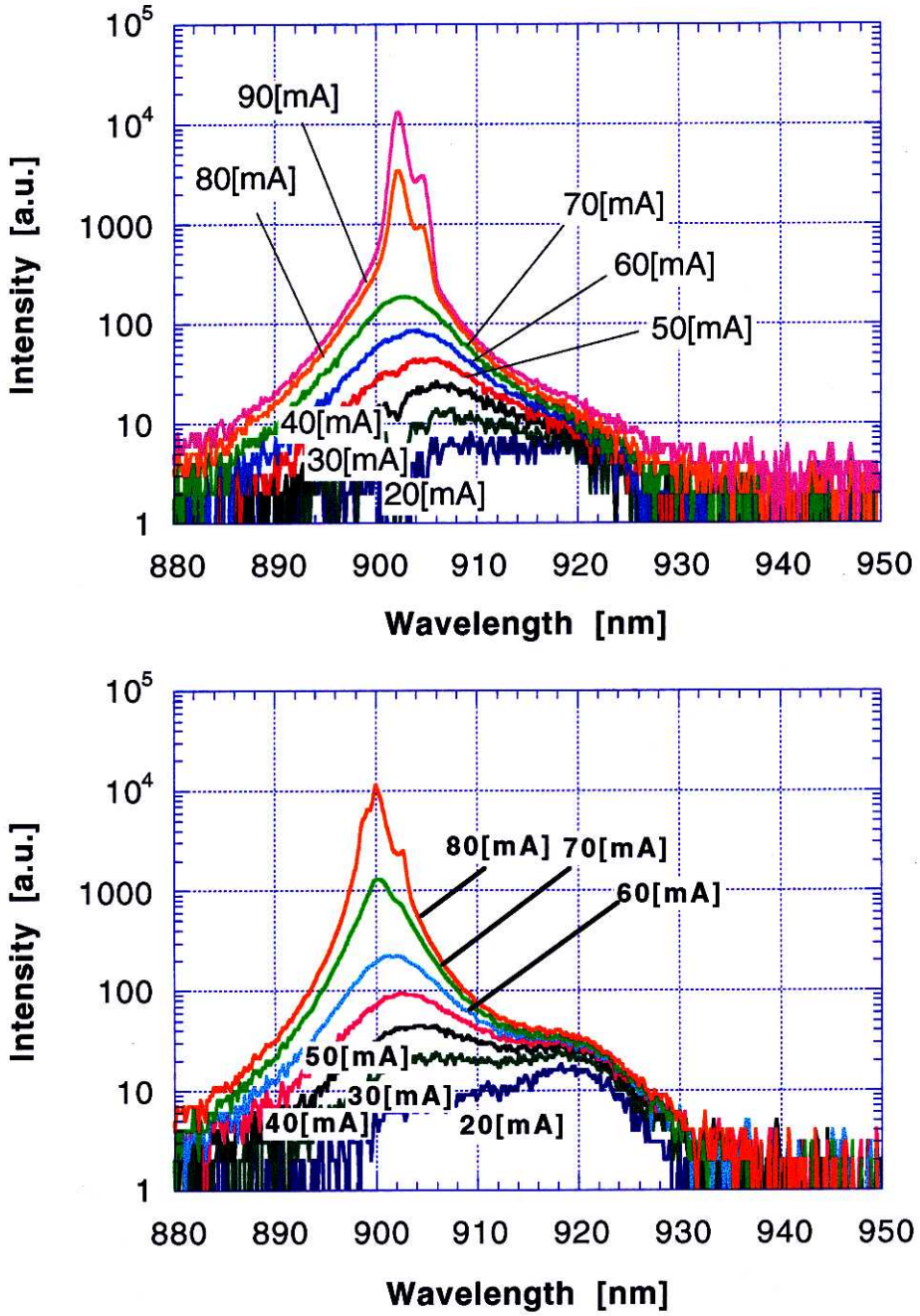

Figure 4-16 EL spectrum above threshold current (at 68K) (above: parallel type, below: vertical type). Inboth cases, lasing happend at last from QWL due to FP cavity.

The comparison of QWR with QWL in Figure 4-14 makes us notice another thing. At low injection current, QWR's luminescence is dominant. As we increase the current, it starts to be saturated and QWL's luminescence become stronger definitively. As a result, lasing occurs from QWLs in both types (Figure 4-16). It means that carrier capturing and recombination is effective in QWRs, but that its amplification is not enough to achieve a lasing operation in this cavity. It was a defect of QWR coming from its small volume, which is often argued in this field. But it is important that QWR's luminescence occurs at

first in the laser cavity in spite of the coexistence of QWLs. And the reduction of optical loss in a cavity is effective for a laser operation from QWRs. Apparently one possibility to improve optical losses in the cavity at a wavelength of QWR's luminescence is to use a DFB cavity.

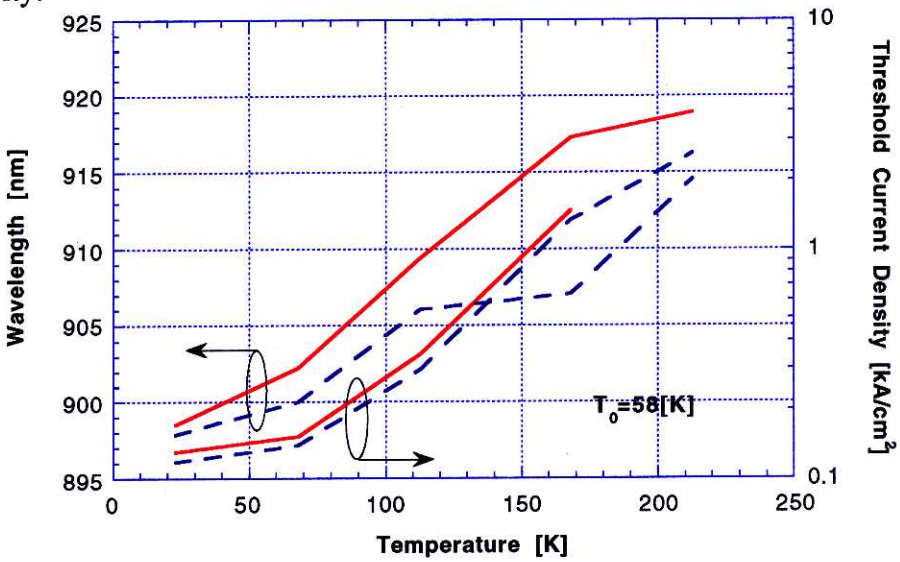

Figure 4-17 Temperature dependence of lasing wavelength and threshold current for vertical (dashed line) and parallel configuration (solid line). Lasing came from parasitic QWLs for both cases. The characteristic temperature was very poor and was about 60[K]. It owes to the poor regrowth quality and a large carrier loss in the cavity by the competition of QWL and QWR emission.

Lasing was observed up to 210[K] for both types of laser. Threshold current density and wavelength variations against temperature are plotted in Figure 4-17. A slight difference between both types would be owing to the difference of cavity direction. For instance, the loss due to a second order grating in the DFB cavity and the difference in effective reflactive index. In the vertical type the apparent mode hopping was also observed at 170[K] because the laser stripe is broad. Considering that fact, the overlap of both types in lasing wavelength and threshold current density is almost certain. It proves again that their lasing comes from QWL which has an isotropic gain in the plane.

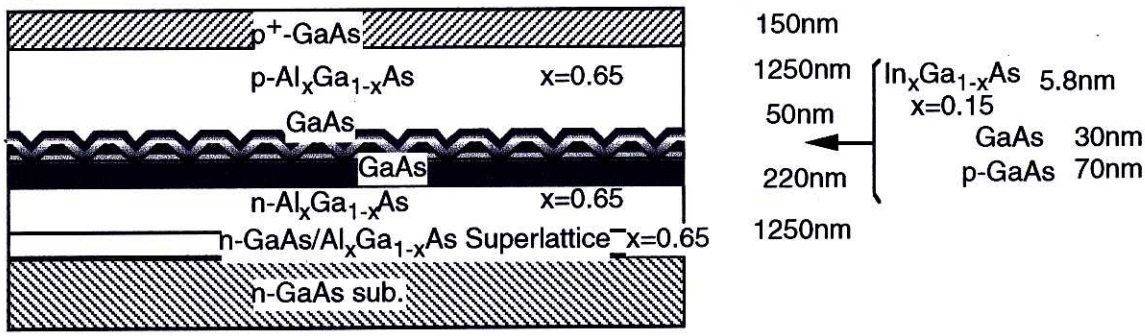

Figure 4-18 Longitudinal layer structure for DFB lasers using QWR array on V-grooved substrates. The grating pitch was set at 274[nm] so that Bragg wavelength matches to QWR gain.

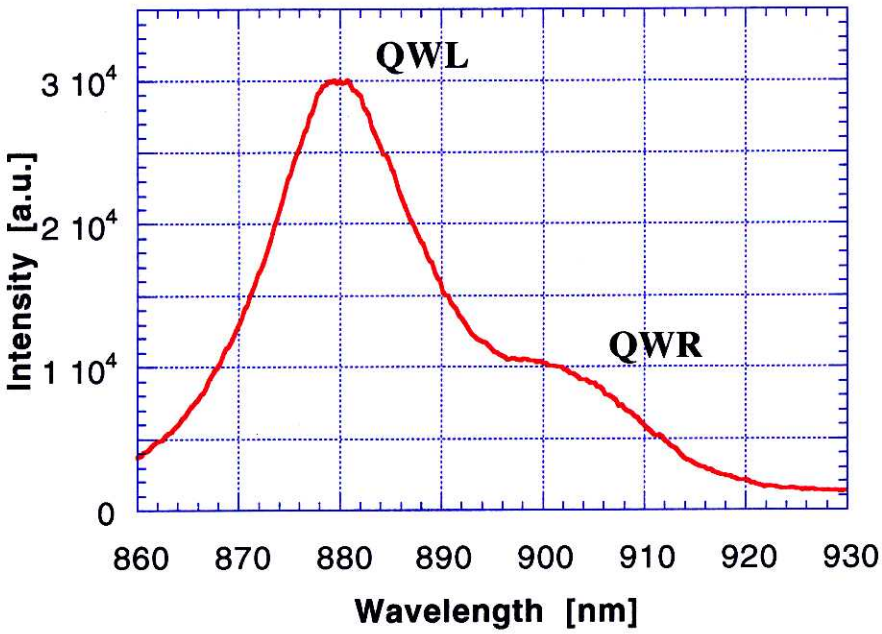

Figure 4-19 PL spectrum of DFB QWR lasers whose structure is shown in Figure 4-18 (measured at 77K from a facet of the sample whose cavity is perpendicular to the QWR array).

4-7 Fabrication of QWR DFB lasers

It was proved in the last section that mathing of Bragg wavelength is needed to fabricate DFB QWR lasers. In addition to this, higher confinement factor and index coupling is expected to play an important role to help the achievement of lasing in QWR DFB lasers. New laser's structure improved in those points is shown in Figure 4-18.

The grating pitch is increased so that Bragg wavelength overlaps with the QWR gain. The concentration of Al is now 65% to strengthen the contrast of material's reflactive index. The previous structure had an almost flat cladding layer on top of a waveguide. But this time a strong index coupling was incorporated by growing the cladding layer on nonplanar substrate. The incresed Al composition also contributes to a higher confinement of the lightwave into a waveguide. A high index coupling is useful to reinforce the selectivity of a lasing wavelength, effectiveness of feedback of lightwave, and suppression of undesirelable emissions by a wider stopband.

Another new important structure is a barrier layer of p-GaAs inserted in a lower waveguide structure before the formation of V-grooves. It is removed away during the wet etching process of V-groove formation, and thus this layer does not exist around QWRs formed in the bottom of V-grooves. But it is left below QWLs formed on the ridges of a V-grooved structure. Hence, it works as a barrier against only parasitic QWLs.

PL spectrum was measured for the sample with such a structure at 77[K] from the edge of braod area lasers of vertical type (Figure 4-19). Only the vertical type was fabricated for this structure. The stripe width was 100[μm], and the cavity length

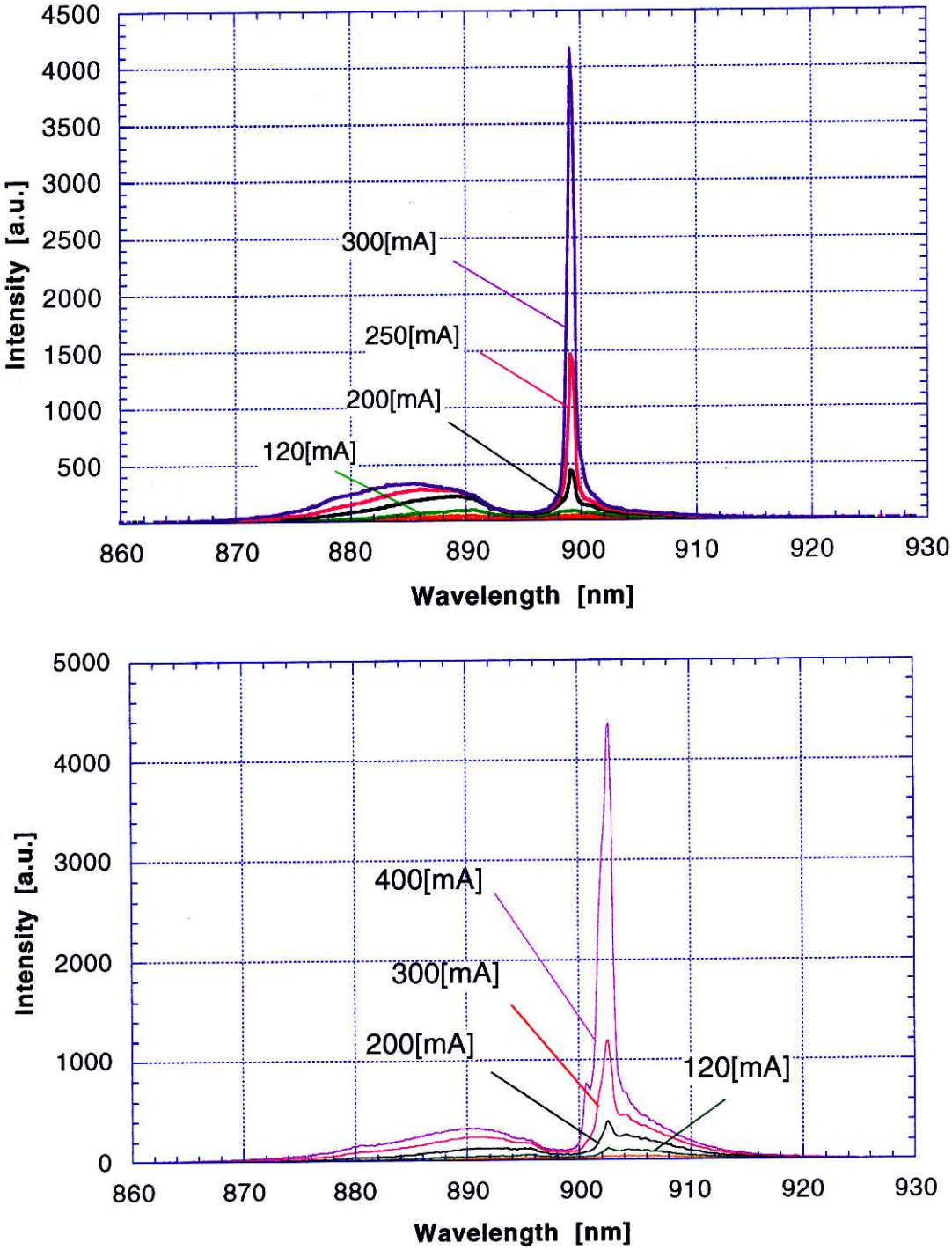

Figure 4-20-1 EL (lasing) spectra measured at various temperature (above:20[K], below:80[K]). Lasing occurred from a QWR side due to the DFB effect. The stopband is not obvious at these temperature because the lasing mode overlaps with the QWR emission peak and rather on its longer wavelength side.

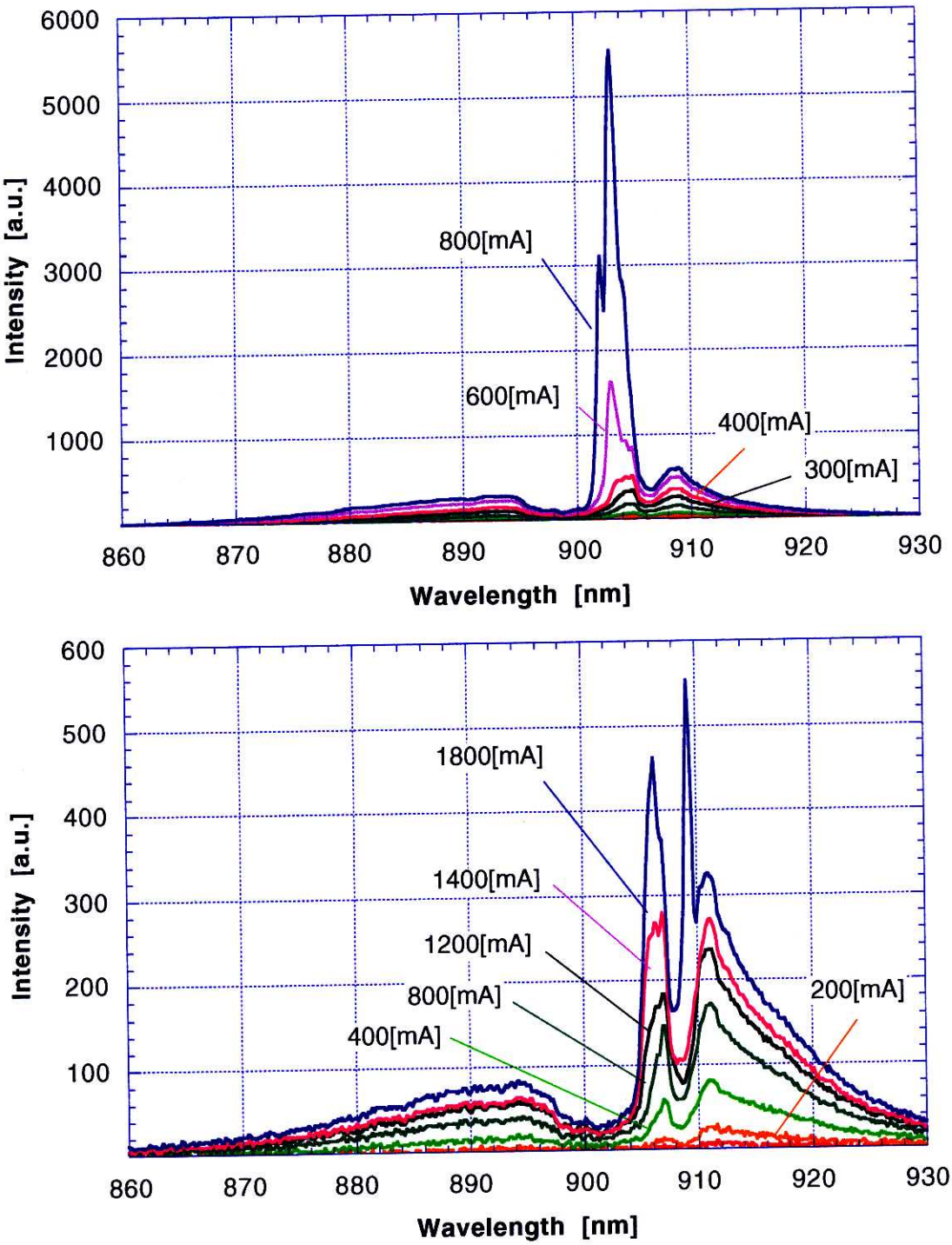

Figure 4-20-2 EL (lasing) spectra at various temperature (above:105[K], below:145[K]). The stopband is oberved in above figure on the right side of a lasing mode. Because the emission peak from QWR moves toward the longer wavelength at the higher temperature, it appeared at 105[K]. At 145[K], because the first peak is far from the gain of QWR, another DFB mode on the longer wavelength side is lased.

was 500[μm]. EL spectra measured for this sample with varying the temperature from 20[K] to 150[K] were Figure 4-20. The difference in spectrum from the previous lasers in chapter 4 is obvious at a glance. The emission from parasitic QWL is suppressed effectively and looks even strained due to the incorporation of strong index coupling. Lasing occurs from the side of QWRs at measured all the temperature. A stopband was found on the right side of a lasing mode in the spectra above at 85[K].

The big hole on the left side of a lasing mode is not a stopband. Its width is much broader than the estimated value of 3.7[nm], or 142[cm^{-1}] in index coupling constant calculated assuming a triangular grating. It is explained as an extra loss resulted from coupling to radiation modes accompanied with a strong index coupling[6]. As we increase the temperature, another peak appears on the left side of a lasing mode. It is the peak corresponding to a QWR gain. The lasing behavior distant from the gain peak with a stopband is permitted only as a DFB mode in the DFB cavity. Considering that lasing at this wavelength was not achieved in the FP laser in the last section, it must be a DFB mode, and not a FP mode from a higher state of the QWR. Thus, this experiment proves that the laser operation as a DFB QWR laser was achieved. Finally we refer to the temperature dependence of lasing wavelength in Figure 4-23. The laser fabricated in this section shows a smaller dependence (0.05[nm/K]) on temperature up to 150[K] than that fabricated in section 4-6 (0.092[nm/K]). It reminds us that the laser (vertical type) fabricated in section 4-6 was operated as FP QWL lasers. The value of 0.05[nm/K] is not so bad a value as a DFB lasers (0.022[nm/K] in [1]: The difference comes from the higher threshold current of our lasers) and it is impossible to expect such a stability of lasing wavelength for FP lasers. Hence the mode observed in Figure 4-19 are concluded as a DFB mode.

But we carefully continue this discussion to attribute this lasing to the QWR. It is still questionable which of QWL and QWR is dominant in the contribution to lasing. Because the separation between QWL and QWR is not so large, the overlapping of both gain is considerable naturally. To contradict this question, the realation of the stopband and lasing mode is useful. As we explain it in chapter 2, its relation depends on the phase of index coupling and gain coupling. From the laser structure in Figure 4-18 its relation is in-phase if lasing happens from parasitic QWL. If it is QWR, anti-phase is realized. Therefore, lasing occurs from a longer wavelength side of stopband in the case of QWL and a shorter wavelength side in the case of QWR. Because the lasing mode of above laser is found on the shorter wavelength side, it proves that above laser is operated as a QWR laser.

Though the result stated in chapter 2 is well proved to be true by many experiments on ordinary DFB lasers, it become another proof of QWR laser to check if the longer wavelength side is lased or not when Bragg wavelength is matched to QWL peak in our lasers. In Figure 4-21, the spectrum of the laser with such a structure is shown. 2 stopbands are found because both TE and TM mode is included in it. As is seen in Figure 4-22, the left hole corresponds to a stopband for the TM mode, and the right hole to a stopband for the TE mode. And lasing occurs as the TE mode because the gain for the TE mode is larger than the TM mode in QWLs. Hence, the spectrum in Figure 4-21 shows lasing of a DFB mode from the longer wavelength side of stopband in this QWL DFB lasers. It was exactly what was predicted for this laser structure by the theoretical result in chapter 2.

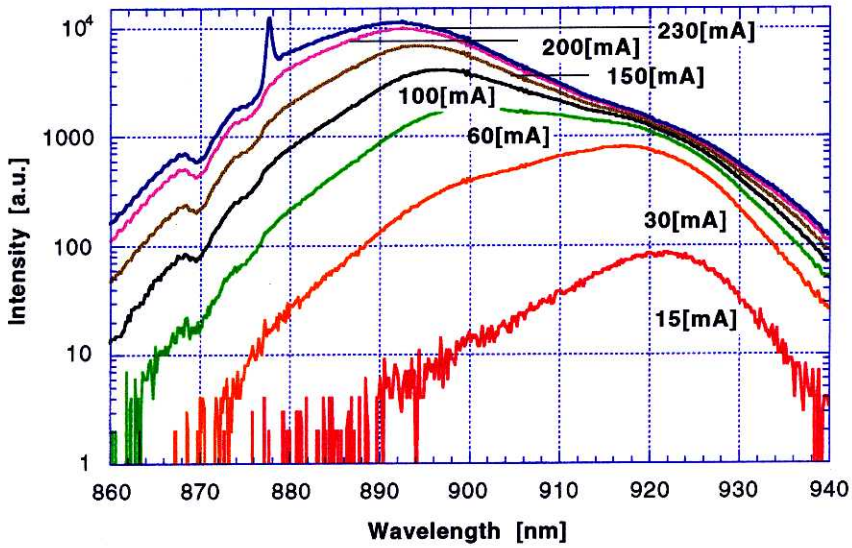

Figure 4-21 EL spectrum of the sample whose Bragg wavelength matches to QWL gain. The 2 stopbands for TE and TM mode are observed as is shown in Figure 4-22.

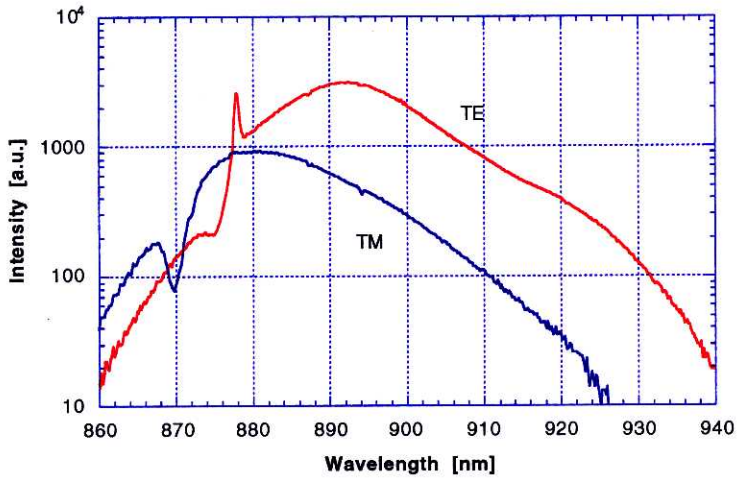

Figure 4-22 TE and TM component of the lasing spectrum shown in Figure 4-20.

One more proof is the variation of threshold curent density against temperatue. In FP lasers, it increases monotonously as the temeperature gets higher. Figure 4-22 is the temperature dependence of threshold current density of our QWR DFB lasers. Because a lasing wavelength is designed independently from the gain peak in DFB lasers, its temperature dependence is unique. In Figure 4-23, the threshold current decreases within the temperature from 20[K] to 60[K]. And it increases as usual more than at 60[K]. It is impossible to conprehend this phenomenon by a lasing from QWL. The gain profile of QWL moves to longer wavelength side as the temperature increases. Then, the better matching of Bragg wavelngth to QWL gain peak brings about the decrease of threshold current density at all the temperature shown in Figure 4-23. But it is not what happened in our lasers. Again it was concluded that lasing must come from QWR. Since the QWR

gain peak is on the shorter wavelength side of Bragg wavelength from 20[K] to 60[K], the increase of temperature improves the detuning of Bragg wavelength from the gain peak, and results the decrease of threshold current density in Figure 4-23. Above at this temperature, a matching of Bragg wavelength becomes worse, and thus the threshold current density starts to increase.

We just add the comment here that we could observe an improvement of carrier capturing in QWRs around at 80[K] when we measured the EL spectrum for the QWL lasers in 4-6. Its effect was observable at low injection current where the QWR emission was strong. A decrease in threshold current density shown in above figure may be explicable by this effect, too. But note that quite a high threshold current was needed due to the competition with QWL in our lasers. And such an effect which is valid only at low injection curent is negligible in our lasers

Lasing operation as DFB QWR lasers was observed up to 150[K]. Temperature characteristic is even worse than the QWL laser made in the last section. This is apparenrly owing to the unnecessary competition with parasitic QWLs and the poor quality of regrowth. The laser samples used in this chapter showed relatively worse quality than that proved in GaAs/AlGaAs QWRs. In this sense it seems that much better characteristics for QWR DFB lasers with the structure used in this chapter can be expected. But lasing operation at room temperature is impossible. Though it is significant that the operation of DFB QWR laser was achieved even under such a disadvantageous condition, this poor temperature characteristics must be improved by introducing a new type of QWRs on V-grooves.

4-8 Conclusion

By using V-groove method, we fabricated a strained InGaAs QWR array. It has been known that this method produces a good quality of QWRs for fundamental researches. Some good results were also obtained in the application to lasers, too.

Useful growth techniques are known as a background of the formation of such uniform QWR array. Self-ordering growth and planarization of V-grooves are those technique. We actually fabricated our laser structures making the best use of them.

At first, the preparation process of V-groove is mentioned. The 2 beam interference method was used in the exposure process, and we showed that excellent V-grooved substrate was prepared for the growth of QWRs on it. The substrate was GaAs, and QWR material was InGaAs. The compressively strained QWR was used to expect a larger gain for TE mode as is confirmed in the case of strained QWLs. In PL spectrum measurement, 2 peaks corresponding to QWL and QWR was clearly observed. One of the defects of the QWR formed by V-grooved substrate is the existence of this parasitic QWL.

The first laser was made to know how QWL and QWR behave under the current injection. For this purpose, Bragg wavelength was detuned intentionally from gain regions. The broad area laser with its cavity perpendicular and parallel to QWR array was lased under pulsed current injection up to 200K. Through this experiment following points were clarified.

- Better luminescence efficiency in QWR at low injection current.
- Lasing from QWL resulted from the saturation of QWR gain.
- Anisotropy of QWR emission in ASE.

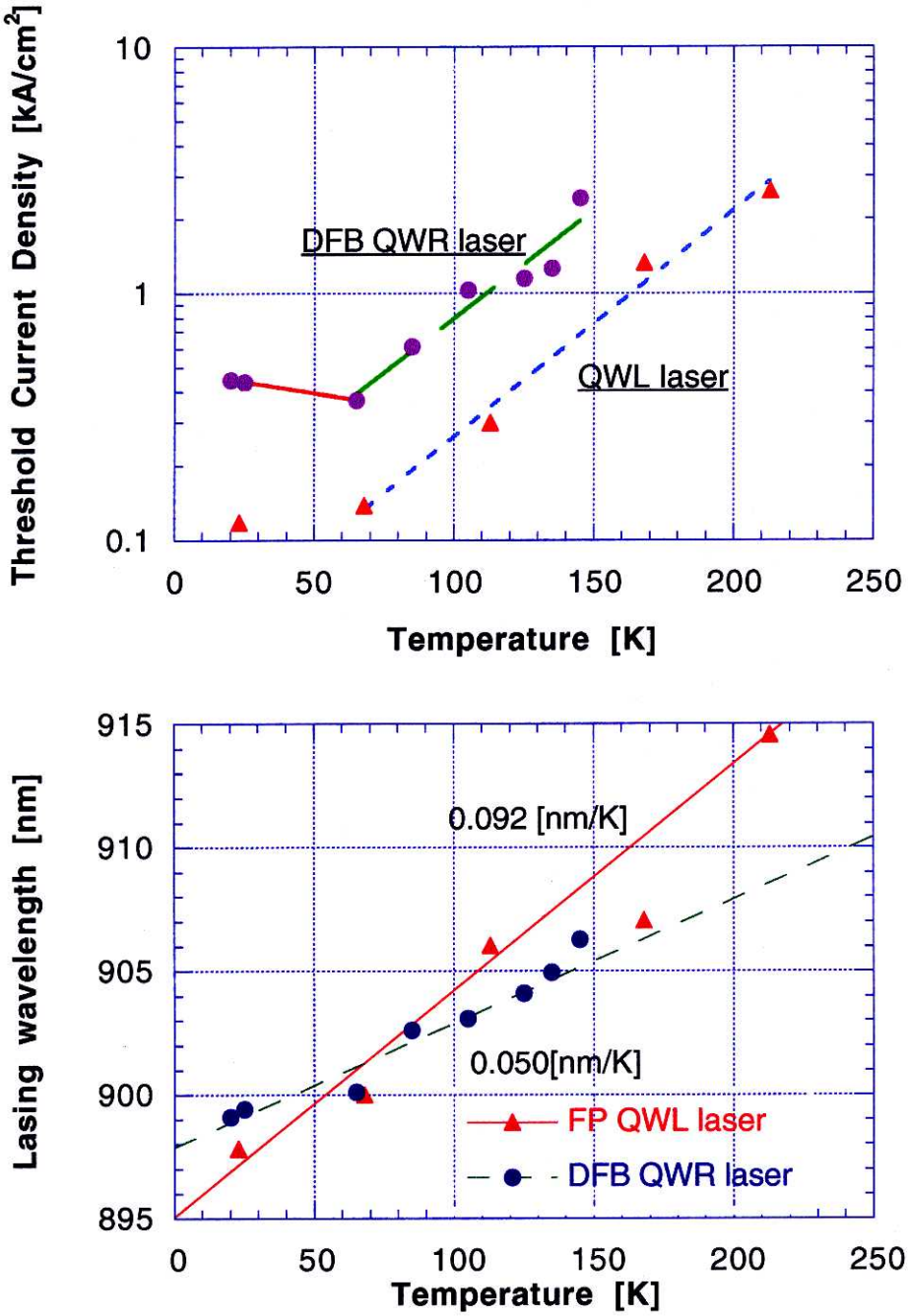

Figure 4-23 Temperature dependence of threshold current density of DFB QWR laser (above) and its lasing wavelength (below). DFB QWR laser is the laser fabricated in this section, and FP QWL laser is that discussed in the last section (vetical type). Both laser's stripe is directed parpendicular to the QWR array.

Based on above results, the broad area DFB laser whose Bragg wavelength matched to the QWR gain was fabricated. Its operation as a DFB QWR laser was observed from 20K to 150K. QWR luminescence was suppressed efficiently by the strong index coupling. It leaded to the loss in a cavity covering a wide bandwidth on the shorter wavelength side of the lasing mode (QWL gain region), which is resulted from coupling to radiation modes.

And the selective feedback of DFB cavity around at Bragg wavelength (QWR gain reagion) was also effective to compensate the cavity loss at the wavelength of QWR luminescence in the cavity. Lasing mode was confirmed as the DFB mode supported by the QWR gain by the followng reasons.

- Anti-phase mode of lasing operation.
- Decrease of threshold current density from 20[K] to 60[K].
- QWR gain peak appearence on the long wavelength side of a lasing mode at higher temperature (105[K], 145[K]).

Consequently, DFB QWR laser was successfully achieved by using strained InGaAs QWR array as active grating. It is also shown that DFB cavity was effective enough to support a lasing from QWRs even under the disadvantageous conditions such as a coexistence of parasitic QWL with the higher optical confinement factor and effective carrier capturing by its larger volume.

Reference

[1]M.Walther, E.Kapon, C.Caneau, D.M.Hwang, and L.M.Schiavone, "InGaAs/GaAs strained quantum wire lasers grown by organometallic chemical vapor deposition on nonplanar substrates", ApplPhys.Lett., vol.62, 2170, 1993.

[2]private discussion with Dr. E.Martinet at EPFL.

[3]S.Tiwari, G.D.Petit, K.R.Milkove, and F.Legoues, "high efficiency and low threshold current strained V-groove quantum-wire lasers", Appl.Phys.Lett., vol.64, 3536, 1994.

[4]A.Gustafsson, F.Reinhardt, G.Biasiol, and E.Kapon, "Low-pressure organometallic chemical vapor deposition of quantum wires on V-grooved substrates", ApplPhys.Lett., vol.67, 3673, 1995.

[5]K.Eberl et al. (eds.), "low dimentional structures prepared by epitaxial growth or regrowth on patterned substrates", Kluwer Academic Publishers, 291, 1995.

[6]V.Mizrahi and J.E.Sipe, "optical properties of photosensitive fiber phase gratings", IEEE J.Lightwave Technol., vol.11, 1513, 1993.

■ Chapter 5

Fabrication of InAsP QWR by mass transport method

5-1 Introduction

In chapter 4, lasing of DFB QWR lasers was demonstrated by using the conventional QWR array on V-grooved substrates. But it necessitated a low temperature for its operation. And several good features expected by the use of QWRs in such DFB lasers had to be sacrificed due to the extra competition with parasitic structures which are unavoidable in the above conventional way. What was new in those experiments was that lasing from QWRs was supportable by the DFB filtering effect even in such disadvantageous conditions and that a DFB cavity can contribute to lasing by the reduction of a waveguide loss, too. Though the decrease of QWR's density as in the DFB cavity in chapter 4 was believed to be definitively negative, the result in the last secton showed that it could be compensated with the particularities of the DFB cavity. And thus, a QWR array is applicable to improve DFB laser properties practically. For the next step to practical DFB QWR lasers, it is undoubtedly necessary to remove parasitic structures from the previous DFB QWR lasers stated in chapter 4, or may be much better to form only QWRs in the growth process from the first.

The most researchers' attention has been simply directed to the first idea, that is, the removal of parasitic QWLs. Because it seemed very difficult to grow only QWRs on V-grooves (especially with a small periodicity of sub-micron) selectively by the conventional growth scheme. That is one of the considerable reasons that has prevented them from paying their attention to the DFB lasers using a QWR array. Even in this simple approach, if a grating pitch of the QWR array gets smaller, the removal process of parasitic structures becomes more complicated. And it makes more difficult to keep the quality of QWR array, itself. Note that the method I in chapter 3 (etching of QWLs) was finally eliminated by the damage in QWRs in this papaers. Then, what method should we take for the improvement of DFB QWR lasers. First, we should understand that it is no more helpful to persist to the old method as has been applied to FP QWR lasers. It never produces better results than FP QWR lasers. A new method is needed for satisfying our purpose.

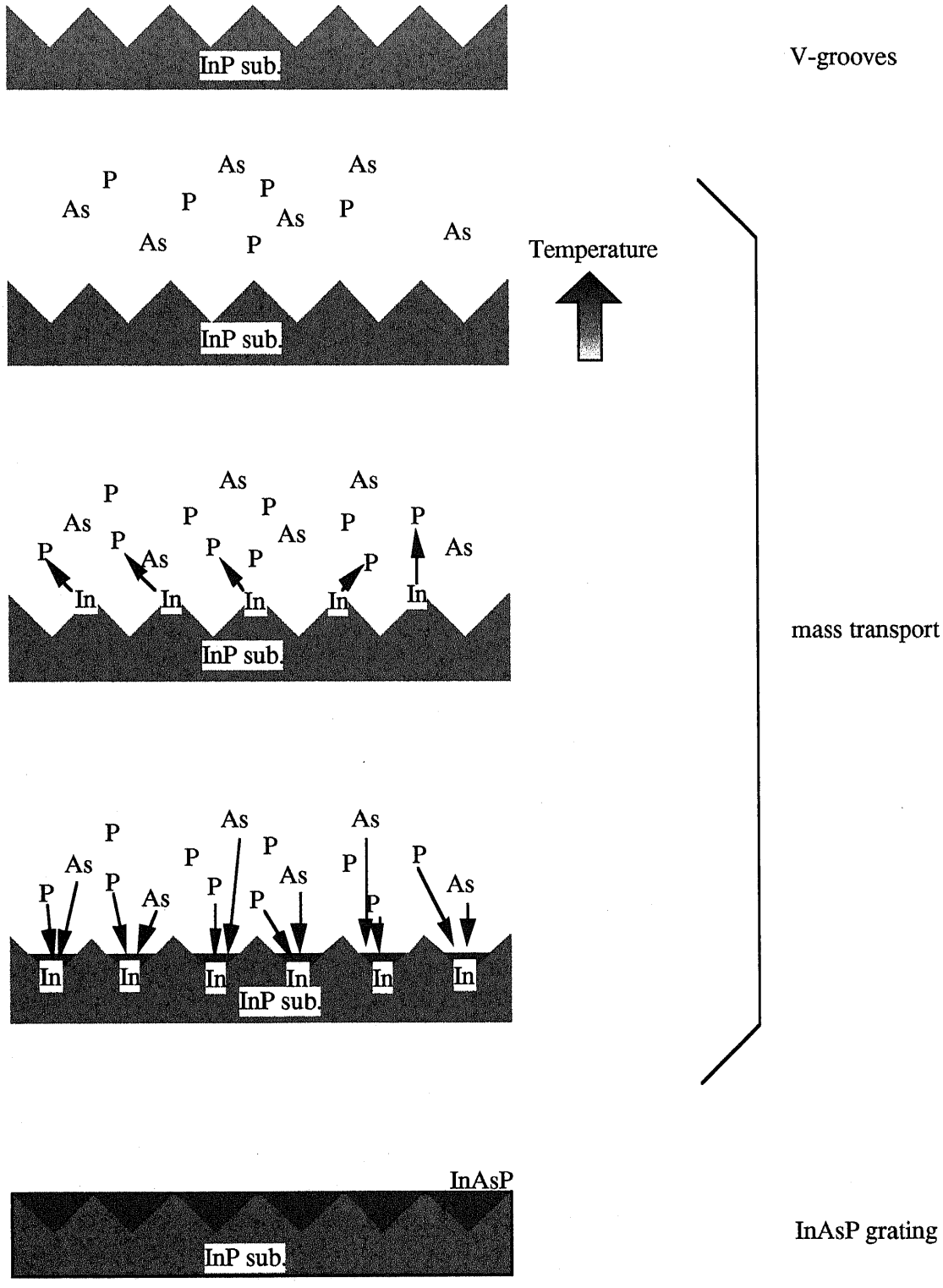

Figure 5-1 The conventional mass transport process for burying InP V-grooved substrates with InAsP. The mass transport process is terminated by the planarization of V-grooves automatically.

And all the discussion in this chapter will be effective under the condition to use InP substrate, which enables the application to optical communication systems in the long wavelength such as 1.3 or 1.5μm.

In this chapter, the new method to solve this problem will be presented. Furthermore, it is also shown that many additional better features are attributed to the new method without losing any merits in the conventional way.

5-2 Mass transport method

Mass transport method as the device fabrication was first applied to form an absorptive grating in DFB lasers on InP substrates[1]. Operable GC(gain coupled)-DFB lasers actually has successfully been fabricated and it showed good properties as DFB lasers as well as an excellent regrowth quality in its process[2]. Expanding this research, the possibility to use this method to form QWRs is naturally considerable. It is achieved by preparing smaller V-grooves as patterns of mass transport. Because mass transport is controlled by the depth of V-grooves, smaller V-grooves enables us to use a small amount of mass transport. Figure 5-1 is the schematic stream of mass transport process. As is understood from above, this method is based on the use of V-grooved substrates. Hence, all the merits which belong to V-groove methods in chapter 3 and 4 are hereditable in this method.

The mass transport process is achieved simply by MOVPE (metal organic vapor phase epitaxy) system. V-grooved substrate (InP) is first prepared. After it is loaded into the reactor of MOVPE, it is heated up to a certain programmed temperature. It is done in the atmosphere containing group V ambient (As and P). Hereat it is important that no group III material sources (Ga and In) are supplied in the reactor. Hence, it is different from a normal growth process in MOVPE. And the reactor temperature is kept at the programmed temperature for about 10 or 15 minutes in such a circumstance. The different material (InAsP) whose group V composition varies corresponding to that of the ambient in the reactor is formed only in the V-grooves. Surprisingly no parasitic QWL is formed during this process except for the very thin layer made by the replacement of P with As on the V-groove surface. This layer is too thin to contribute to the optical characteristics effectively. Therefore, only QWRs are formed in this method when it is applied to small V-grooves. Then, group III material sources are supplied for the first time to switch the mass transport process to a normal growth mode. In fact, the effective mass transport is already finished by the planarization before this switching. It is important to keep the stability of processing. And the successive growth process follows as usual. In this process, the V-grooves are filled with mass-transported materials until that a flat surface is recovered completely on them. Precisely saying, the obtainable surface may be quasi-plain with a micro corrugation on it originating from V-grooves when mass transport is not sufficient against the given V-grooves.

The wire size is supposed to be determined only by that of V-grooves in the above process. The stable control of a size in wire structures become possible in this case because it is free from other conditions such as temperature, heating rate and mass transport time. They can influence on the composition of materials on V-grooves. However this scheme is too simplified and is inconvenient for stacking wires and controlling as small a size of structures as QWRs. The reason for the former one is evident. Because V-grooves are planarized in one mass transport process, only

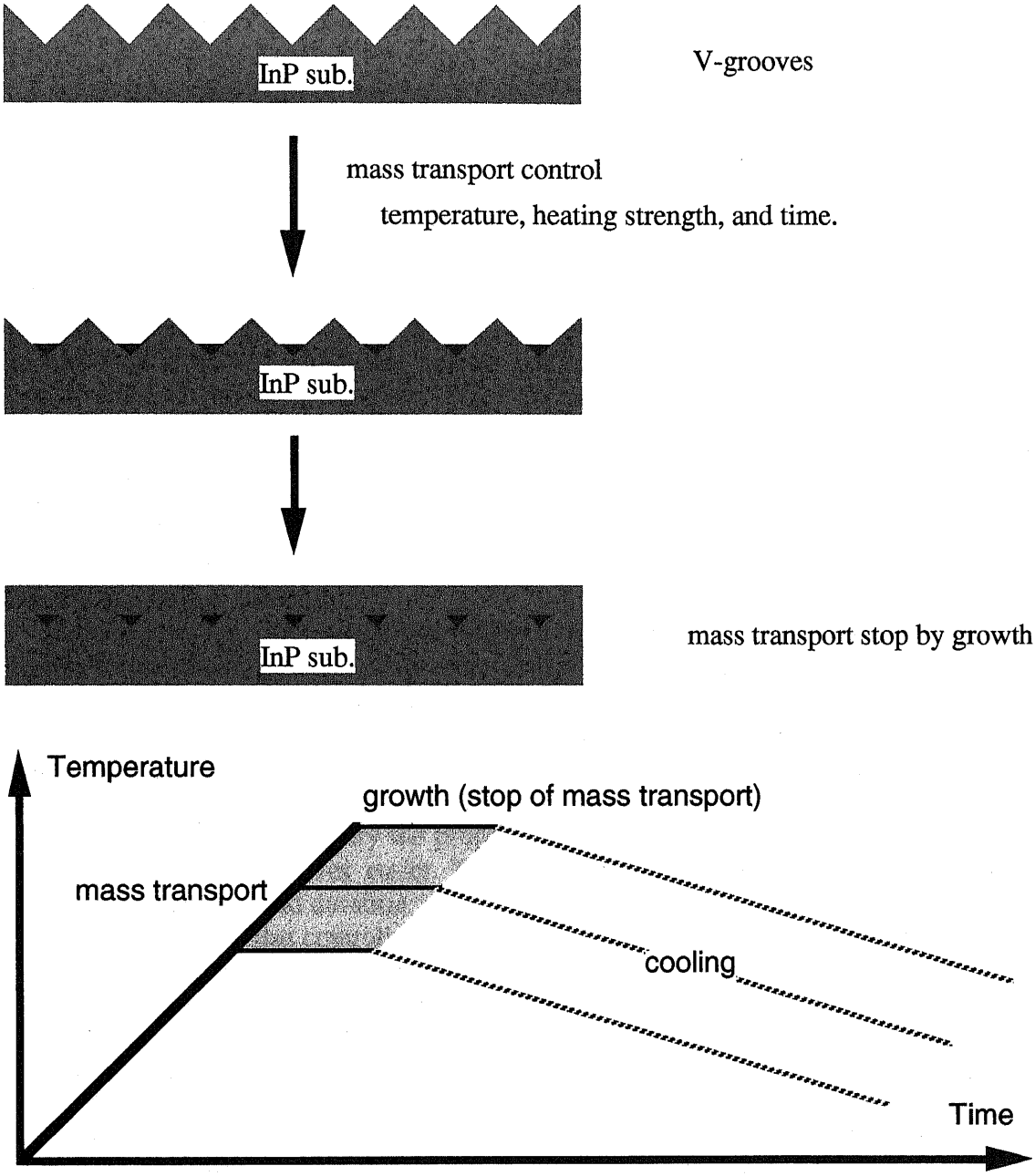

Figure 5-2 Schematic process stream in new mass transport for the stable fromation of QWRs applicable to QWR devices. Temperature diagram in new mass transport is shown in below.

single wire array is producible in the above case. Since the improvement of optical confinement factor is necessary in all the lasers using QWRs as an active part, it is considered to be disadvantageous in laser structures. The latter is a problem of processing. If we control the size of wire by that of V-groove, the accuracy of several [nm] is needed for the formation of V-grooves. The fabrication of V-grooves with the size of a few tens [nm] is possible, but its optical quality and reproducibility is doubtful in the available process technology. Actually the reported smallest size of wire in the above absorptive grating was as small as 30[nm] in width [3]. However, its cross-sectional

shape was obviously different from triangular shapes for the much larger one used in DFB lasers. It was flatten and far from a triangular shape originating from a V-groove. It means that the control of a cross-sectional shape of wires on such small V-grooves is very difficult and that the resulted shape is very unfavorable to expect a quantum effect by the 2 dimensional confinement in the QWR structure. The reproducibility for such an irregular shape is not possible, either.

Therefore, it is concluded that the control of mass transport by the V-groove size enables us to obtain QWRs, but that the quality of obtainable QWRs is not tolerable for the application to devices. It is apparently resulted from the difficulty in the preparation process of small V-grooves and also from differences in the mass transport phenomenon to bury V-grooves with a different size. In general, the smaller the V-grooves is, the less controllable the process is and the more serious the modification in V-groove's shape during mass transport become.

Consequently, we propose to utilize mass transport temperature, heating rate, and mass transport time actively in order to achieve more flexible controllability and improved quality of QWRs. In this scheme, we don't need to depend on a V-groove size when we design a QWR. If self-ordering process (see 4-3) is available for InP, stacking of QWRs become possible in that case.

Moreover, as the QWR size is now independent from the V-groove size, the control of confined states in the QWR is easily achievable without changing the geometry of grating. It is very useful to accomplish a matching of the luminescence peak in the QWR emission profile to Bragg wavelength. Otherwise, we must prepare new V-grooves at each time when the condition is changed or fluctuates. That is actually a considerable case when the conventional way is applied as it is. In the newly improved method, we don't need any change in a substrate to modify the property of QWRs as we want. It apparently makes the preparation of V-grooves easier. The size control of QWRs are achieved by mass transport temperature and duration.

In addtion to the size controllability, the variable composition in the QWR material is also important. This operation is achieved independently from the size adjustment by ustilizing the gas source condition in MOVPE reactor during mass transport. It means that the emission profile of QWR can be shifted in energy (or wavelength) axis without the serious variation in QWR size. Hence, this method satisfies the necessary condition for the QWR application to devices. Our mass transport is what makes the simultaneous optimization of QWR size and its luminescence peak on a given laser structure possible only by the MOVPE process. It is equivalent to the free design of QWR properties for (DFB) lasers. It is needless to say that additional one more parameter is necessary for the control of strain in QWRs.

The essence of our mass transport is shown in Figure 5-2. In the conventional way, the mass transport process was spontaneously stopped by the planarization of a substrate, and the precise condition for the mass transport time is not important. But in the new method, the mass transport process must be stopped just at any time when we want, and its switch must be as discrete as possible in viewpoint of controllability. For this compulsory termination of mass transport, we utilize the introduction of group III materials into the reactor. It is also explained as a switch to the normal growth mode from the mass transport mode. In Figure 5-2 (above), the mass transport process is finished by the growth of InP.

Mass transport is controlled through the temperature (T_{target}) and group V ambient pressure ratio in the reactor of MOVPE with the heating rate (a) constant. And the mass transport time ($t_{masstransport}$) is determined automatically by the next equation in our case.

$$t_{masstransport} = \frac{T_{target}}{a} \quad (1)$$

The reason why we chose only 2 among 3 parameters to control the mass transport process is explained as follows. The heating rate is deeply related with the amount of mass transport occuring until the reactor temperature reaches a programmed value. The higher the heating rate is, the smaller amount of mass transport is controlled when the same target temperature is set. It is because mass transport duration is shorten at the higher heting rate. The mass transport time is a main contribution to the QWR size. Considering that heating process is incidental in all the growth process in MOVPE, this initial mass transport is unavoidable. If we could avoid this unfavolable initial mass transport during the heating process, it would be nicer to enhance the freedom and the stability in the whole processing because it , for instance, makes it free to choose a reactor temperature and the successive mass transport and growth at constant temperature are advantageous in the MOVPE process. This is rather an ideal case, but at least this initial mass transport should be suppressed or controled below the size of QWRs. In our experimental apparatus, only this heating process was found to be sufficient for the mass transport process of structures as small as QWRs. No further mass transport at a constant temperature was needed. And thus, the highest heating rate was necessary to keep the size controllability in mass transport for QWRs. Even if it affords an additional mass transport time, the highest heating rate is also desirable to set up the mass transport temperature as high as those necessitated by a normal growth. Eventually, the heating rate is fixed at the maximum permitted in an attached heating apparatus.

Figure 5-2 (below) is the temperature profile of our mass transport. The highest heating rate of IR lamp system of our MOVPE was around 0.6~0.7[℃/s], and was fixed at this value in the following experiments. Subsequently the mass transport time was also determined by setting temperature from (1). And only the heating process corresponded to the mass transport process. This mass transport style is universal in all the experiments in this paper. After reaching the set temperature, the normal growth terminates mass transport and the successive recipe follows. In Figure 5-2 the profile is specilaized for the simple formation of a single QWR array in InP. In the case of device structures, more complicated growth recipes follow after the heating process for mass transport.

	conventional way	proposed way in this paper
dependence on heating rate (h)	small	high (size)
dependence on temperature (T)	small (composition)	high (size and composition)
mass transport time (t)	small	=T/h
control of QWR size	by V-groove size	by 2 elements among h,T,t
material composition	by V group ambient pressures	by V group ambient pressures

Table 5-1 The differences between the conventional way and our method in the mass transport process.

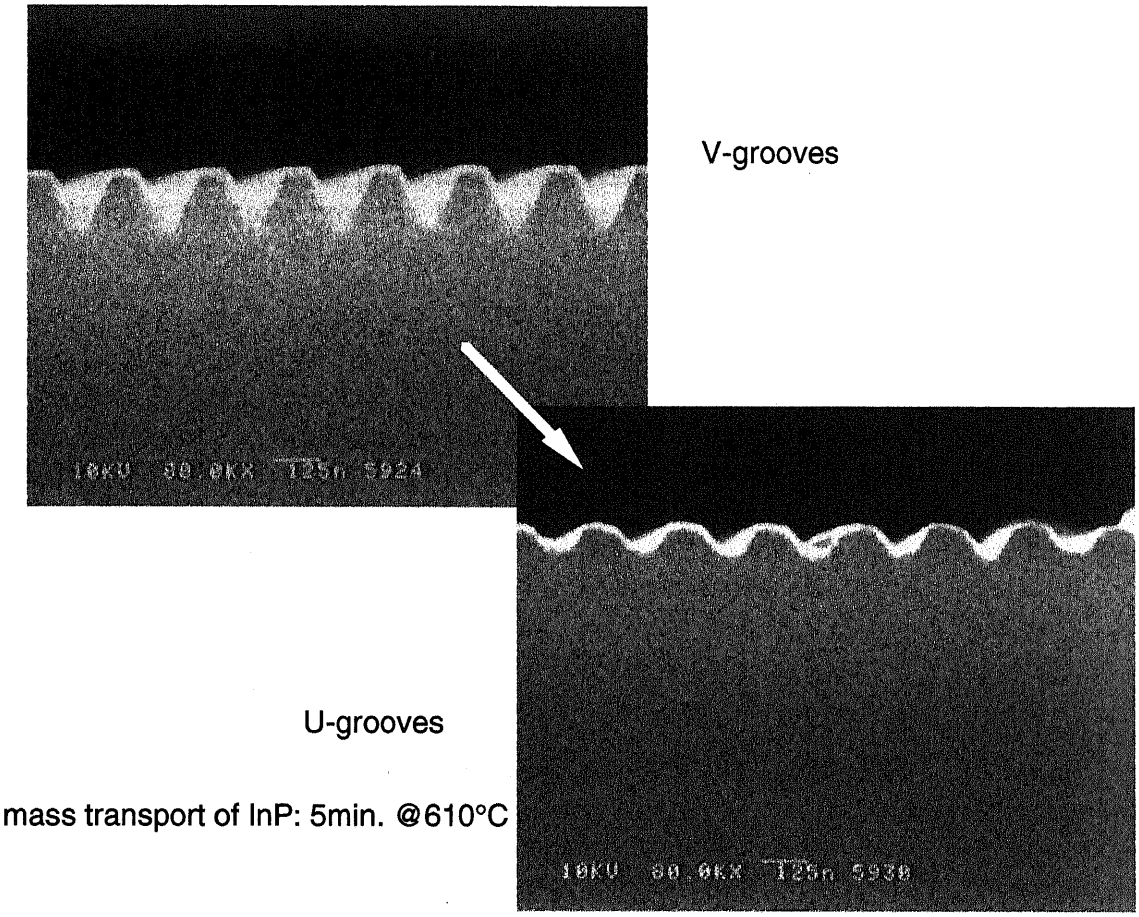

Figure 5-3 U-grooves made from sharp V-grooves after the heating process up to 610[℃] in P ambience.

As a result, it is summarized that the controllable parameters for the mass transport process is reduced to a target temperature for mass transport and group V ambient ratio in the MOVPE reactor. If an ideal heater to set the temperature in instant were available, more parameters would be permitted and it would ease the stability of mass transport.

In Table 5-1, the differences between the conventional mass transport and our new mass transport is resumed. It is shown from viewpoint of influences of each parameter on mass transport or the difference of control parameters.

5-3 Meaning to form QWRs for a long wavelength domain

InP was considered to be difficult to apply the regrowth on V-grooved substrates for the formation of QWRs[4]. What prevented us from a successful formation was a migration of In on the surface. Comparing with that of Ga and Al, the migration of In on the V-groove surface is very active and the V-grooves are filled with In so that the corrugation of the substrate becomes minimum. And thus, as far as we use the conventional growth method, V-grooves are embedded before the regrowth starts. The regrowth on the dull V-grooves leads to a lateral size enhancement or a low confinement of carriers, which is essentially a serious problem for quantum structures. The preceding reports on the QWR made on V-grooves were not sufficient as QWRs. Concerning to this point, the

application of mass transport method is very attractive to realize QWRs on V-grooves for the long wavelength region. Moreover, such QWRs are not accompanied with any parasitic QWLs. It opens the way to apply QWRs on V-grooves to long wavelength lasers for the first time.

In fact, this unfavorable phenomenon observed in the conventional growth method is a simple mass transport process. InP substrate is very suitable for the mass transport process because of its large migration. The phenomenon that the V-grooves are palanarized before the growth is understood as a mass transport under P ambience. In the formation of QWRs, this P ambience is replaced with P and As mixed one. It tells us that the mass transport method is effective for the materials where the growth method is not applicable. It also suggest the possibility that the compound materials which contains both types of materials enable us to utilize both self-ordering growth and mass transport process in MOVPE method. Traditionally mass transport has been known for InP substrates. The same effect is naturally expected for GaP substrate, and heterostructure is possibly made using the same principle. InP is the material for long wavelength (1.0[μm]~1.6[μm]), and GaP for short wavelength (620[nm]~850[nm]).

In this paper, InP will be treated for the realization of QWRs suitable for long wavelength lasers applicable to telecommunications.

5-4 Preparation of V-grooves on InP substrates

It was explained in the last section that the self-ordering growth was difficult to be applied to InP substrates contrary to GaAs substrates. In migration on the surface was more effective to planarize it than to form a crystallographic structure. Therefore, QWRs should be formed directly on a chemically etched V-grooved substrate in either conventional growth method or mass transport method. It is possible only when the mass transport method is applied because quite a high temperature is needed for the epitaxial growth. It means that the size and shape of QWRs formed on InP substrates must be determined by the preparation process of V-grooves.

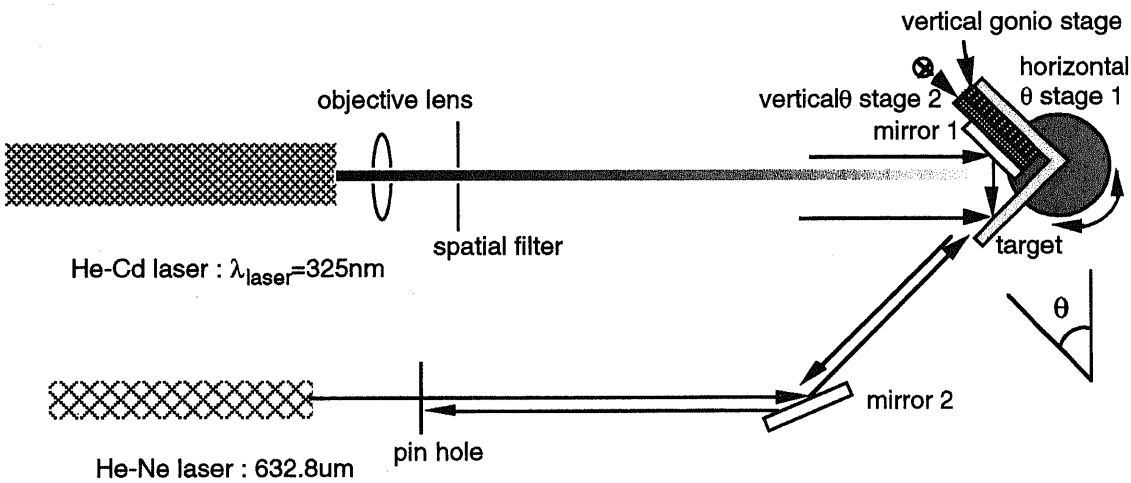

Figure 5-4 Corner cube type holography system.

solution for etching	*mask material*	*quality of grating*	*SEM photo*
20%HCl	resist	not reproducible	Figure 5-6
Saturated Br Water:HBr:H_2O	SiO_2	fast underetching of mask, dull V-grooves	Figure 5-7
Bromine methanol	SiO_2	rapid underetching of mask, non-uniform patterns	Figure 5-8
Saturated Br Water:H_3PO_4:H_2O	SiO_2	slow underetching, uniform and sharp V-grooves, stable processing	Figure 5-9

Table 5-2 The formation of V-grooves on InP substrates.

However, the processing that was used for a GaAs substrate in chapter 4 did not give enough a good quality of V-grooves owing to the rapid side etching under the SiO_2 mask. This time we must be more careful to choose a wet etching solution suitable for our purpose. We shall start from reviewing the whole process to make V-grooves.

The simplicity is one of the merits in processing. Hence, we considered both cases using only a resist mask and using a SiO_2 mask. The processing was approximately the same as Figure 4-4. Holography was made by using a corner cube type system (Figure 5-4) with He-Cd laser (325[nm]) as a coherent light source. This system is more stable and simpler than 2 beam interference method used in chapter 4. Because there is only one adjustable mirror and a lightwave is not splitted in the system, it is resistive against the unexpected perturbation and alignment of the set-up. On the other hand, the uniformity depends on the quality of a quasi-plain wavefront as a limit of spherical one. The patterned grating pitch (Λ) and the angle of mirror (θ) are related by the following equation.

$$\Lambda = \frac{\lambda_{laser}}{2\cos\theta} \qquad (2)$$

All the results on wet etching are summarized in Table 5-2. HCl, HBr:Saturated Br Water:H_2O=1:10:40, Bromine methanol 0.1%, Saturated Br Water:H_3PO_4:H_2O=2:1:15 were tried as a wet etching solution. Definitively, Saturated Br Water:H_3PO_4:H_2O + SiO_2 mask was selected. This method is superior to the others in the following points.

- very slow side etching rate under the SiO_2 mask.
- controllability of a duty of SiO_2 grating mask by a dry etching process.
- protection of InP surface by SiO_2.

The sharp and uniform V-groove grating was obtained as is seen in Figure 5-8. And Figure 5-9 is an example of the controllability of duty ratio in SiO_2 mask. ECR (electric cycrotron resonance) dry etching was used for the transfer of resist mask (25% diluted TSMR CRB-2).

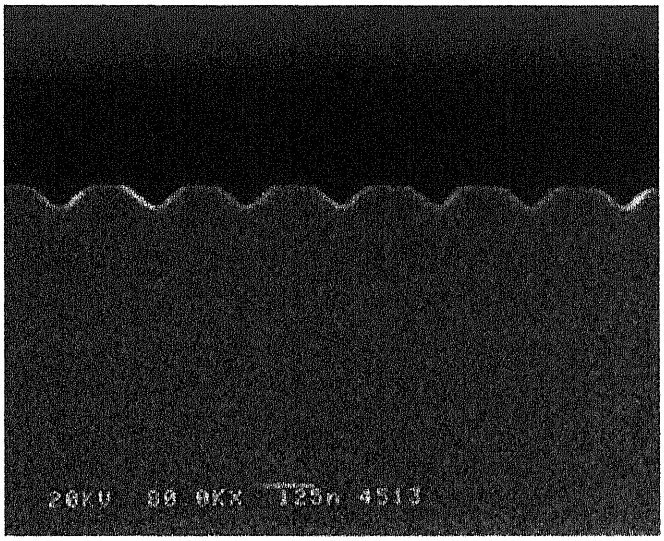

Figure 5-5 V-grooves made by HCl solution with resist mask. Wet etched for 30[s] at 5[℃].

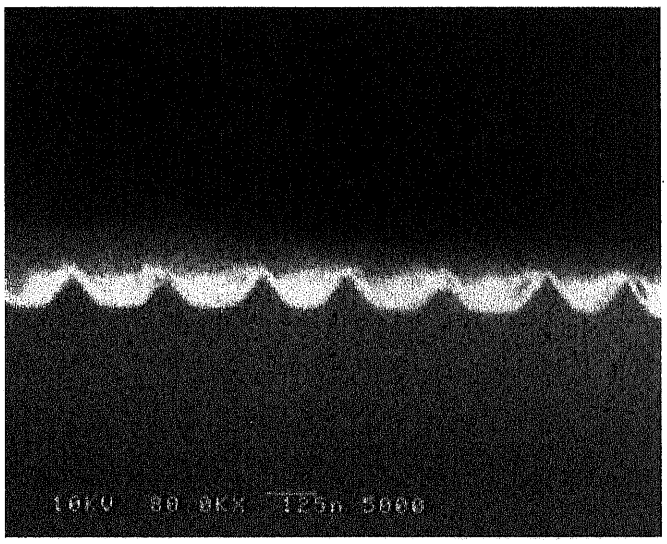

Figure 5-6 V-grooves made by Saturated Br Water : H_3PO_4 : H_2O solution with SiO_2 mask. For 2[min.].

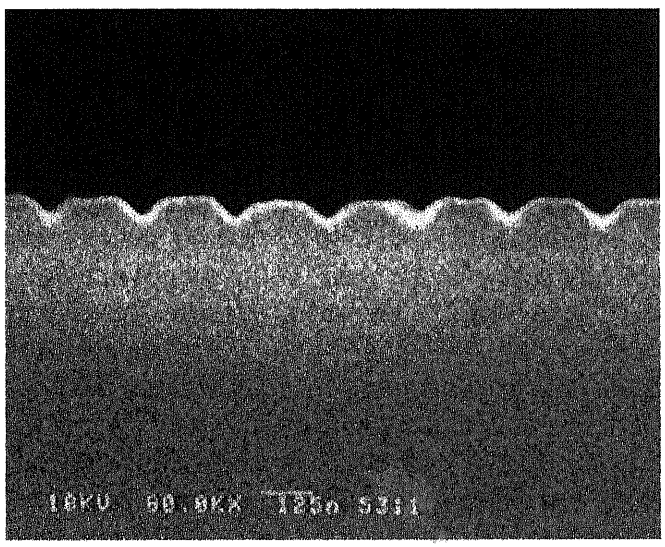

Figure 5-7 V-grooves made by 0.1% Bromine methanol solution with SiO_2 mask. For 10[s].

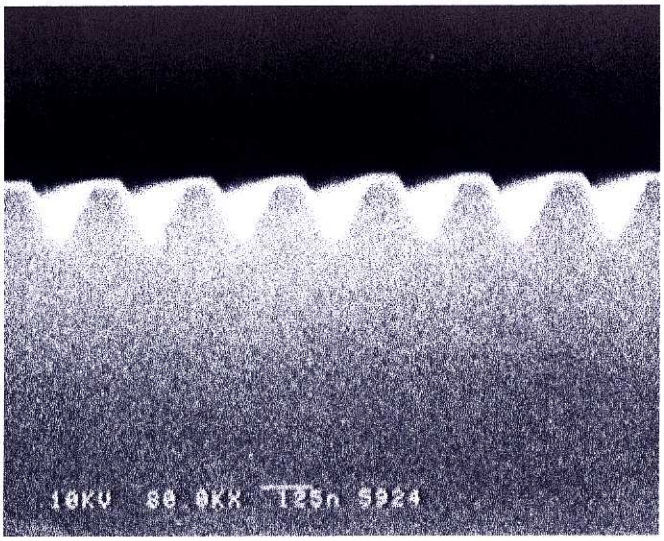

Figure 5-8 V-grooves made by Br Water : H_3PO_4 : H_2O with SiO_2 mask. Wet etched for 15[s].

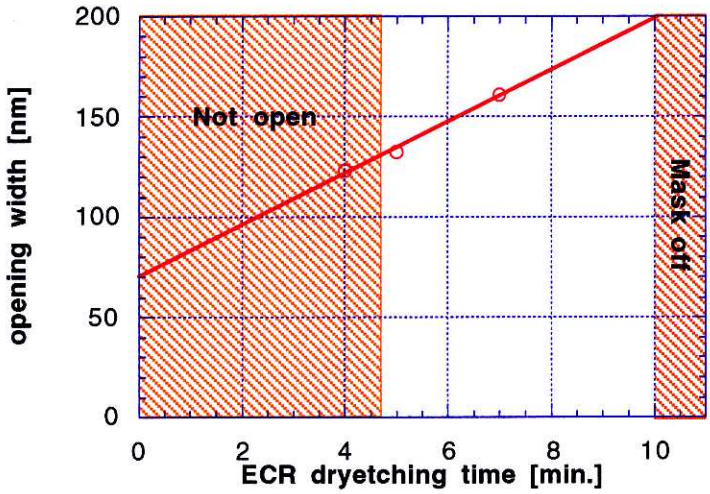

Figure 5-9 controllability of duty ratio in SiO_2 mask by dry etching process

The difference in the quality of V-grooves between this one and that in chapter 4 is evident in SEM photos (Figure 5-8 & Figure 4-7). Almost all the problems seen in chapter 4 are solved. The flat parts is also left on the substrate thanks to the controllable wet etching process. The SEM cross-sectional photos for the other etchants are also shown in Figure 5-5~7. They are all worse than Figure 5-8 in the points of sharpness and uniformity. Among them, HCl looks good, but its reproducibility was not proved experimentally.

After the formation of a grating by wet etching, cleaning process followed. Because SiO_2 mask was deposited on the substrate, Buffered HF cleaning was necessary anyway. And this processing was also helpful to get rid of impurities on the surface, and effective to keep the quality of V-grooved substrates as high as is tolerable for the successive regrowth. We also added a sulfuric acid solution to clean oxides on V-grooves. And the preparation process was finished by ordinary organic cleaning.

The cleaning of resist was done by 3 steps. The first one was during dry etching of SiO_2, the second was ashing in O_2 plasma, and the final was organic cleaning. Remover

for the resist was not used in this process. And a descumming process to raise the transfer quality of stripes resist pattern to SiO_2 was inserted before the dry etching process

To obtain supreme quality of sharpness and smoothness at the bottom of V-grooves, the orientation of V-grooves is important, too. Because the V-groove is engraved in the direction of $(0\,\bar{1}\,1)$ on a (100) substrate, the grating pattern exactly must be aligned in this $(0\,\bar{1}\,1)$ direction to avoid a roughness at the bottom of V-grooves. The QWRs luminescence broadening is influenced by its structural uniformity along the axis. Therefore, the alignment of the orientation is indispensable especially for small QWRs. The He-Ne laser in Figure 5-4 was utilized for this alignment. The edge of a cleaved substrate is precisely corresponds to $(0\,\bar{1}\,1)$ or (011) orientation. And thus the orientation of a substrate is adjustable by monitoring the reflected light of He-Ne laser from this edge. Because its wavelength is located out of the sensitivity of resist, it has nothing to do with the exposure. Figure 5-9 is the aligned pattern on the substrate. The orientation of $(0\,\bar{1}\,1)$ is parallel to the stripe pattern of the substrate.

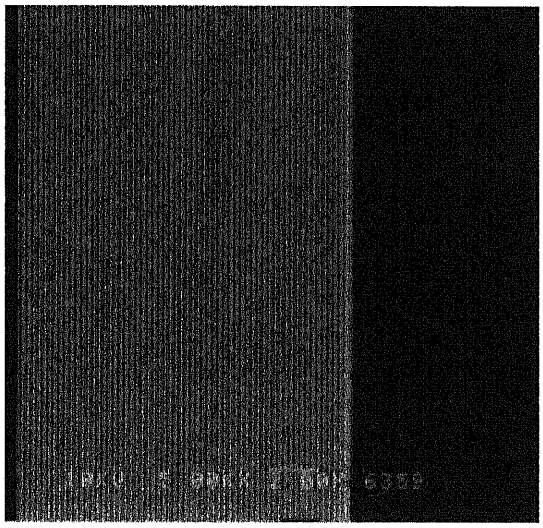

Figure 5-10 Alignment of V-grooves to $(0\,\bar{1}\,1)$ orientation.

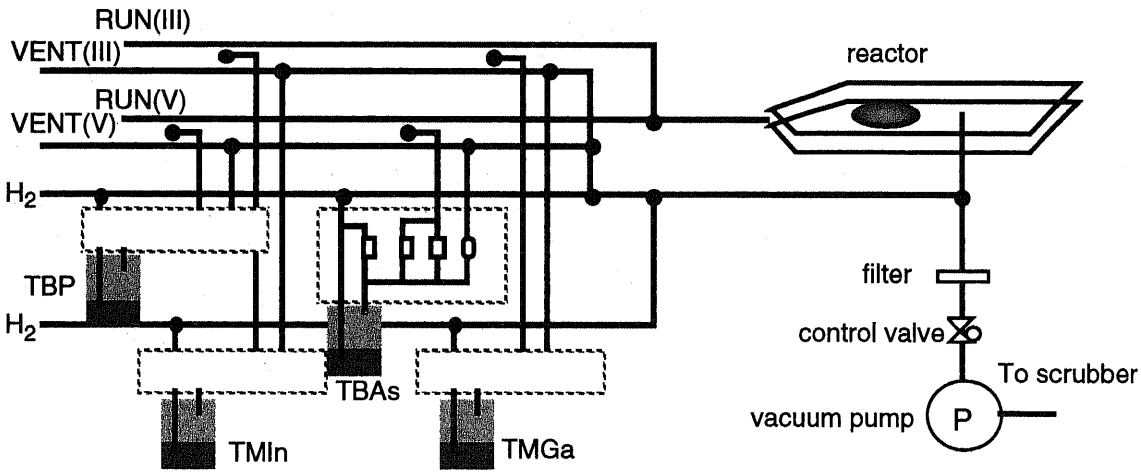

Figure 5-11 Schematic figure of MOVPE system used for mass transport on InP substrates.

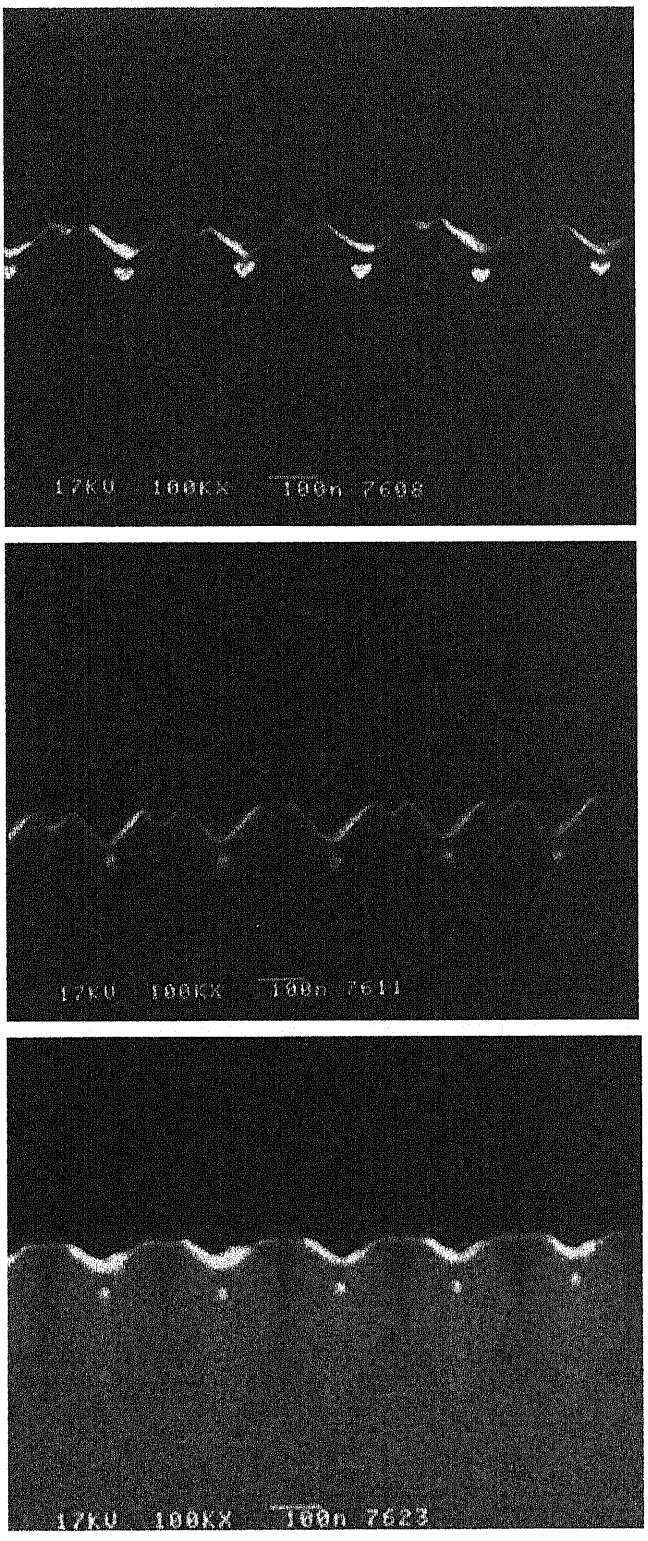

Figure 5-12 QWRs formed at various temperatures by mass transport. (above : 580[℃], middle : 550[℃], below :530[℃]). Stain etched by 20%HCl for 10[s].

5-5 MOVPE system used in our experiment

Schematic figure of MOVPE system is shown in Figure 5-11. Source materials are TBP(tertiary butyl phosphine), TBAs(tertiary butyl arsine), solution TMIn(tri methyl indium), and TMGa(tri methyl gallium). DMZn(di methyl zinc) for p type doping and H_2S for n type doping are equipped. Our system is Aixtron Aix200/4 with a horizontal reactor. 2 inches wafer is accommodated on a graphite susceptor which is rotative by the gas stream. The outer tube has windows for ellipsometry attached to the system and is surrounded by the infrared heater. The system is run with the total flow keeping at 13000[sccm] by balancing with a purified H_2 carrier gas.

5-6 Formation of QWRs by mass transport

The temperature diagram for mass transport is as is shown in Figure 5-2. Mass transport process starts from room temperature (mass transport phenomenon itself appears over at a few hundreds[℃].). As soon as the temperature reaches a programmed value (530, 550, 580[℃]), the growth of InP follows with the temperature constant. This growth is to stop the mass transport process on the substrate as is mentioned above and is also for covering QWR with InP so as to form a heterostructure. Finally the reactor was cooled down to room temperature. Apparently, this diagram is for the formation of a single QWR array. After the formation of QWRs, to enhance the contrast of materials of InAsP and InP, HCl stain etching was done for all the samples.

Figure 5-13 TEM image of QWRs fabricated by mass transport at 550℃ (low magnification).

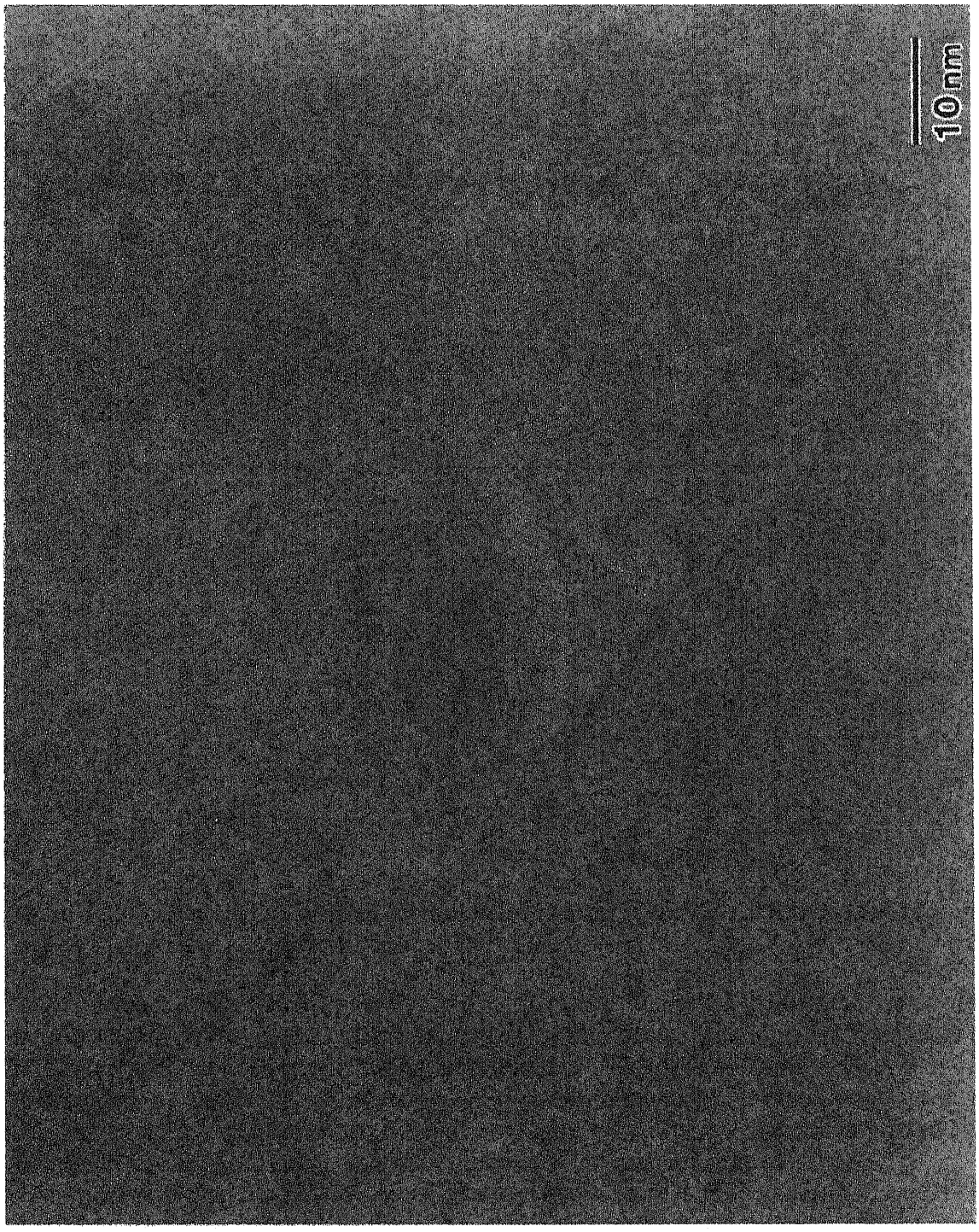

Figure 5-14 Lattice image of QWRs fabricated by mass transport at 550℃.

The other condition used in this experiment was;
heating rate 0.6~0.7[℃/s]
TBP pressure 1.83×10^{-1}[mbar]
TBAs pressure 2.70×10^{-3}[mbar]
Group V ambient pressures were kept at above values in this experiment.

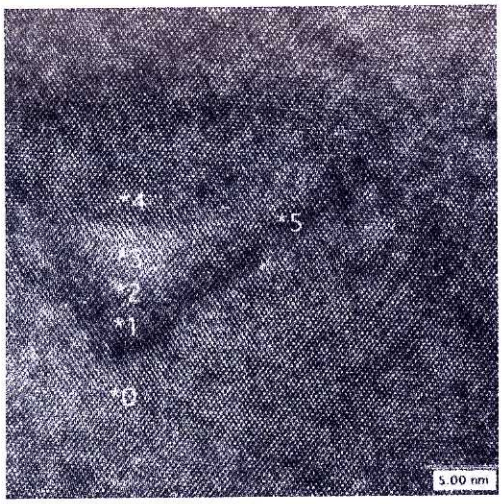

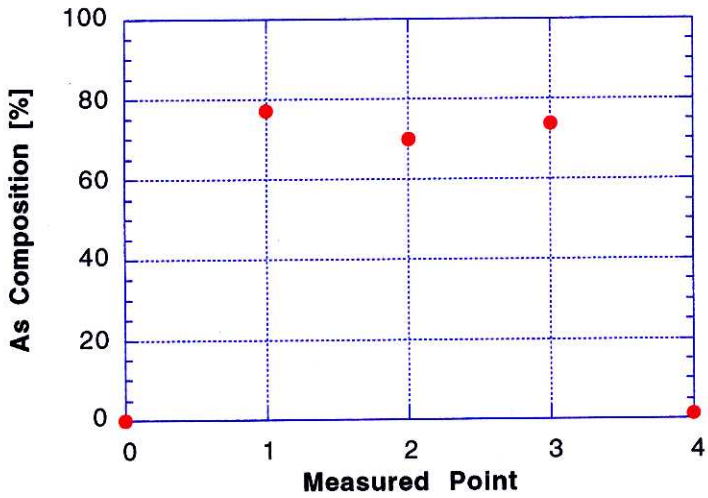

Figure 5-15-1 Estimated As composition spatial distribution in QWR made by mass transport at 550[℃]. The same specimen as Figure 5-13.

The surface was etched away by HCl in Figure 5-12, and V-groove-like structure appeared again. It was caused by the existence of a thin InAsP layer made by replacement of P in InP with As in ambience during mass transport. This layer is found to be as thin as a monolayer by the later TEM (transmitting electron microscope) observation. It worked as a temporal etch stop layer against HCl in Figure 5-12. The fragility coming from its thinness is known from etching on the flat part of V-grooved substrate.

The size variation of QWR by mass transport temperature is obvious from these SEM (scanning electron microscope) photos. At lower mass transport temperature, QWRs with a quantum effect size were realized. Even the wire made at 580[℃] has at most 40[nm] of the side of triangular shape. These wires' size is smaller than ever reported one using InP V-grooved substrate. Their shape is not flattened and the confinement is rather equivalent in lateral and transverse direction. The sharp V-groove bottom is kept even for small QWRs. Quite a strong quantum confinement is expected in such QWRs. In addition to that, InAsP is strained compressively by the surrounding material; InP due to its lattice mismatch. This strain can enhance the confinement of carriers into QWR. Even 40[nm]

wire structure may serve as a QWR thanks to the strain effect in spite of its geometrical largeness.

The TEM image of QWRs made by mass transport at 550[℃] is shown in Figure 5-13. The image at low magnification, and lattice image are presented there. Uniform triangular shaped QWRs were successfully fabricated. Its base side is about 20[nm], and the height is bout 10[nm]. The thin layer on the side wall is unmeasurable even at this magnification. The interface of lattice mismatched materials are very smooth on the atomic level. No dislocations and defects are found in the images. Good interfaces seen in these images make it sure that the reordering effect exists in the mass transport mechanism. Because it is difficult to imagine that only the wet etching and cleaning process produces so good a quality of regrowth interface, it is expected that the surface repairing and stress relaxing phenomenon like annealing process also works in the mass transport process. Hence, mass transport contributes both to improve damaged surfaces and to form QWRs with a good geometry. The lattice mismatch is also confirmed in this image as a shadow around the interfaces or a starined lattice image at interface in Figure 5-13.

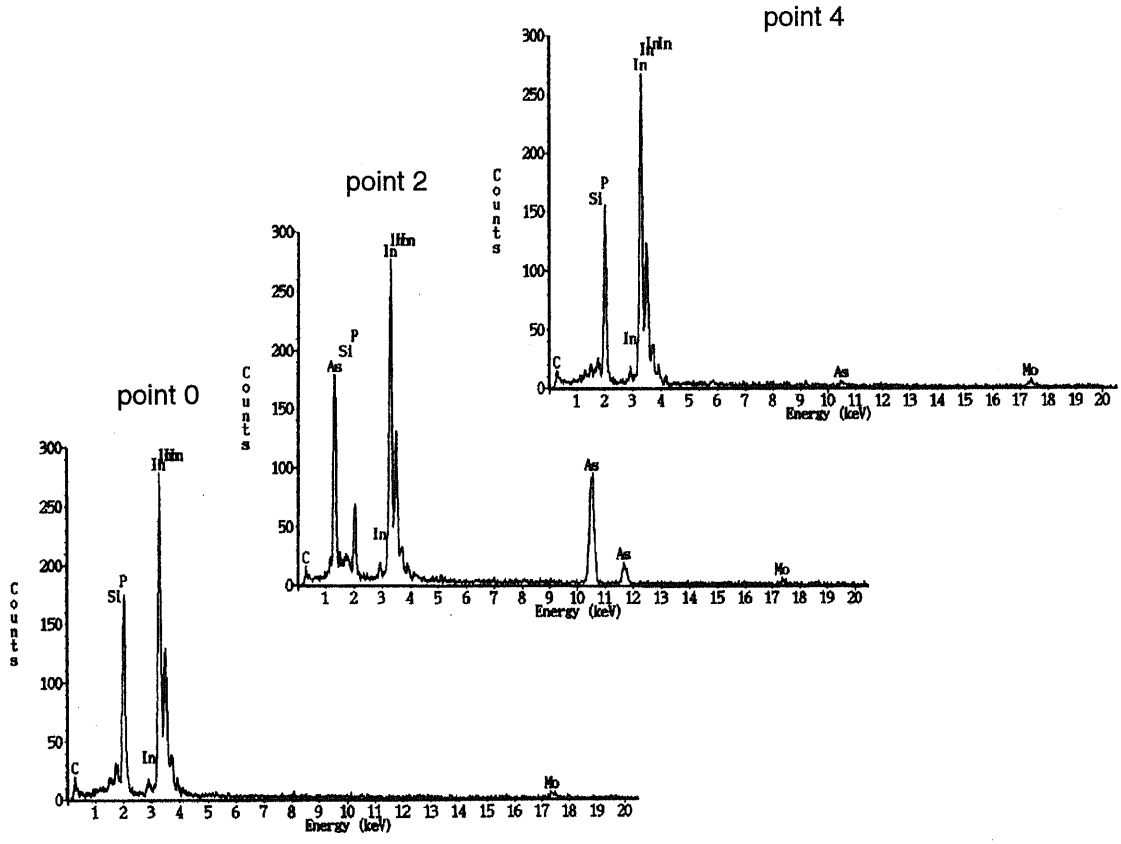

Figure 5-14-2 EDX spectra of QWR in Figure 5-13. Each point corresponds to that of Figure 5-14-1. As is nearly contained in point 0 and 4.

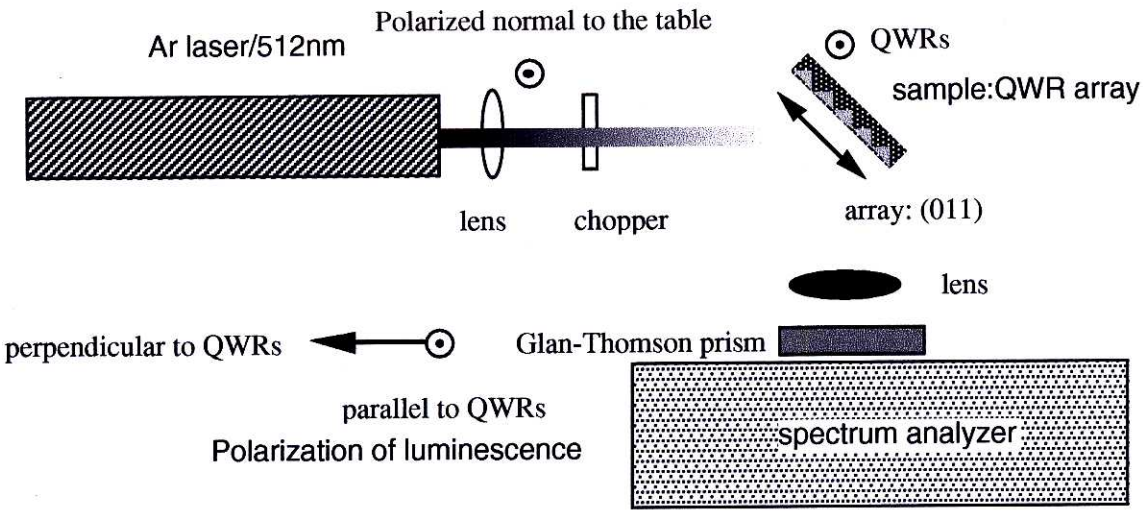

Figure 5-15 Configuration of PL measurement.

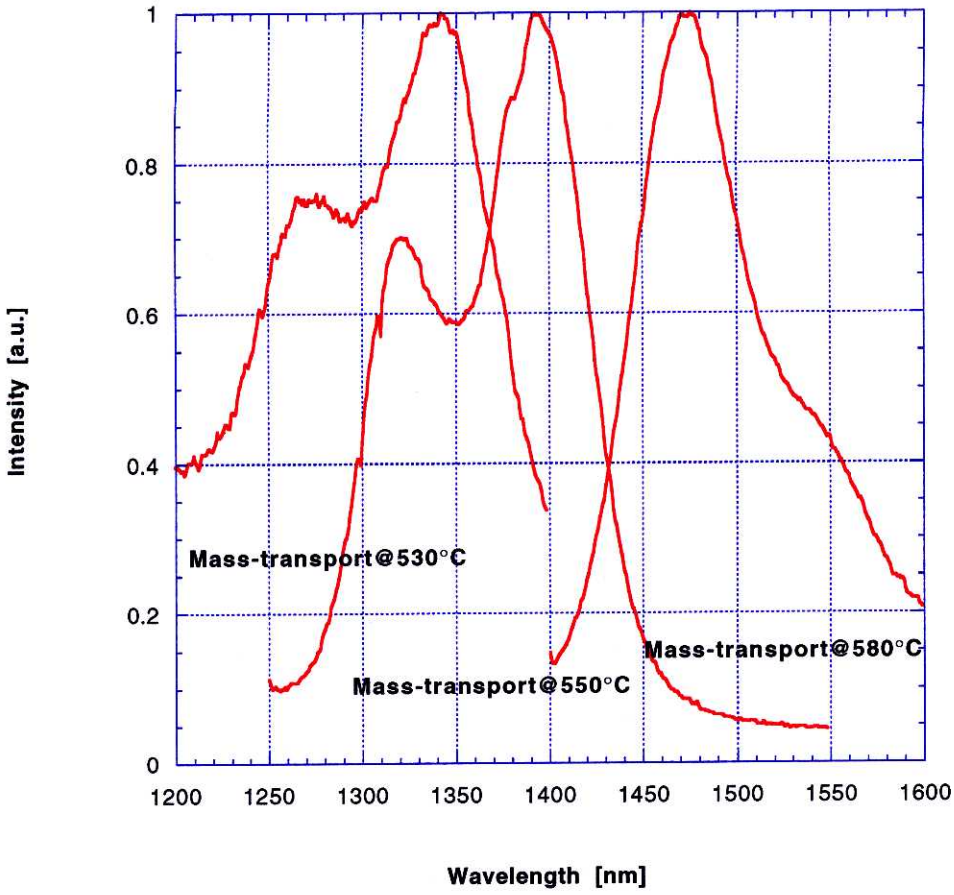

Figure 5-16 PL spectra at 77[K] of QWR array made by mass transport at 530, 550, and 580[℃].

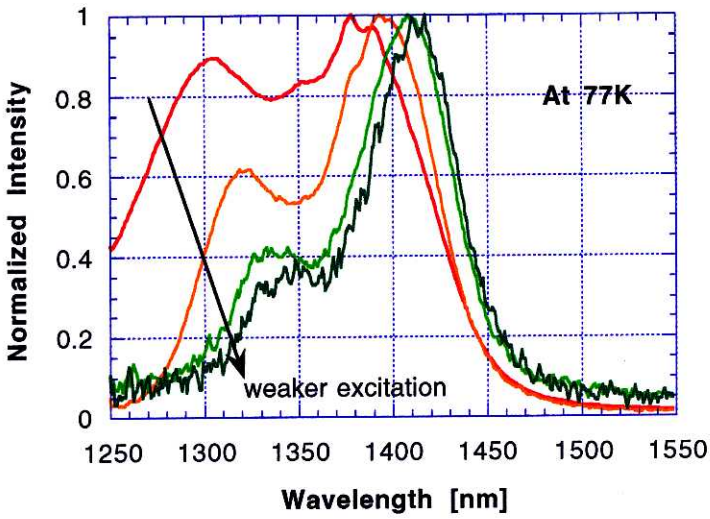

Figure 5-17 Dependence of PL spectrum (at 77[K]) of QWRs on excitation strength. QWRs are made by mass transport at 550[℃]. The peak intensity on the higher energy side decreases as the excitation power gets weaker.

The composition analysis by EDX (energy dispersive X ray analysis) shows that As composition is as rich as 80% in InAsP (Figure 5-14-1). It was reported that As is relatively easy to be incorporated in a newly formed material at the bottom by the mass transport process using PH_3 and AsH_3[4], and this was again demonstrated in the case of TBP and TBAs. At the outside of QWR (2.5[nm] above and below QWR), 0% of As was

5-7 Characterization of optical property of QWRs formed by mass transport

It was proved in the last section that QWR structures can be fabricated by the mass transport method. The good controllability and the excellent crystal quality was shown by SEM and TEM observations. Then, as a n

Photoluminescence (PL) spectra were measured for each sample made in the last chapter. The lightwave for the excitation was polarized parallel to a QWR array (Figure 5-15). Excitation strength were approximately $3W/cm^2$. It was rather a high excitation as a PL measurement. Figure 5-16 was measured at 77K without the polarization prism in the measurement set-up.The peak shift is mainly due to a size difference of QWRs. Its size is controlled by the mass transport temperature so as to cover the whole region called long wavelength in telecommunications. The peak wavelength of each sample was reproducible. And the dependence on a V-groove's quality that may be different at each time of production was small in our processing. It is resulted from above stable V-groove preparation process. Considering that the luminescence peak of QWR made at 550[℃] is 1390[nm] at 77[K], the estimated As composition in QWR by the EDX measurement was not so bad.

2 peaks were always observed for these samples. As was mentioned above, it was caused by a strong excitement of samples. As the excitation strength is reduced by the variable ND filter, the peak intensity on the shorter wavelength side or the higher energy side is also decreased (Figure 5-17). It shows that the peak on the shorter wavelength side

is a second peak coming from the recombination between the higher energy states. The exchange of a dominant peak between 550[℃] and 580[℃] is probably due to the strain effect in QWRs. At a higher temperature, the As incorporation in QWRs is expected to be more. This trend is natural because mass transport is caused by releasing P from the InP V-grooved surface and is activated by the higher temperature. On the other hand, the formation of QWRs at the V-groove bottom is the inverse phenomenon, and the QWRs contain more As in them by the reduction of fixed P. And thus, the strain induced from the lattice mismatch is harder in QWRs at 580[℃]. This inference related on the strain in QWRs is based on the PL measurement of samples with their As composition varying, but with their size approximately unchanged. When the strain is increased by the more As in QWRs, the second peak became dominant again. Because now the size of QWRs are fixed, it must be resulted from the strain in QWRs or the barrier hight change. The common term between these 2 experiments is now the strain in QWRs. But above explanation is not still certain. What is sure that this phenomenon was repetitively observed and it was always between these 2 temperatures in our experiment.

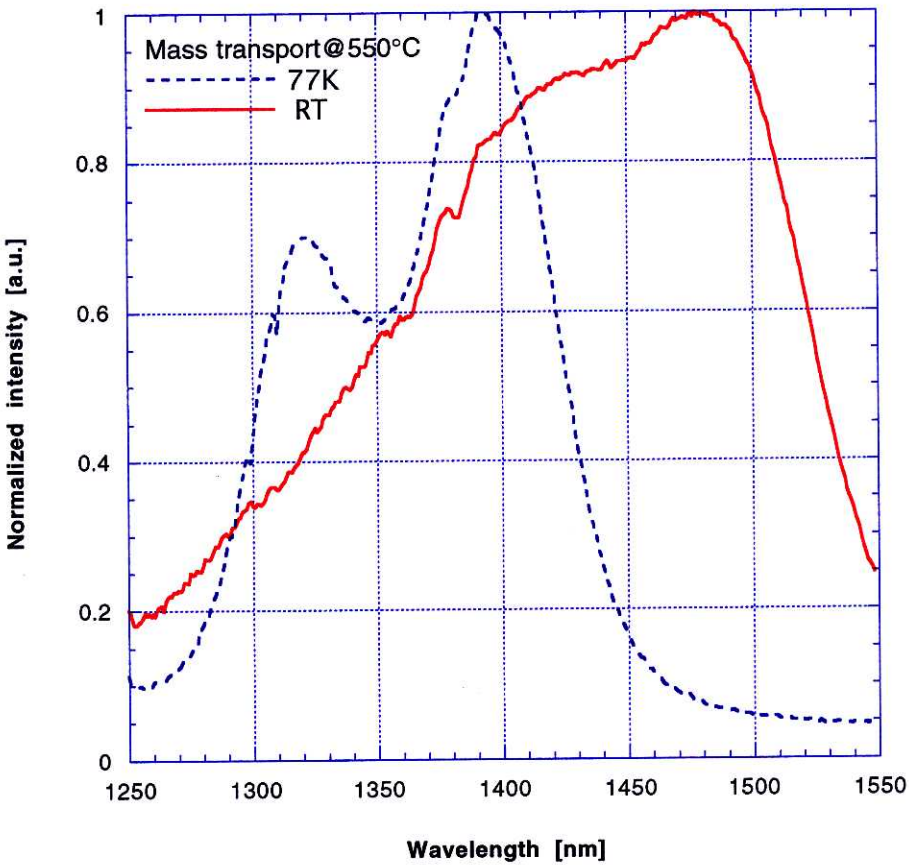

Figure 5-16 PL spectrum at room temperature of QWRs made by mass transport at 550[℃]. The dotted line is a reference measured at 77[K]. In both spectra, 2 peaks are clearly recognized.

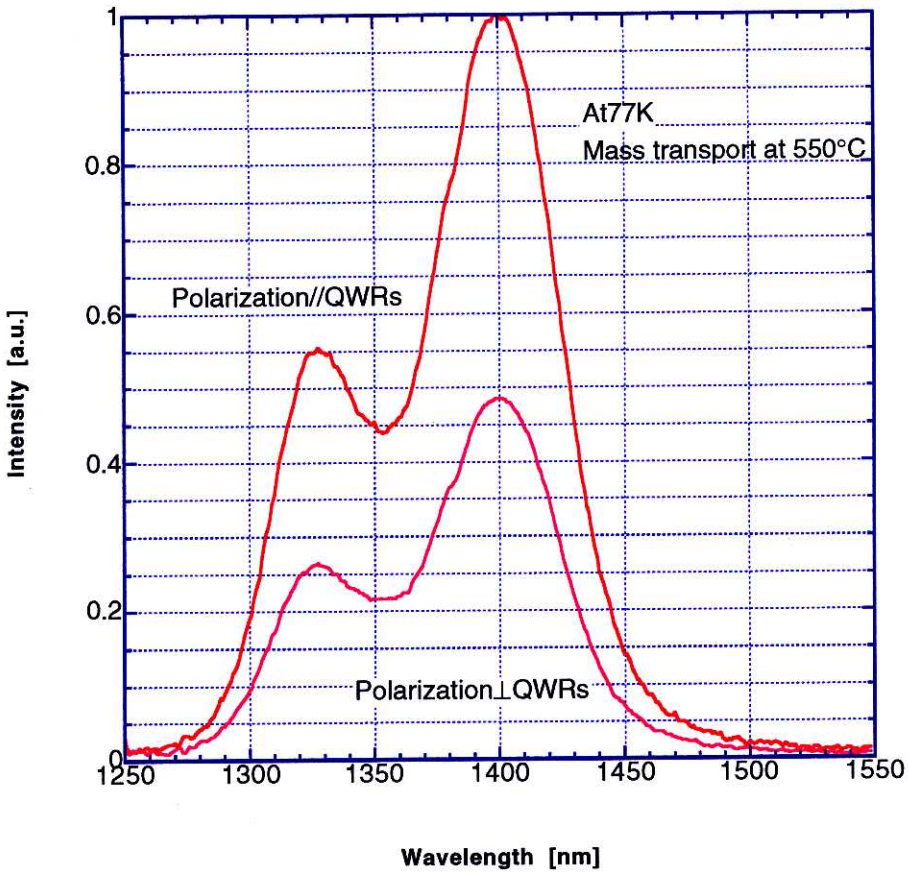

Figure 5-17 Linear polarization dependence of QWR's PL signal at 77[K]. For the sample made by mass transport at 550[℃]. Note that the luminescence whose polarization is parallel to QWRs is always stronger than the other.

The PL spectrum of these sample (mass transported at 550[℃] and 580[℃]) was observed even at room temperature (20[℃]). Figure 5-18 is for the sample made at 550[℃]. The excitation power was the same as at 77[K] in Figure 5-16. 2 peaks were obviously observed at room temperature, too. It was impossible to observe such a luminescence when we used a conventional growth on V-grooves for the QWR. One of the causes was apparently the coexistence with parasitic QWLs. This fact is also enough to show how much the quality of QWR was improved by mass transport method comparing with other methods in chapter 3. The PL peak at room temperature was around at 1480[nm] for the higher wavelength one. FWHM (full width at half maximum) of the this luminescence peak was 30[meV] at 77[K], and 40[meV] for the same peak at room temperature. This is a good value as an experimental one though it is larger than the theoretically expected value. And the broadening of FWHM at room temperature is suppressed very well. The excellent quality of our QWRs was shown again.

As is often quoted as an excuse for a broadening of a spectrum, the non-uniformity of QWRs in the array would be the most serious reason in our case, too. Though the TEM observation shows a good uniformity of QWRs, its observed area is local, and the dispersion of a size and a cross-sectional shape in the whole wafer is not negligible because our process includes a wet etching for the V-groove formation. We carefully

considered this problem by the selection of the wet etching solution and the alignment of a substrate in the previous sections, but much more effort is needed to obtain so excellent a quality as QWLs. The simplest way to show the peculiar optical property of QWRs is to check the anisotropy of a PL luminescence intensity. Its effect purely comes from anisotropic quantum confinement of carriers in 1 dimensional structure in the plain of a substrate. In its plane, one direction is confined, and the other is free for carriers.

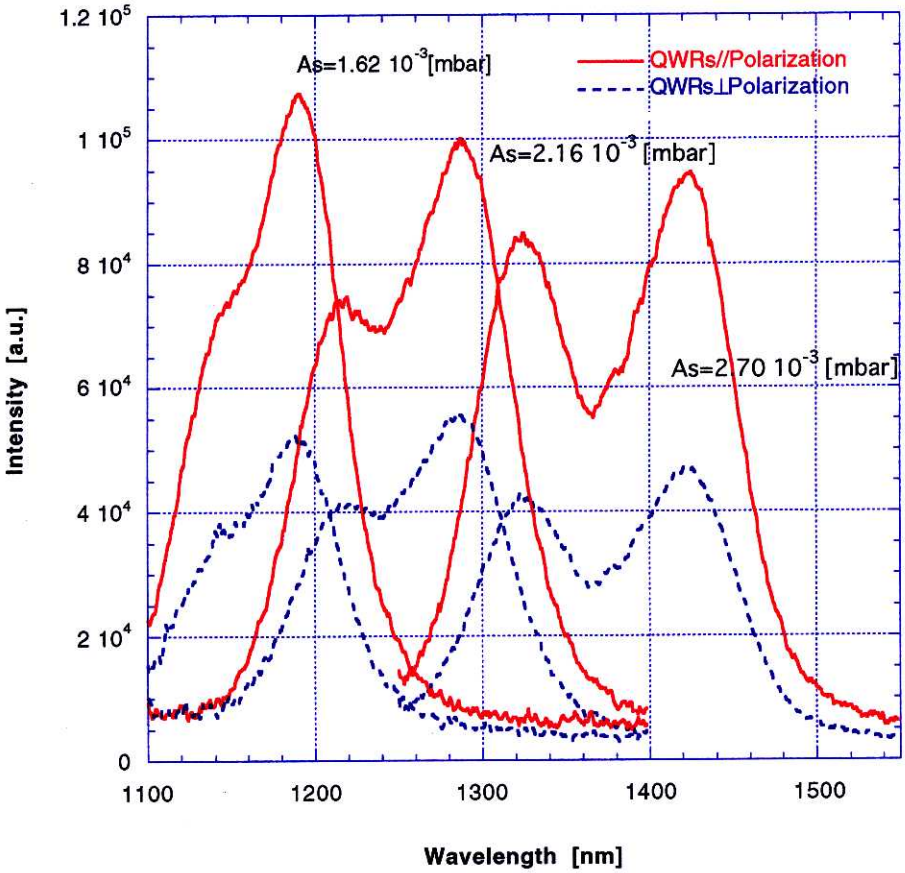

Figure 5-20 PL spectra of QWRs made by mass transport with different As/P ambient pressure ratios. Linearly polarized anisotropy is also shown for each one.

For such a measurement, the grating effect must be separated carefully since the QWR array is also a grating as it is and it can also be a cause of anisotropy. But this structural effect comes from the excitation process, and not from the luminescence property of QWRs because the grating pitch is now the 1st order of a luminescence wavelength of our QWRs. Therefore, for instance, by changing the orientation of QWRs against the polarization of a lightwave for the excitation, we can estimate the strength of a disturbance by the grating on PL signals. But we see that this effect is quite small even if it exists, and is even negligible. Because QWR size is so small comparing with the surrounding bulky barrier materials that the directly excited carriers contributing to the luminescence is very little. As is understood in QWLs, most carriers for the recombination in QWRs are transported from barrier regions. In this model, no dependence of the PL spectrum on the

excitation polarization is found because excited carriers belongs to the bulk regions apart from the QWR grating. Our result was exactly in good agreement with this model. No dependence on excitation polarization was found. Therefore, the measured spectrum is precisely the polarization dependence of QWRs and the existence of the grating does not influence on it.

The orientation dependence of the PL spectrum for QWRs made at 550[℃] is shown in Figure 5-19. The intensity was stronger in the direction parallel to QWRs. It was the same results as the previous reports on QWRs made by various methods[5]. Hence, the effect of a quantum confinement on optical properties is proved to be true in the QWRs made by mass transport. The same anisotropy was obtained for all the samples made by varying the mass transport temperature.

The emission wavelength tuning only by a mass transport temperature is inconvenient to apply them to devices because it is accompanied by the change in a QWR size. Tuning must be ideally achieved with the size constant for the practical use. A control of As composition of QWR is useful for compensating this aspect. In this case, both bandgap of material and strain are modified. In the previous results on mass transport temperatures, the ambient ratio of TBAs and TBP was always constant at 0.01477. This ratio is changed by controlling TBAs pressure in the reactor but with that of TBP constant. As pressure varied from 1.62×10^{-3}[mbar] to 2.70×10^{-3}[mbar] in our experiment.

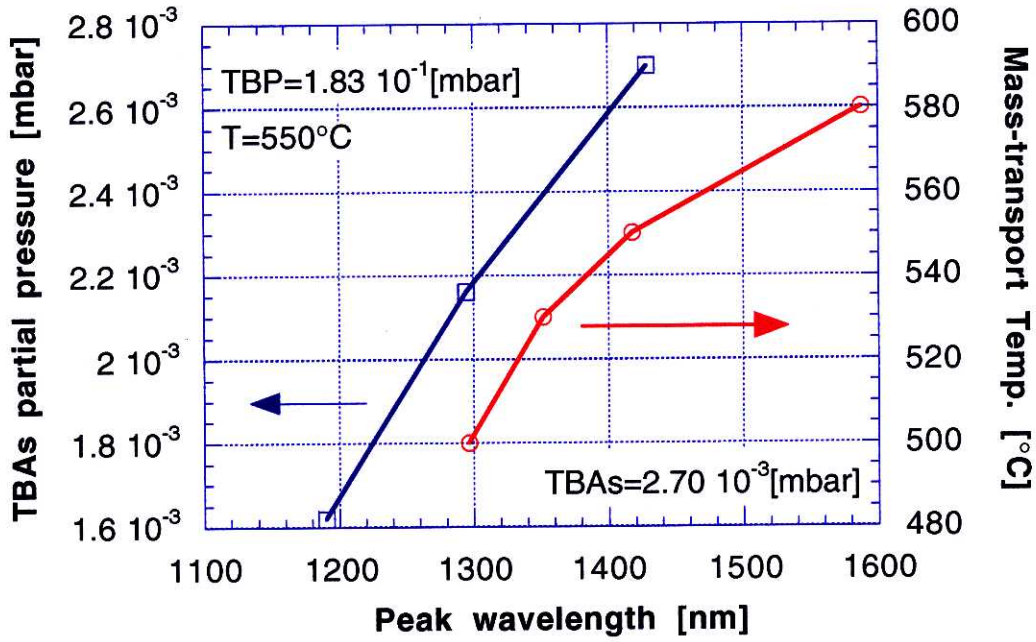

Figure 5-18 PL peak wavelength (at 77K) of QWRs fabricated by mass transport. Temperature and group V ambient pressure ratio dependence. The former contributes to the shift mainly by changing the QWR size, and the latter does by varying the composition and strain in the QWR. Both parameters (size and composition) are approxmately controlled such as ones that are independent from each other, and thus, the design of QWR size and emission peak wavelength is simply achieved by adjusting these 2 elements in MOVPE system.

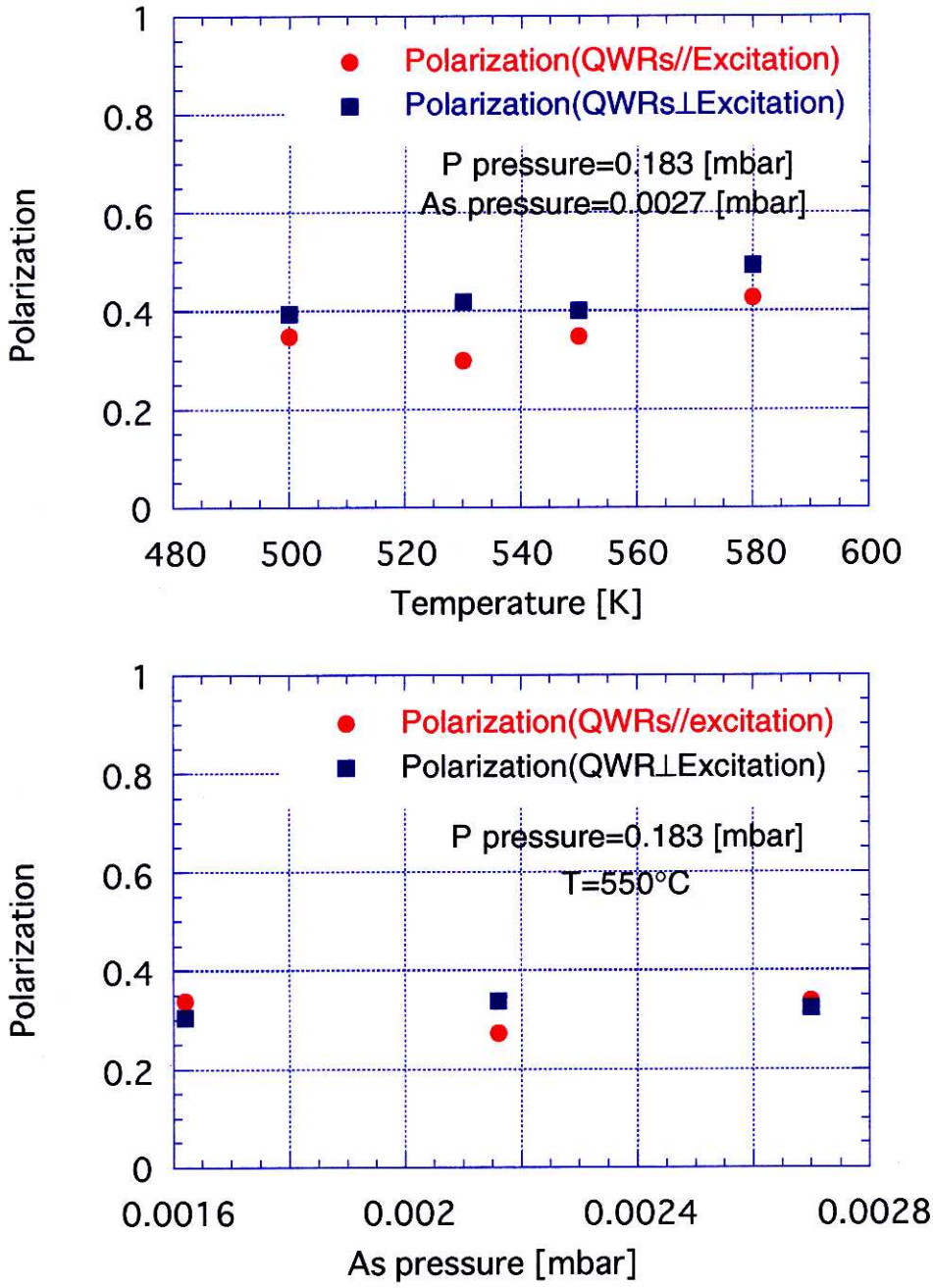

Figure 5-19 Polarization anisotropy of QWRs made by mass transport method at various temperatures and various As/P ambient pressure ratios.

PL spectra of such QWRs of which As composition changed are shown in Figure 5-20. It clearly shows that the peak wavelength shift potentially covers the same entire region of long wavelength as before. And the SEM observation proves that the QWR size remains almost the same in these conditions. Hence, the control of a peak wavelength of gain with the QWR size fixed becomes possible by using this way. The polarization anisotropy is also shown in Figure 5-20. The quality was kept at the same level as before when As pressure moves in the above region. But the upper limit for As pressure certainly exists due to the enhancement of the lattice mismatch and then the quality of

QWRs get worse, off course. PL signals of QWRs were observed until the As pressure of 3.70×10^{-3}[mbar] at 77[K]. But its intensity was much weaker than those of Figure 5-20 and the profile was noisy. The measurement of a polarization dependence in such a case was impossible in our measurement set-up of Figure 5-15.

As a result, the tuning of QWR emission wavelength was achieved in the bandwidth shown in Figure 5-21. Note that these are the wavelength at 77[K], and thus around 100[nm] shift toward the long wavelength side must be considered for the application to devices operable at room temperature. The polarization anisotropy of PL spectrum for all the samples in this section are also summarized in Figure 5-22. There, the anisotropy is defined as

$$D_{\text{anisotropy}} = \frac{I_{//} - I_{\perp}}{I_{//} + I_{\perp}}$$

5-8 Conclusion

To ameliorate the defects clarified on the conventional growth method using V-grooves, the mass transport method on V-grooves was newly proposed as an alternative. This method is particular in the point that the migration of materials are positively used. Because its process is different from a growth, several new good features are expected. Especially, because the formation of QWRs on InP V-grooved substrates has known to be difficult and no sufficient results have ever been reported, it is epoch-making as a method to offer a QWR array on V-grooves for the long wavelength domain.

Mass transport was carried out by MOVPE system. To innovate its controllability for the high quality QWR formation, we introduced mass transport temperature, heating rate, and mass transport time as new parameters in addition to V group ambient ratio in reactor.

The formation of high quality V-grooves is more important in this method than before. The use of Saturated Br Water:H_3PO_4:H_2O solution, the pattern transfer to SiO_2 mask, and the orientation alignment of substrate enables us to obtain sharp, smooth and uniform V-grooves on InP substrates. Holography of corner cube type was used for this purpose.

Mass transport was carried out for these V-grooved substrates. And QWRs as small as to expect 2 dimensional quantum confinement effect were successfully fabricated at the bottom of V-grooves. Only QWRs were selectively formed without any parasitic structures. The As and P exchanged layer on the side wall was too thin to contribute to the optical properties in these samples. The uniformity and the quality of regrowth interface was excellent on TEM photos in spite of the large lattice mismatch of InAsP QWRs and a InP barrier material. The material contrast at the interface of QWRs is also understood sufficient from EDX measurement. The sharpness was kept at the bottom of V-grooves and it offered triangular shaped comparatively strained QWRs. Their size was well controlled and QWRs whose base side of less than 20[nm] and the hight of less than 10[nm] was achieved by changing the mass transport temperature. The PL measurement of these samples at 77[K] proved its excellent optical property. Above all, the observation of PL signals at room temperature (20[℃]) was undoubtedly a proof that this method can offer much better quality of QWRs than the conventional one in the point of view of parasitic structures and the crystal quality. FWHM of the PL spectrum for the QWR array made by mass transport at 550[℃] was 30[meV] at 77[K] and 40[meV] at room

temperature. The luminescence of these QWRs made by varying the mass transport temperature covered the entire region for long wavelength lasers needed in telecommunication systems. Moreover, the control of As composition in the QWRs enabled to adjust the PL peak wavelength in the same wavelength domain with the QWR size kept almost constant. Anisotropy of QWR luminescence was observed from all the QWRs made by mass transport and it was in good accordance with theoretically predicted results and the reported experimental ones.

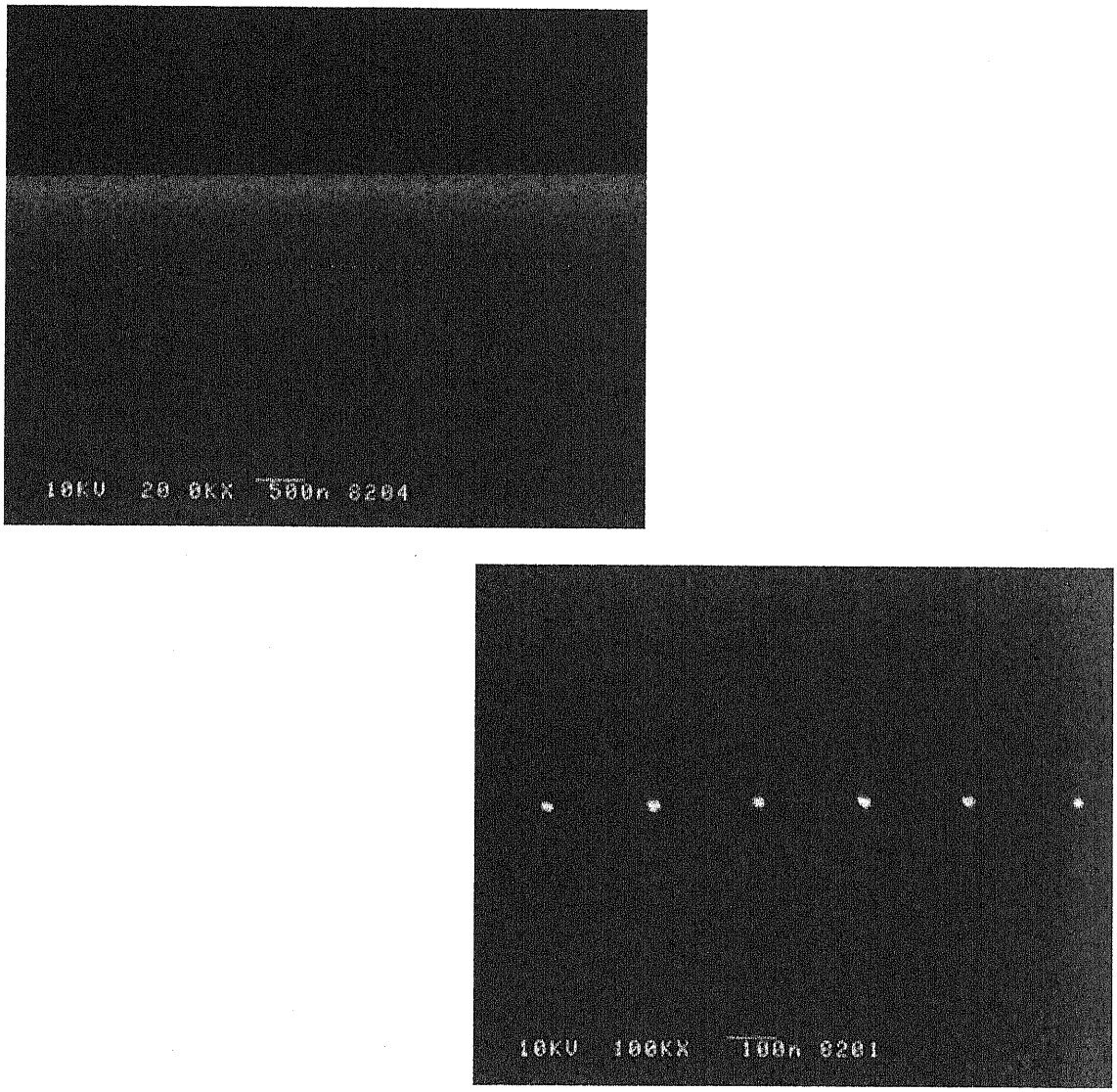

Figure 5-20 QWR array embedded in a InP homojunction PIN structure (above: ×20K, below: ×100K). HCl stain etching is used for the contrast.

These results are very effective to fabricate DFB QWR lasers which is operable under the practical conditions. QWR's quality is improved in almost all the aspects comparing with the conventional one. Though such QWRs are for long wavelength so far, the same method is applicable to the other materials on which the migration of group III materials can happen, too. Figure 5-23 is an example of a simple device on a InP substrate using mass transported QWRs embedded in it. It is a simple InP homojunction PIN structure where non-doped QWRs are equipped. Homogeneity, geometrical size, and regrowth quality is apparently satisfied. QWRs are brightened in relief due to the stain etching in HCl. A beautiful dotted line of QWR array is shown in semiconductor layer structures.

Reference

[1]D.H.Jang, J.S.Kim, K.H.Park, S.Nahm, S.W.Lee, J.K.Lee, H.S.Cho, H.M.Kim, and H.M.Park, "InAsP phase formations during the growth of a GaInAsP/InP distributed feedback laser diode structure on corrugated InP using metalorganic vapor phase epitaxy", ApplPhys.Lett., vol.66, 3191, 1995.

[2]M.Kito, S.Nakamura, N.Otsuka, M.Ishino, and Y.Matsui, "new structure of 1.3mm strained layer multi-quantum well complex coupled distributed feedback lasers", Jpn. J. Appl. Phys., vol.35, 1375 (1996).

[3]M.Kito, N.Otsuka, Y.Yabuuchi, S.Nakamura, M.Ishino, and Y.Matsui, "formation of InAsP layer on corrugated InP substrate by MOVPE for buried grating of DFB lasers", Proc. 9th Int.Conf. on Indium Phosphide and Related Materials, 606, 1997.

[4]M.Kappelt, M.Grundmann, A.Krost, V.Turck, and D.Bimberg, "InGaAs quantum wires grown by low pressure metalorganic chemical vapor deposition on InP V-grooves", Appl. Phys. Lett., vol.68, 1996, 3596.

[5]F.Vouilloz, D.Y.Oberli, M.-A. Dupertuis, A.Gustaffson, F.Reinhardt, and E.Kapon, "Effect of Lateral Confinement on Valence Band Mixing and Polarization Anisotropy in Quantum Wires", Phys. Rev. B, vol.57, 12378-12387 (1998).

■ Chapter 6

Fabrication of InAsP/InP DFB QWR laser using mass transport

6-1 Introduction

The difficulty of the realization of DFB lasers by using the conventional QWRs on V-grooves were already discussed in chapter 4. The proposal of new mass transported QWR arrays discussed in the last chapter was for this application to DFB lasers. They actually showed better characteristics as QWRs and the process itself was very useful to improve the laser substrate quality. In this chapter we try to impress how new DFB QWR lasers with a mass transported QWR array is effective in the innovation of laser characteristics. We confirms that several epoch-making features in mass transported QWRs reduce the barrier toward the realization of DFB QWR lasers operable at room temperature. High quality of QWRs, QWR array as an active grating, materials for long wavelength, and no parasitic structures, such new features in QWRs on V-grooves are significant in our work of this chapter.

6-2 Discussion on layer structures of DFB QWR lasers

No matter how good the properties of QWRs are, lasing of devices is difficult to be achieved if their structure is not well designed. Because a single QWR array's gain is limited to be small due to its volume, the laser structure design must be optimized so that the waveguide loss is constrained effectively. The most important question on our design is where to place a QWR array. For example, our QWRs in chapter 5 was obtained on InP V-grooves as is shown in Figure 5-11 and was embedded in InP finally. Because PL peak wavelength and size dependence of QWRs on mass transport temperature and As/P ambient ratio was well investigated in chapter 5, this knowledge should be made the best use of in the design of laser structures.

From the luminescence intensity and structure size of QWRs, the condition for mass transport temperature was best at 550[℃] in the previous experiment. It offered QWRs whose PL peak wavelength is around 1.5[μm] and the triangular shaped cross section with less than 20[nm] of its base side (see chapter 5). QWRs obtained at this temperature was, in general, small enough to expect a quantum confinement of carriers. And the

subtle tuning to match the luminescence peak to 1.55[μm] is possible by an additional modification of As composition in QWR materials.

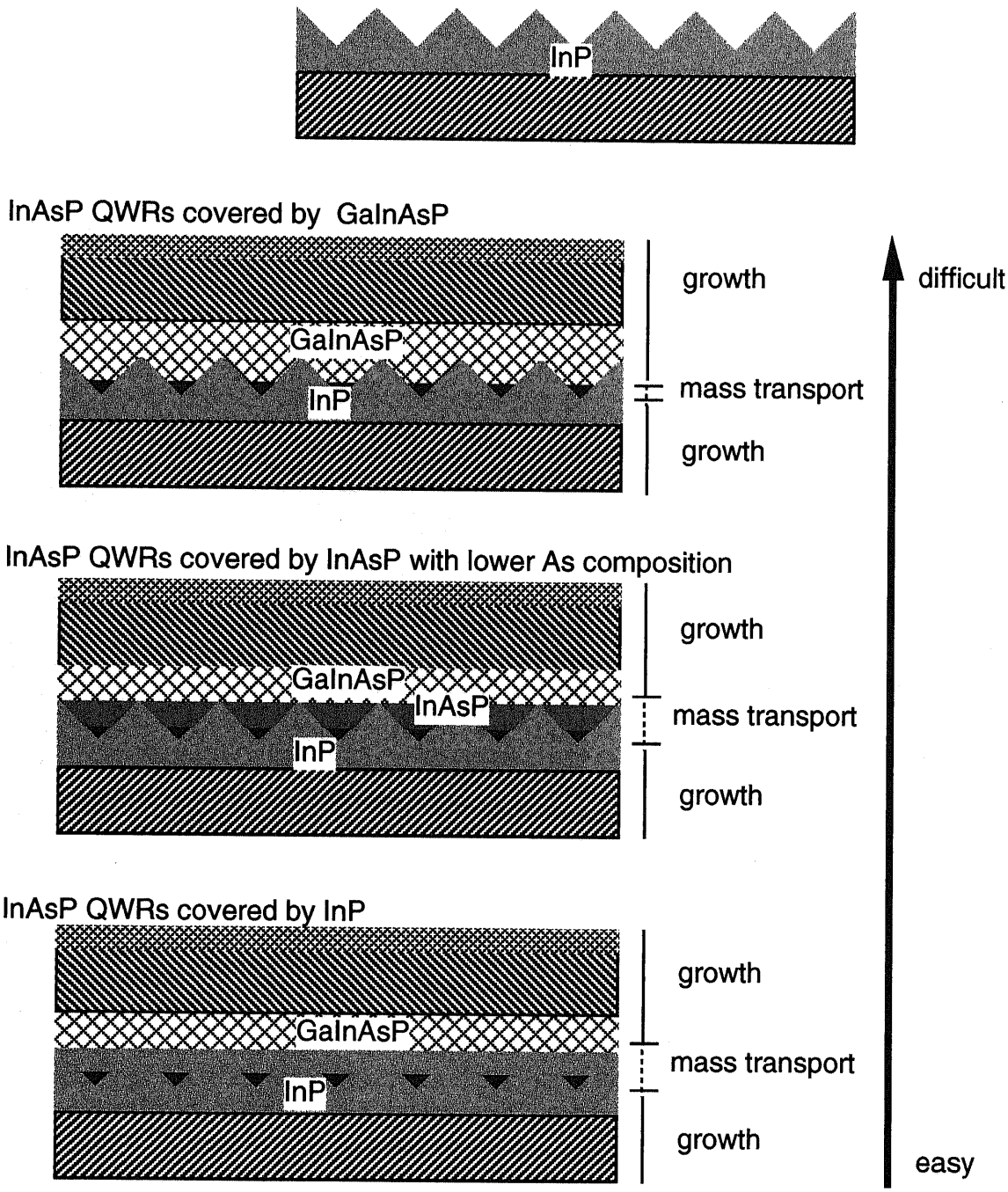

Figure 6-1 Schematic layer structures of possible DFB QWR lasers made on a InP V-grooved substrate. 'Easiness' and 'difficulty' are used with respect to that of regrowth process.

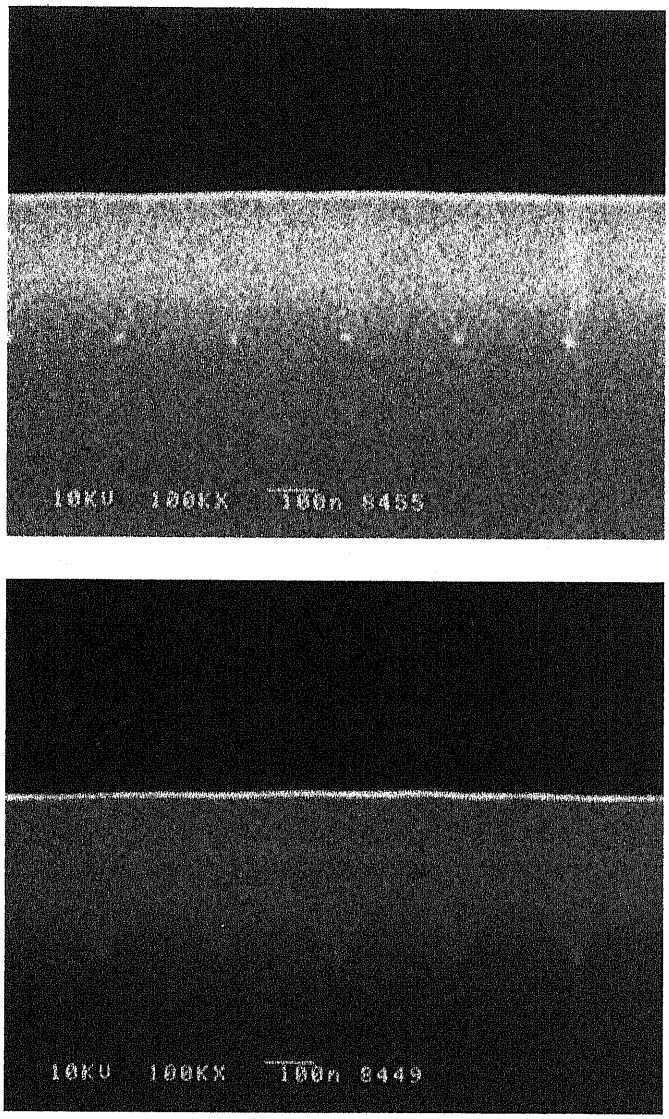

Figure 6-2 Cross-sectional SEM photos of InAsP QWRs buried by mass transported InP (above) and InAsP (below) (after HCl stain etching).

To incorporate such a QWR array on V-grooved InP substrates into the waveguide of laser structures, GaInAsP must be grown directly on it as an ideal case (Figure 6-1). This GaInAsP layer works as a waveguide in these structures. But it is difficult to control the growth of such a compound material with multiple compositional parameters on non-planar substrate. We must always consider the lattice matching condition to regrow a thick layer structure like a cladding layer in lasers. The careless regrowth of materials which potentially give a strain in the structure often leads to the low quality of produced devices.

One possibility to avoid this complexity of growth conditions is to bury and planarize V-grooves with simpler materials before a growth of GaInAsP layer. For this purpose, the growth of InP or the mass transport of InP is considerable (Figure 6-1: upper). But in neither case, QWRs are located in the waveguide. QWRs are distant from a p-doped GaInAsP waveguide just like a grating in conventional DFB lasers (Figure 6-1: lower). Though it is true that this type of lasers is easier to be fabricated, carrier capturing into QWRs is never efficient in such a structure. Because InP used for a planarization works as a barrier against the carrier injection, it is fatal to lasers with a QWR array where leaky current is essentially indispensable due to a large space between QWRs. Therefore, it is

necessary to fill the V-grooves with the different material whose bandgap is lower than InP to reduce the barrier hight. Only InAsP with lower As concentration than QWRs was the possible material in our conditions (Figure 6-1: middle).

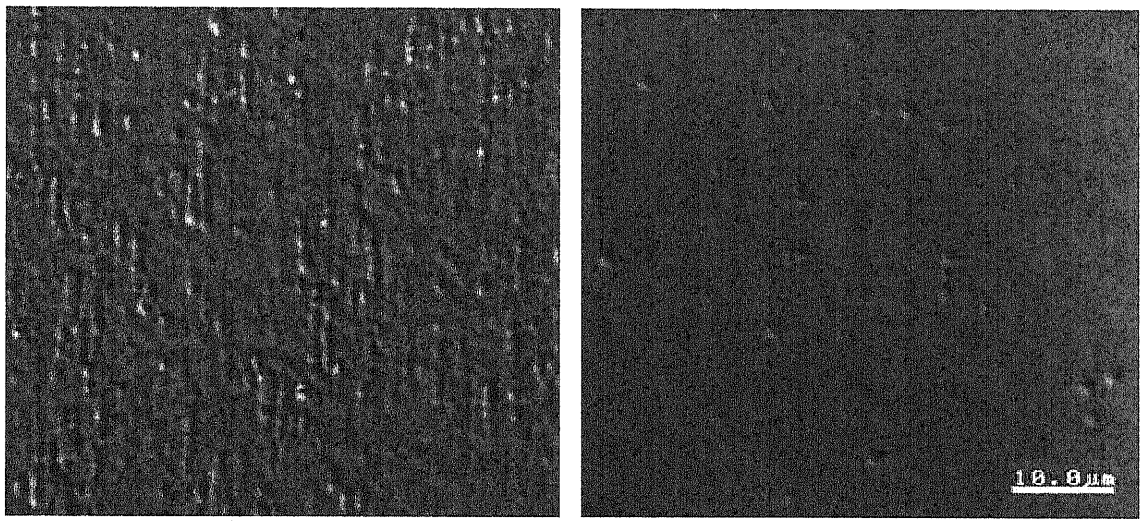

Figure 6-3 Morphology of GaInAsP(Q1.25) layer lattice-matched to InP grown on InP V-grooves, which were planarized by mass transported InP, with InAsP mass transported QWRs (550[℃]). (left: after 30 sec. of InP mass transport for planarization, right: after 5 min. of InP mass transport, both done increasing temperature up to 610[℃]).

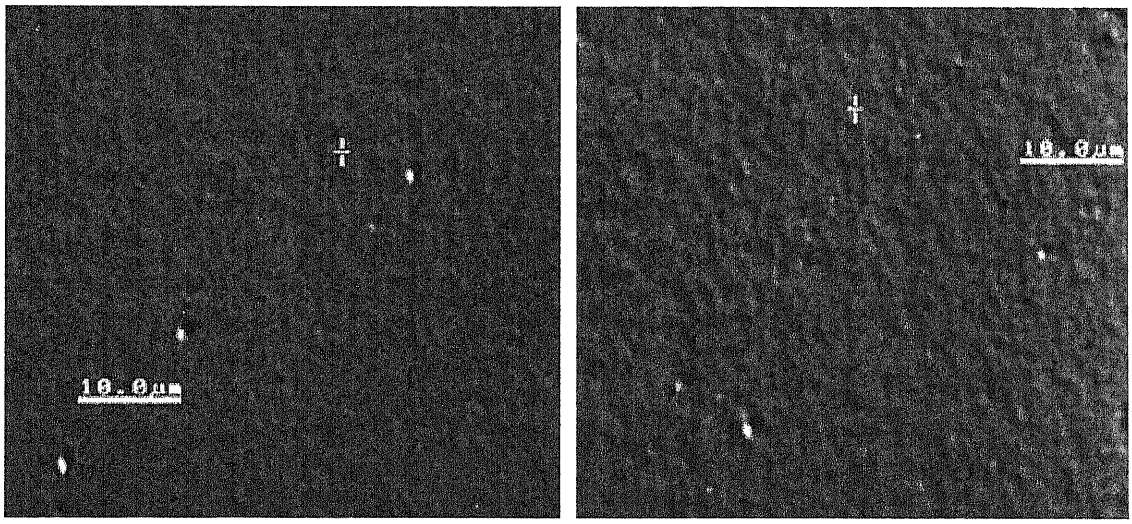

Figure 6-4 The difference of GaInAsP surface morphology by mass transported materials for a planarization. InP V-grooves with InAsP QWRs were planarized by mass transported InP heating and staying at 610[℃] for 10 min. (left), and mass transported InAsP under the same condition (right). And then GaInAsP lattice matched to InP was grown on it. In the right case, mass transported InAsP has less As composition than QWRs.

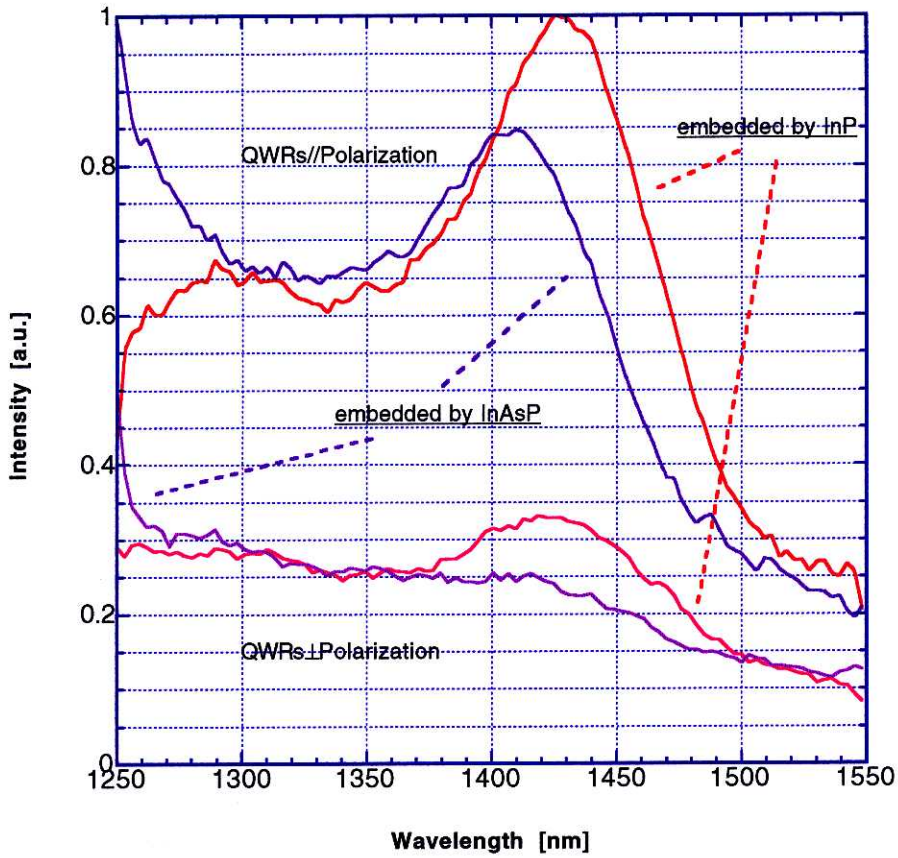

Figure 6-5 PL spectra at 77[K] of InAsP QWR array embedded by mass transported InP and InAsP barriers for the planarization of a V-grooved substrate. Polarization dependence is also shown for each one.

Figure 6-2 is the QWRs on V-grooves embedded with mass transported InP or InAsP of which As/P ambient ratio was 0.00886. It was 0.01477 for mass transported InAsP as QWRs. Though the material contrast by stain etching is naturally weak in the case of InAsP mass transport, it shows the formation of QWRs at the bottom in both cases, and the introduction of a successive mass transport after the formation of QWRs doesn't disturb the processing to fabricate lasers. It was also experimentally observed that the regrowth quality was certainly improved through the planarization (Figure 6-3). It is clear that the surface morphology of GaInAsP (Q1.25) grown under the condition of matching to InP is better when the V-grooves are planarized for a longer time by InP mass transport. When we compare the surface morphology of planarized substrates by mass transported InP and InAsP, its quality is worse in the case of InAsP (Figure 6-4).The condition of mass transport for InAsP planarization is the same as before. Though the use of InAsP reduces the lattice mismatch to QWRs, it, to the contrary ,is enhanced against the InP on the side wall and the uniformity of the composition of mass transported InAsP is seriously influenced by the strain distribution on the surface. It is possibly the cause of lower quality observed in above.

Because the mass transport phenomenon is a sort of thermal annealing in a MOVPE (metal organic vapor phase epitaxy) reactor, the material contrast at the interface of QWRs and mass transported barriers for the planarization is weaken owing to the mixture of

composed materials. It is shown on the SEM (scanning electron microscope) image in Figure 6-3 as an ambiguous contrast of QWRs. The intermixing happens only on the mass transported side of QWRs. It is an unfavorable phenomenon for QWRs which need a sharpness of heterostructure interface for a stronger confinement and a better carrier transport. Hence, it is significant to check whether this phenomenon is fatal on the optical characteristics of QWRs or not.

Figure 6-5 is the PL spectrum of such QWRs planarized by mass transported InP or InAsP. They are the same sample as those in Figure 6-4. The peak wavelength shift compared with samples whose V-grooves are filled by the ordinary growth of InP was about 30[nm] on the long wavelength side (see Figure 5-19). The decrease of a quantum confinement by the interfacial intermixing reflects on it. The difference between InP and InAsP is probably due to the strain effect and the influence of this intermixing. The peak for InAsP is found on the shorter wavelength side of InP. Because the barrier hight surrounding QWRs is asymmetric in the case of InAsP and decreased comparing with the case of InP, the confinement energy of the ground state of QWRs is lower than that of InP with the other conditions unchanged. But its contribution is contrary to the experimental result and is concluded to be very small in this case. The strain relaxation effect must be considered and it results the wavelength shift on the shorter wavelength side of the peak originated from the heavy hole. Furthermore, because the compositional difference of QWRs and barriers is little in the case of InAsP, the intermixing has to be more suppressed. It apparently contributes to the wavelength shift in the same direction as the strain. Therefore, above difference is possibly explained as a complex effect of the strain and the intermixing. Note that the symmetric barrier potential of InP shows 2 peaks just as before, but that the asymmetric barriers of InAsP shows only one peak. The peak expected on the left side of InAsP case belongs to GaInAsP. The hidden second peak in InAsP can be explained as the influence of a relatively strong luminescence of GaInAsP because of the low quality of QWRs and also as the asymmetric potential shape of this structure. It is impossible to decide which is dominant only from these PL spectra.

The linear polarization trend in QWRs are kept for both types in Figure 6-5. In this sense, The optical characteristics as QWRs are judged to be basically conserved even after the planarization of V-grooves. As a result, though QWR's characteristics are certainly modified by the mass transport planarization, such QWRs still keep a quality applicable to devices. The planarization technique is useful for the device application.

6-3 Mass transport method for irregular V-grooved structure on InP substrates

We discussed on the possibility of a fabrication of DFB lasers using QWRs on a V-grooved InP substrate. Though the mass transport for the planarization was new and effective for the improvement of a regrowth quality, the laser structures were suitable for neither carrier capturing nor optical confinement factor. We fabricated such a structure as is shown in Figure 6-1 by using the planarization technique during the growth. But it just showed the difficulty of carrier transport into QWRs in those structures, and thus, no electric luminescence were observed eventually. New laser structures without the regrowth of GaInAsP must be considered. It means the necessity of QWRs formed on a substrate with different structures from simple InP V-grooves.

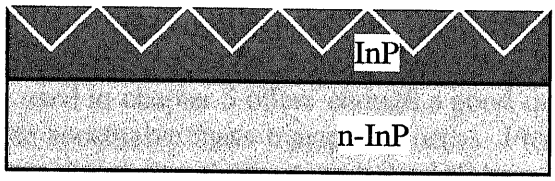

Substrate used in chapter 5
without a waveguide

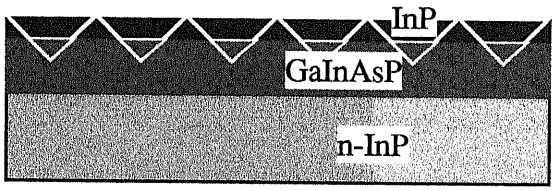

Substrate for a laser structure
with a waveguide

Figure 6-5 Lower laser structures before making V-grooves. The above one is the simplest, but not appropriate for a laser fabrication owing to the regrowth problem on a non-planar substrate. Thebelow one is the new type which should be discussed in this chapter.

The additional growth processing for a GaInAsP waveguide prevented us from obtaining a simple and excellent laser structure. And even if its growth problem is cleared, QWRs are not structurally formed in the middle of the waveguide as far as we use a simple V-grooved InP substrate (Figure 6-1). Anyway it is not a wise way to form a waveguide on the upper side of QWRs for the device fabrication, though it was very convenient to investigate fundamental properties of QWRs.

The simplest idea to avoid the problem of GaInAsP growth is to grow it before the formation of V-grooves. Then the regrown material is only InP for a cladding layer and InGaAs for a capping layer. Figure 6-6 is a new structure prepared for a test of this idea. The GaInAsP waveguide is already inserted in the substrate and is embedded by InP. InP serves as a mass transport layer to offer In for the migration on the non-planar substrate. The thickness of this layer is significant to control the position of QWRs. Now we assume that the V-groove size is fixed. About 100[nm] depth of V-grooves were used in the chapter 5. 2 types of substrates including GaInAsP layer were prepared with regard to the position of QWRs. One has a thin InP layer on top of GaInAsP to make a deep V-grooves in the GaInAsP layer, and the other has thicker one so as to place the bottom of V-grooves just at the upper interface of GaInAsP layer. As far as we concern the optical confinement factor and carrier capturing, the former type is much better than the latter because QWR is located closer to the center of a waveguide and has a much larger surface area surrounded by GaInAsP. But the latter also seems good if GaInAsP can be grown on it. Then, QWRs are located just at the narrow path between the barriers of InP and it leads to the carrier injection confinement to QWRs. But we don't discuss further in detail on this challenge in this chapter because it brings the same problem as the last section again. It is less useful to persist to such a problem now.

Because not only InP but also GaInAsP must be wet etched for the above substrate, we have to reconsider the wet etching process to make V-grooves. We have already known that the solution used in chapter 5 offers enough a good quality of etched surfaces to be compensated by the successive mass transport process. From this point of view, it is convenient for us to use the same solution to etch the InP layer at first. The question is if the GaInAsP layer is also etched by the same solution and how fast its etching rate comparing that of InP. The wet etched substrate are displayed in Figure 6-7. One is etched only by Saturated Br Water:H_3PO_4:H_2O used in chapter 5 for 25 sec., and the other is stopped the wet etching once at 15 sec. and followed by H_2SO_4:H_2O_2:H_2O for 5 sec. All these wet etchings were done at room temperature (20℃).

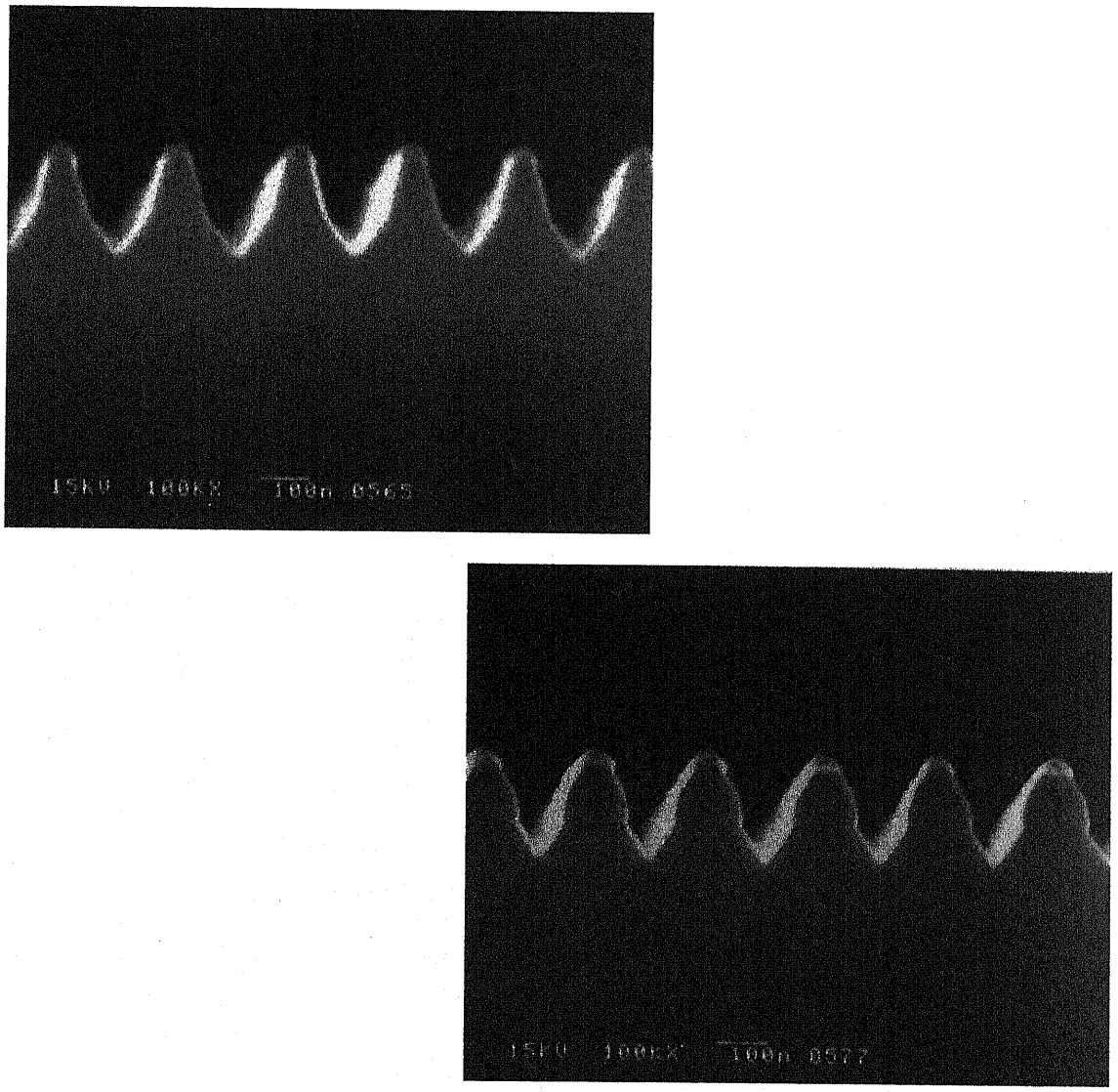

Figure 6-6 V-grooved structure made on new substrates with GaInAsP waveguiding layer. The etchant was Saturated Br+H_3PO_4+H_2O (2:1:15) (25 sec.) for above, and Saturated Br+H_3PO_4+H_2O (15 sec.) & H_2SO_4+H_2O_2+H_2O (1:1:5) (5 sec.) for below. In both pictures, the boundary of InP and GaInAsP layers in Figure 6-5 is evident as a step of side walls.

It shows that the solution used in chapter 5 also works for GaInAsP. Though the etching rate is a little bit different, there is not a serious influence left such as underetching at the boundary of InP and GaInAsP except for a disappearance of the smoothness on the side wall. This discrete change of the orientation of exposed surface on the side wall corresponds to the interface of both InP and GaInAsP layer. The index of orientation of side walls in the InP layer is higher than before in Figure 6-7 (the above SEM picture), and the sharpness of a V-groove bottom in the GaInAsP layer is different from that of InP. Considering the high index number of InP side walls, the wet etching rate in GaInAsP layer is faster than in the InP layer. Because underetching in GaInAsP with above InP layer as a mask occurs, the floating InP layer is eaten because it has a (100) exposed surface beneath it. Side walls are successively etched in the solution in spite of an appearance of the (111)A stable surface of which wet etching rate is very slow. And V-grooves are sharpened with the angle proper to GaInAsP while it happens. This variation in the cross-sectional shape of V-grooves directly reflects on the difference in a confinement energy of QWRs.

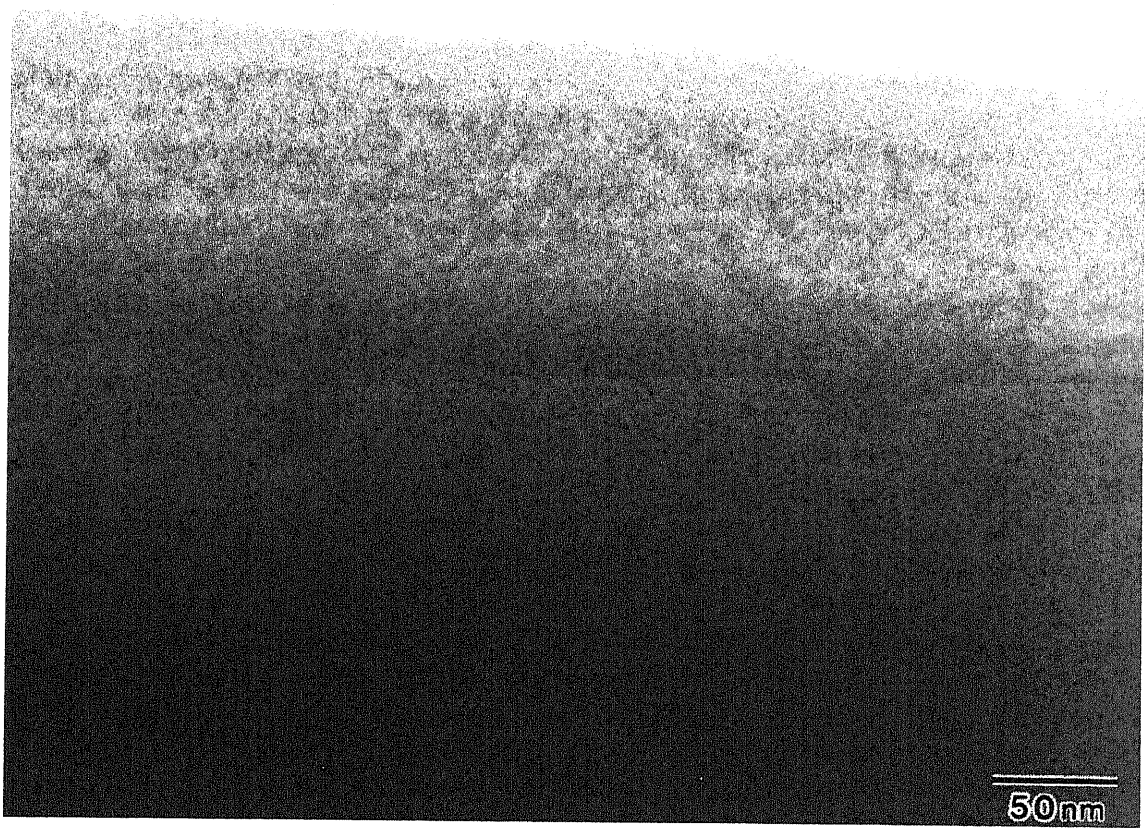

Figure 6-7-1 Cross-sectional TEM image of QWRs formed by mass transport on GaInAsP V-grooved substrate. Triangular QWRs are observed at the bottom of V-grooves. And the boundary of InP and GaInAsP runs in the middle of this image. The As and P exchanged layer is also found on the side walls.

The sharpness of V-grooves can be achieved by the other solution, too. As an etchant for GaInAsP the solution based on a sulfuric acid is well-known. After making holes in the InP layer with the previous Br based solution, GaInAsP is etched with this sulfuric acid solution. But underetching in GaInAsP layer is much faster than InP in this solution due to the selectivity of wet etching. And thus, the cross-sectional shape is more complicated than before. The large side etching in the GaInAsP layer is conspicuous in the below image of Figure 6-7.

The first solution is evidently much better in the point of simplicity as a method and as a resulted structure on substrates. The controllable side etching in GaInAsP layer is useful and it never cause a mushroom structure on the substrate because both InP and GaInAsP is etched with the same solution without an interval. The avoidance of irregular structures like a mushroom is important to induce a stable and controllable mass transport phenomenon in the next step. It is equivalent to the reproducibility of QWRs with the same optical characteristics. As a conclusion, we could successfully obtain a good quality of V-grooves on the new substrates again.

6-4 Formation of QWRs at the bottom of GaInAsP V-grooves by mass transport

It was demonstrated in Figure 6-6 that V-grooves were formed in the wafer with an GaInAsP waveguide in it. The edge of V-grooves penetrated into the waveguide, and its position was controllable in the waveguide. The same mass transport process as in Chapter 5 was done for these samples following the temperature diagram of Figure 5-2. 550[℃] and 530[℃] was selected as a mass transport temperature. The heating rate was set at 0.6~0.7[℃/s]. And TBP and TBAs ambient pressure stayed at $1.83\ 10^{-1}$[mbar] and $2.70\ 10^{-3}$[mbar] respectively.

Because the contrast of InAsP (QWR) and GaInAsP (waveguide and barrier) is very weak even with the stain etching due to the similar chemical property in the etchants known for these materials, it was difficult to check a formation of QWRs in the V-grooves by the SEM observation. Therefore, only the results by TEM (transmission electron microscope) observation are shown in this section. The sample was made by mass transport at 550℃. The TEM photo at low magnification (Figure 6-7:×500K&×2M) clearly show the formation of QWRs at the bottom of V-grooves. Their size is almost the same as ones in chapter 5 (It was made using totally the same conditions except for the difference of substrate). The P and As exchanged thin layer on the V-grooved surface is also found again. The rounded corner of V-groove's shoulder suggests that the migrated In during the mass transport process is supplied from this convex part again. It is notable that 2 surface with different orientations appear as side walls of InP. It is because that the original side walls of InP before mass transport had an orientation with a high index number and 2 stable orientations reformed as side walls disappeared by mass transport. The above lines which are far from QWRs are (111)A surface which was also observed in Figure 5-2. The other surface corresponds to higher index such as (211).

The lattice image of the QWR is also presented in Figure 6-7. No dislocations and defects are found at the interface as it was in chapter 5. It does not prove only the high quality of QWRs of this sample made in GaInAsP V-grooves, but also the effectiveness of using mass transport method for the formation of nanostructures. The excellent

interface of QWR and barrier materials was shown again in spite of the difference of used substrates. From this point of view, the quality of mass transported QWRs is high enough to be applied to optical devices employing them.

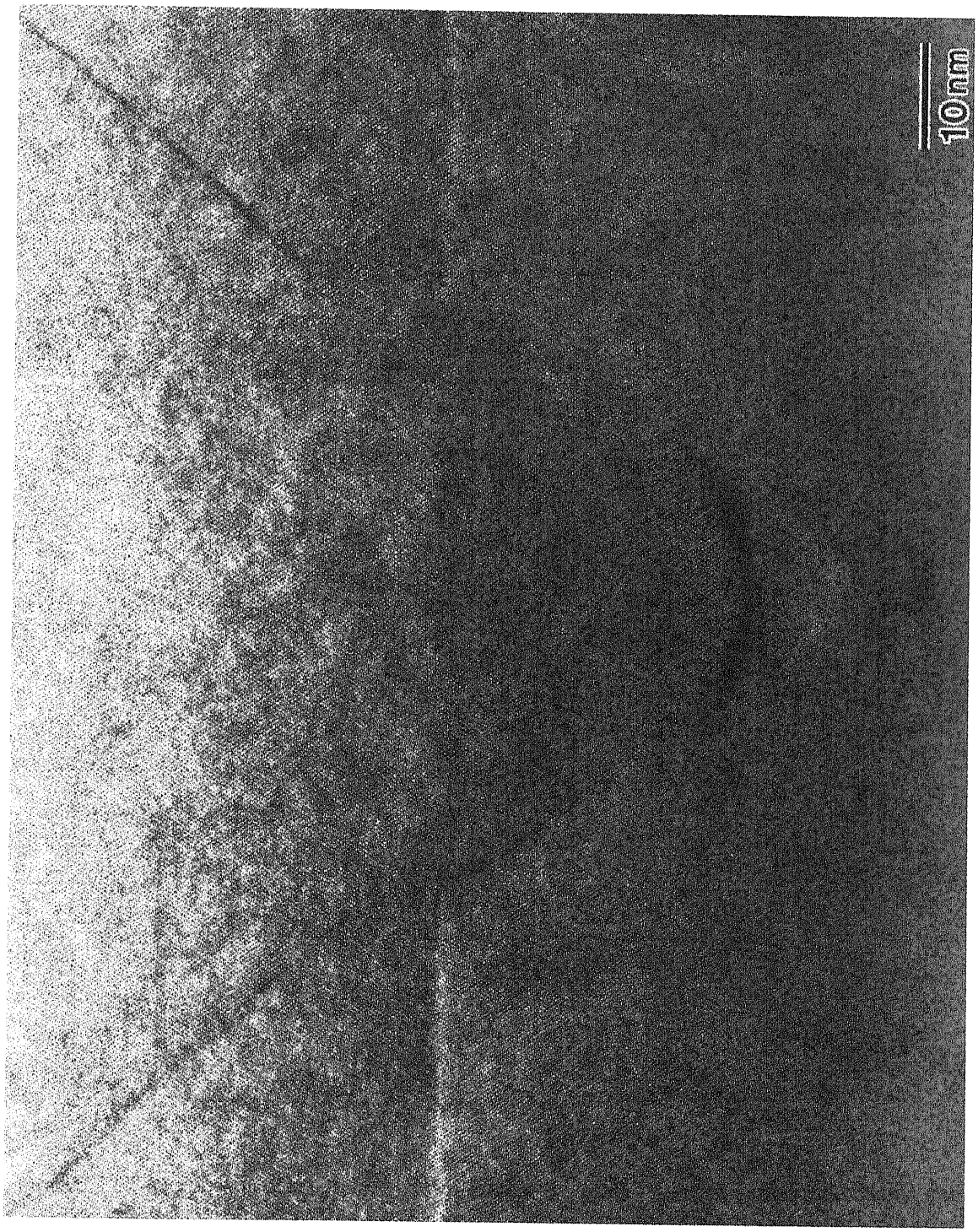

Figure 6-7-2 Lattice image of QWRs made by mass transport on GaInAsP V-grooves. No defects and dislocations were found in spite of the strained heterostructure on the non-planar substrate.

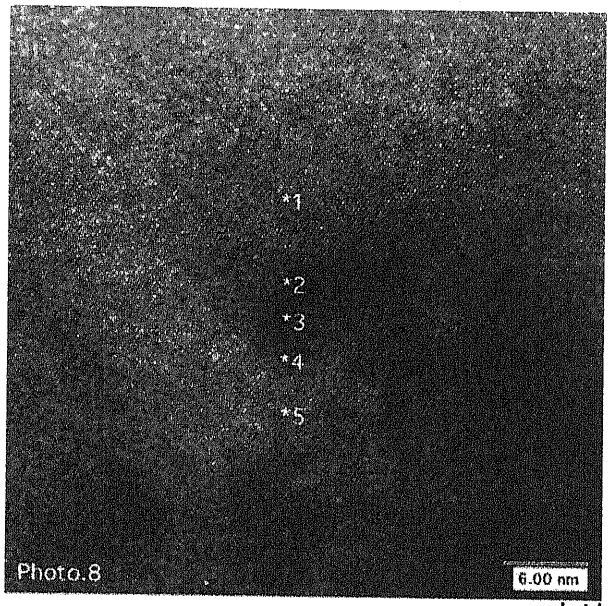

point1

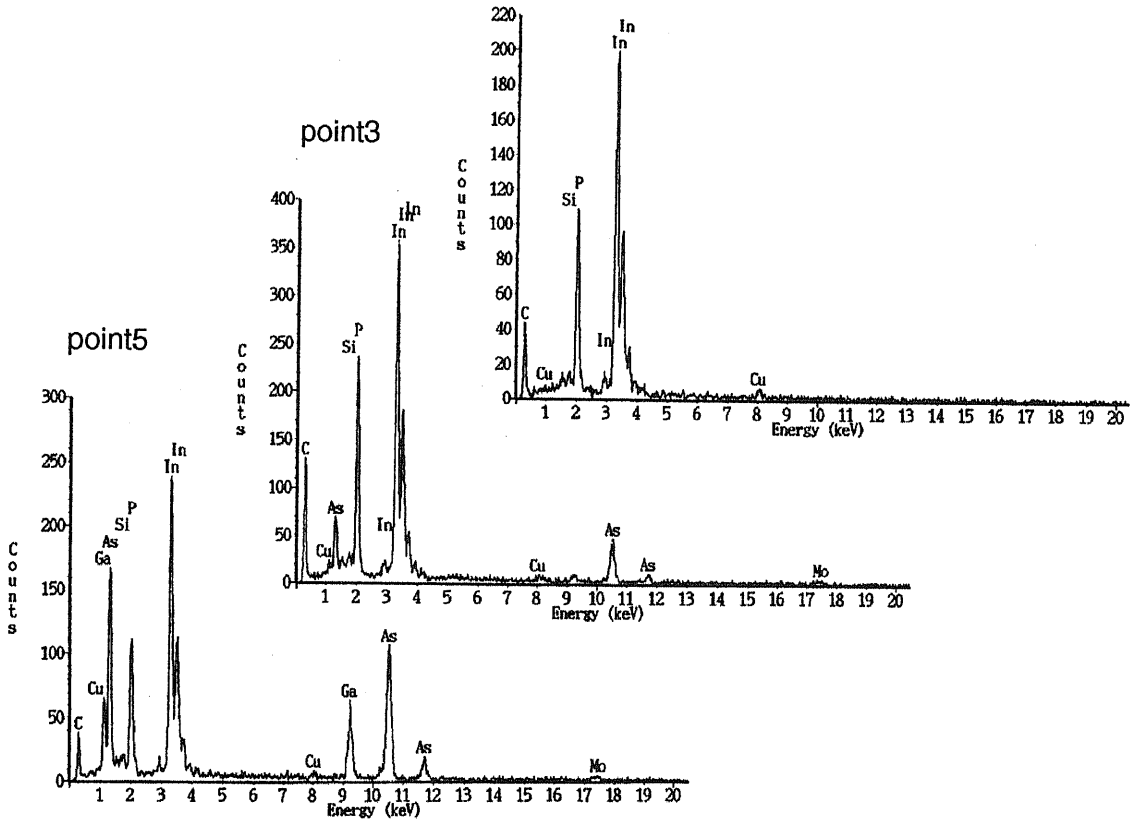

Figure 6-8 EDX spectrum of the new QWR formed on GaInAsP V-grooved substrates. Almost no Ga was contained in the QWR. It means that the strained InAsP QWR is formed again as was observed in chapter 5.

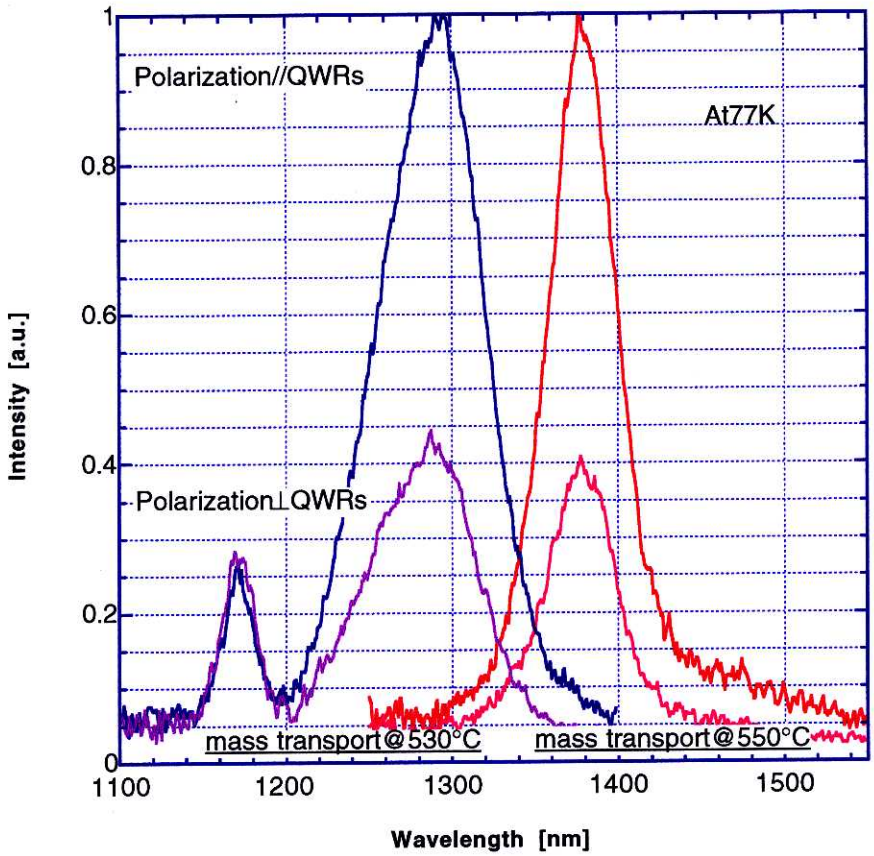

Figure 6-9 PL spectrum of new QWRs made on GaInAsP V-grooved substrates. Polarization dependence is also shown. The peak at 1170[nm] corresponds to a bulk GaInAsP. It shows a different polarization characteristic between QWRs and a bulk material.

EDX (energy dispersive X ray) analysis showed a quite interesting results on the mass transport phenomenon (Figure 6-8). They are the spectrum at 3 points designated by the number in the photos. In GaInAsP layer, 4 elements were found naturally, but in QWRs almost no Ga is found. The recognized small peak was as small as to be judged as the background influence. And InP layer, only In and P was found. It means that no influence on the composition of QWRs is given by the GaInAsP V-grooved materials. The mass transport is suppressed by containing Ga or Al as is understood from the self-ordering phenomenon in GaAs or AlGaAs (see chapter 4). Hence, In the new QWRs are supplied by the InP layer grown on the GaInAsP layer. The rounded convex part of In layer is where the mass transport occurred. In this sense, it is natural to think that the material composition in new QWRs are almost the same as that of chapter 5.

This EDX results also tells us that the sharp material contrast at the interface of a mass transported QWR was achieved again.

6-5 Photoluminescence spectrum of new InAsP QWRs on GaInAsP V-grooves

As a next step, the difference in QWR properties from those of chapter 5 must be clarified. The V-groove shape is different at first because it is made in the GaInAsP layer

this time. And the barrier height is decreased on the GaInAsP side and is asymmetric in the case that the V-grooves are filled with InP. Moreover, the side walls of the V-groove is constituted of InP and GaInAsP, and thus ,the composition of InAsP QWR is unknown. Ga might be contained in QWRs during the mass transport process.

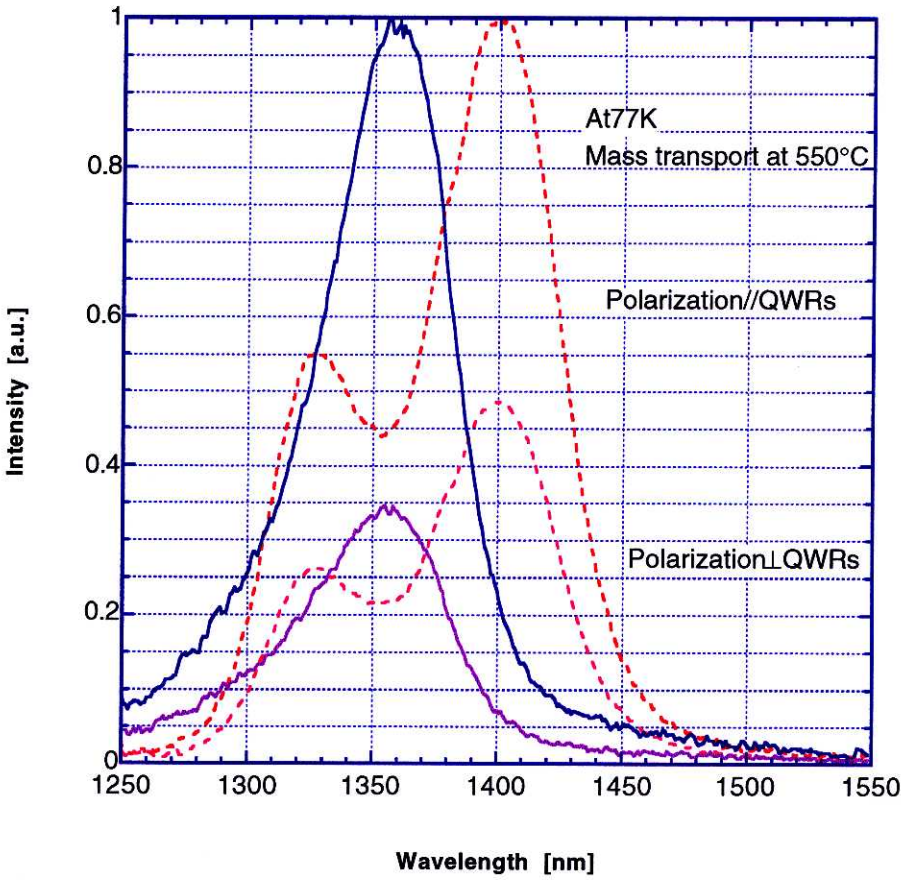

Figure 6-10 PL spectrum of QWRs made by mass transport at 550[℃] (with and without GaInAsP layer beneath QWRs). The spectrum with 2 peaks is for the QWR array on InP V-grooved substrate. The spectrum with a single peak is for the new QWR array on GaInAsP V-grooved substrate. Both are covered with InP.

PL (photoluminescence) spectrum is shown in Figure 6-9. Both QWRs were formed under the same mass transport condition by changing only their mass transport temperature. As is mentioned in the last section, the result of both QWRs at 530℃ and 550[℃] are shown. The V-grooves were filled with InP in these samples. The small peak around at 1170[nm] comes from bulk GaInAsP waveguide layer. The linear polarization of PL signal is also shown in Figure 6-8. The signal intensity parallel to the QWR array is stronger than that perpendicular to the QWR array. Its different property between the QWRs and the bulk GaInAsP is revealed. The bulk material has no polarization dependence.

The comparison of PL signal at 77[K] with QWRs in chapter 5 is displayed in Figure 6-10. The newly formed QWR's peak is shifted toward the shorter wavelength side comparing the counterpart in chapter 5. It is needless to say that the difference in both

samples was only the prepared V-grooved substrate and that the mass transport condition was completely the same. It is known from TEM observation (Figure 6-7) that the most part of new QWRs are surrounded by GaInAsP and that only the upper side is covered with InP. The shift would rather be explained by the effect of strain and the change of a cross-sectional shape of V-grooves similarly to the discussion in 6-2. There the cover material of QWR was InAsP and the V-grooved substrate was InP instead of InP and GaInAsP respectively in this case. Both cases have a asymmetric potential profile around QWRs in common. Though the decrease of barriers comparing with the QWRs surrounded by InP results the shift to a long wavelength side, it is not the case observed in PL spectrum. And thus, the strain relaxation on the GaInAsP side and the sharpen V-grooves in GaInAsP by the introduction of Ga and As is the main reason of a shift on the short wavelength side. Both contributes to pull up the ground state of electrons and heavy holes on the higher energy side.

In the new QWR's spectrum only a single peak was observed. It was probably caused by the asymmetric potential and the second peak originating from the higher energy states disappeared. It is not certain whether it is brought by the disappearance of those confined states or the decrease of emission efficiency from such energy states. But the disappearance of confined states with high index is not surprising when the barrier potential is not symmetric.

6-6 Laser structure for DFB QWR lasers

Based on the knowledge obtained in the previous sections, we design the DFB laser structure. The most important parameter is Bragg wavelength. Because the mass transport on GaInAsP V-grooves is considered to be the same as that on InP V-grooves, we can utilize the accumulated data in chapter 5 for various cases. This approximation is based on the result on EDX analysis. According to this In is always supplied from the top InP layer, and thus the amount of mass transport is more or less the same whether we use InP V-grooved substrate or GaInAsP V-grooved substrate. It means that the QWRs formed at the bottom is the same in composition and volume if a mass transport condition is kept the same. We take this assumption. Hence, all we have to do is to add the influence by the difference of structural parameters like barrier materials.

The barrier hight, strain, and the V-groove's sharpness should be reflected on such a modification of expected emission peak wavelength of QWRs (Figure 6-10). In addition to this, we have to consider the case where QWRs are embedded by mass transport. In that case, the shift of emission peak is also observed due to the modified potential profile on the mass transported side of QWRs. It is estimated by comparing Figure 6-3 with Figure 5-19. And finally the shift caused by the difference of mass transport process itself must be added. Therefore, the expected emission peak wavelength of QWRs is expressed as

$$\begin{aligned}\lambda_{cavity} &= \lambda + \Delta\lambda_{barrier} + \Delta\lambda_{strain} + \Delta\lambda_{sharpness} + \Delta\lambda_{planarization} + \Delta\lambda_{masstransport} \\ &= \lambda - 40 + 30 + \Delta\lambda_{masstransport} \\ &= \lambda - 10 + \Delta\lambda_{masstransport}\end{aligned} \quad (1)$$

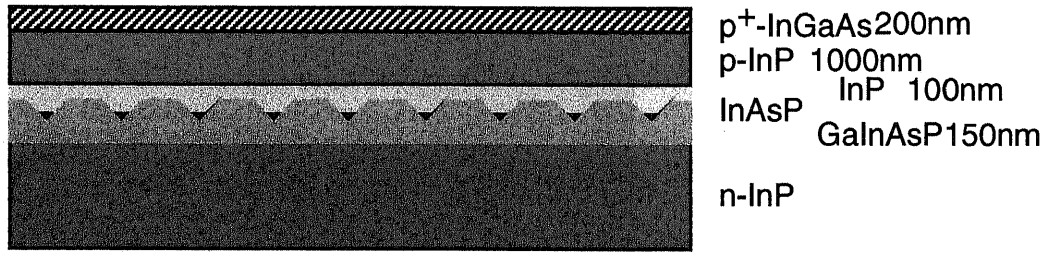

Figure 6-11 Longitudinal layer structure of a DFB laser using mass transported QWR array as an active grating. The layer thickness shown above is for placing QWRs in a waveguide. The InP of 100[nm] should be replaced with that of 120[nm] for locating them on the border of GaInAsP and InP.

The first term is the wavelength in Figure 5-20. It is determined by choosing 'As and P ambient ratio' and 'mass transport temperature'. Note that those wavelengths are measured at 77[K]. We must add around 100[nm] to know the wavelength at room temperature. The next terms from second to forth are the condition of barrier materials. And the fifth is for the QWRs embedded by mass transport. The final term is for the case where the TBP ambient pressure is varied. Remember that all the experiments in chapter 5 were done with this TBP ambient pressure constant. But in this paper, it is always kept at the same value, and thus the last term may be considered to be zero. This is the process to achieve the matching of Bragg wavelength to a QWR gain profile.

Figure 6-11 is the longitudinal laser structure employing a new QWR array as an active grating. The detail of each layer is added on the right side of the figure. It has already been mentioned that there are 2 possible samples with regard to the QWR location in a waveguide. One is in the waveguide and the other is at the boundary on the upper side of the waveguide. Both types were prepared. V-grooves are buried and planarized by mass transported InP after the formation of QWRs. QWRs were made using the following condition:

mass transport temperature: 550[℃]

TBP pressure: 1.83×10^{-1} [mbar]

TBAs pressure: 2.70×10^{-3} [mbar]

The succeeding InP mass transport process was done by simply stopping the supply for As in the above and raising the temperature in MOVPE reactor up to 610[℃]. 610[℃] is the temperature condition for p-InP growth. The SEM cross-sectional observations of such a structure is presented in Figure 6-12. HCl stain etching was added to take these photos. And the InP cover layer was grown, not mass transported in this case. The InAsP of QWRs is not contrast to GaInAsP of the waveguide very well due to a similar etching property against HCl. But it is observed that the QWR array is successfully fabricated at the bottom of V-grooves (Figure 6-11: above) by the fact that the sharp V-grooves are originally made in GaInAsP layer and now that their edge is ambiguous because of the existence of InAsP at the bottom. If the V-grooves were filled only with InP, the sharp V-shaped contrast in materials would appear by the stain etching. On the other hand, the QWRs made at the boundary of a waveguide (Figure 6-12:below) is clearly seen in the SEM image as sticking out structures.

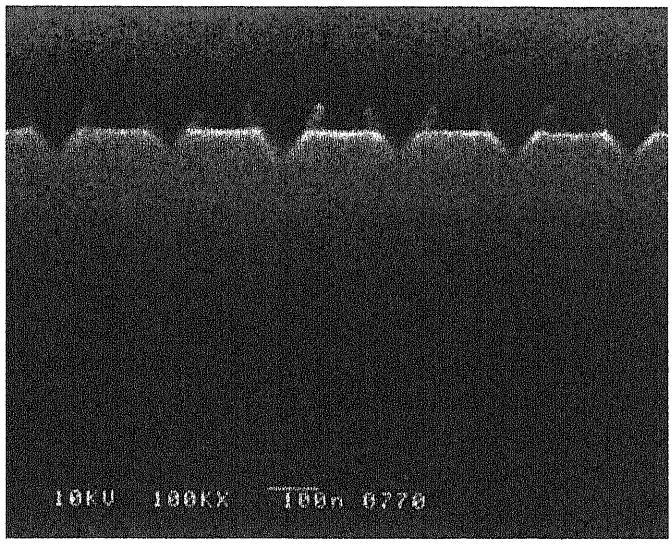

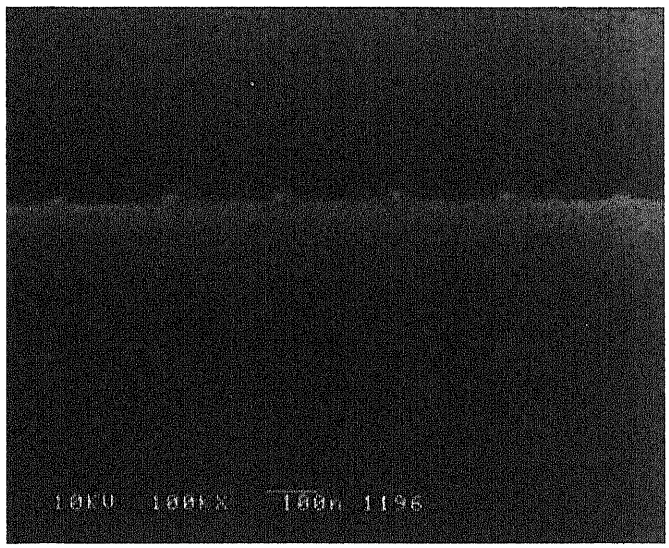

Figure 6-12 Cross-sectional SEM observation of DFB QWR laser structures with an InAsP QWR array in the GaInAsP waveguide (above) and on the upper waveguide border (below). In the above, QWRs are formed at the bottom of V-groove, and the horizontal line is the boundary of the InP cladding layer and GaInAsP waveguide. The interface of the original InP capping layer for mass transport and the regrown InP is highlighted due the existence of a very thin InAsP layer on the side walls. In the below, each sticking out dot in the picture is a QWR. The samples are stain-etched in HCl.

6-7 Fabrication of 1.5μm DFB lasers using InAsP QWR array by mass transport

Broad area lasers with the structure of Figure 6-11 were fabricated. Both types of lasers whose QWRs were located in the GaInAsP waveguide and on its boundary were prepared. The other conditions were completely the same for these 2 lasers. The mass transport condition for QWRs was

mass transport temperature: 550[℃]
TBP pressure: 1.83×10^{-1} [mbar]
TBAs pressure: 2.70×10^{-3} [mbar].

Only TBAs pressure was modified so that the emission peak wavelength of QWRs is found around at 1550[nm]. This modification was determined by taking other conditions into consideration following the process mentioned in the last section. After the formation of QWRs, the planarization by InP mass transport was introduced for the improvement of the surface morphology of laser samples. The preparation of V-grooves were previously completed. The Bragg wavelength was designed at 1536[nm]. The effective index in the structure shown in Figure 6-11 was estimated as 3.20 assuming the waveguide thickness of 185[nm] from TEM observation. And the grating pitch was about 240[nm]. It results above Bragg wavelength. But it is just an approximated value. For instance, the error of ±4 [nm] in the grating pitch equals that of ±25[nm] in Bragg wavelength. Therefore, we set Bragg wavelength at 1530[nm], not at 1550[nm] so that the DFB lasing mode overlapped with the gain profile of QWRs with its peak wavelength at 1550[nm] even in the worst case.

A contact hole on SiO_2 layer was made after depositing SiO_2 film on the p-side of a laser substrate and Ti/Au was evaporated as electrodes on both sides. The stripe width was 100[μm]. It is aligned in the perpendicular direction to the QWR array for the formation of DFB cavity. The samples with a 750[μm] cavity were cut out from it and measured with their facets as cleaved under pulsed current condition. The pulse repetition was 1kHz and its duty was 0.01%. The measurement was carried out at room temperature (20℃).

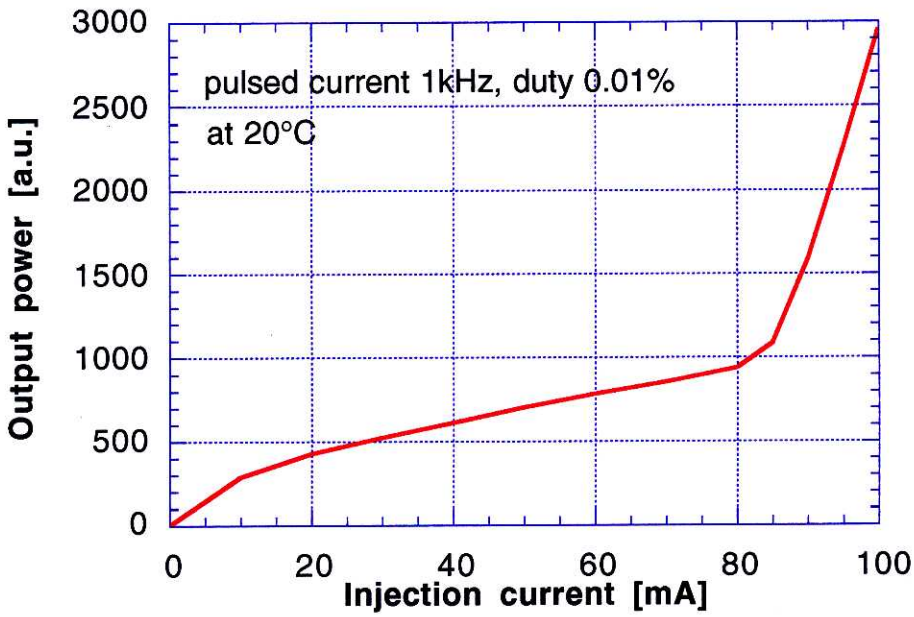

Figure 6-13 L-I curve of the DFB laser with a QWR array as an active grating. The QWRs are located in the waveguide. The cavity length was 750[μm], and the stripe width was 100[μm]. Pulsed current of 1[μs] repetition rate and 0.1% duty ratio was injected at room temperature.

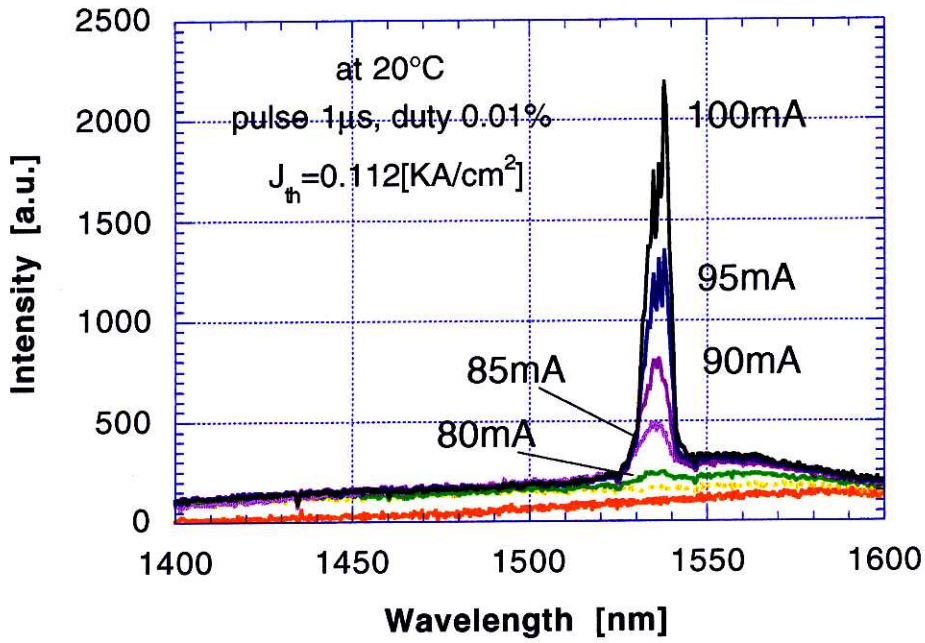

Figure 6-14 Lasing spectrum of DFB QWR lasers at room temperature under pulsed current injection. The same sample as that of Figure 6-13 under the same conditions. Lasing at 1535[nm] is observed. The emission peak is around 1560[nm] and away from the lasing mode by 25[nm].

No emission was found for the samples where the QWRs were formed at the boundary of a waveguide. In this case, the waveguide did not work as a pool to store the carriers temporarily and convey them to QWRs. It also proves that the carriers captured in QWRs directly are very little. The weak luminescence of GaInAsP was observed under the current injection. From this result, the difficulty to expect the lasing of DFB QWR lasers made on InP simple V-grooved substrate that we discussed in the beginning of this chapter is inferable. In such lasers QWR array has to be located at the edge or outside of a waveguide. And thus, its structure is disadvantageous. The lack of SCH (separate confinement heterostructure) was understood to be a serious problem in DFB QWR lasers. SCH was originally introduced in QWL lasers to improve the optical confinement structure, but it also worked for the improvement of carrier capturing in QWLs. The carrier escape from saturated QWLs was not a negligible problem in QWL lasers, either. And the carrier leakage through the pass between QWRs is also to be considered in devices using QWRs. Hence, the necessity of SCH structure in QWR laser is more significant. The larger contact to SCH in laser structure helps carrier capturing into QWRs the more. In this sense, it would be better to use the laser cavity where QWRs are embedded in the middle of a waveguide. Especially when the QWRs are strained like in our case, it is surrounded by the barrier potential induced by the strain. In such a case, it is needless to say that a laser structure considering the carrier transport into QWRs are more favorable.

The DFB QWR lasers with their QWRs at the center of their waveguide were next measured in the same manner of the previous lasers. L-I curve at room temperature (20[℃]) is shown in Figure 6-13. It showed a lasing operation of the laser, and the threshold current was about 84[mA] for the contact region of 750[μm]×100[μm]. It corresponds to the threshold current density of 0.112[kA/cm^2].

It is a small value as QWR lasers operable at room temperature. The realization of a long wavelength QWR lasers at room temperature itself is still rare in the world. And the threshold current density reported here is the smallest value, as far as we know, in the ever reported long wavelength QWR lasers operated at room temperature. But note that it was the value for broad area lasers. It is simply a threshold current divided by the electrode space without considering the filamentation in broad area lasers. But the threshold current of our laser is also a very small value. We just could not find the comparable good data ever reported on long wavelength QWR lasers.

The proof of a DFB and QWR laser is given in Figure 6-14. The lasing spectrum was measured at room temperature. At low current injection, the emission peak appeared around at 1560[nm]. But lasing occurred definitively from the wavelength detuned from this emission peak. It was about 1535[nm]. It was just close to the designed value of Bragg wavelength (1536[nm]). Owing to the broad stripe, the multiple lateral modes broaden the spectral linewidth and it makes difficult to distinguish the stopband in the spectrum. Apparently lasing comes from QWRs because no other materials with the emission near 1550[nm] than QWRs exist in our laser structure. The waveguide is GaInAsP whose PL peak is found at 1250[nm]. InP for a cladding layer is around at 900[nm]. And InGaAs for a capping layer with its lattice matched to InP is more than 1600[nm] though it is highly p-doped until 10^{19}[/cm^3]. Hence, only InAsP of QWR has an emission which can contribute to lasing. As a result, DFB lasing can be concluded from the fact that the lasing mode is distant from the gain peak and is in good agreement with the designed value. And the emission from a QWR array is evident because no other materials than QWRs cannot contribute to the emission at 1535[nm].

The achievement of DFB lasing using QWR array at room temperature (20[℃]) is the first time in the world. Moreover, our laser belongs to long wavelength semiconductor lasers which is considered to be more difficult than short wavelength ones due to the degradation of emission efficiency by the influence of irradiative recombinations such as Auger recombination. This excellent results in DFB lasers, especially in long wavelength, is significant to develop ideal DFB lasers based on nanostructure technology. Considering that a DFB cavity has been thought to be against the application of QWRs superstitiously, it shows experimentally another possibility in QWRs. Most of the results in this chapter surely depends on the development of new QWRs with the highest quality in long wavelength. But we would also like to emphasize the effectiveness of the combination of excellent QWRs and the DFB cavity.

6-8 Conclusion

Based on the discussion on how to apply the mass transport method to a fabrication of DFB QWR lasers, we adopted a lower laser structure with a GaInAsP waveguide previously grown on the n-InP substrate. It is capped by InP layer making mass transport possible. A new V-groove structure was prepared for it, and the QWRs formed on it were

proved to have as good a quality as previous one on the normal V-grooved substrate in chapter 5. The shift of PL peak wavelength coming from the difference of a barrier material and a planarization method to bury the V-grooves were well considered in the design and is utilized to achieve the matching of Bragg wavelength of DFB QWR laser to the QWR gain profile. By changing the InP capping layer thickness on the waveguide, 2 laser samples were prepared. One has QWRs on the upper edge part of a waveguide, and the other has them in the waveguide. The comparison of these 2 lasers results that QWRs must be in the waveguide to make the best use of its role as a SCH. Such a laser with QWR in the waveguide was fabricated as a broad area laser with 100[μm] stripe width, 500[μm] cavity length, and as cleaved facets. Naturally the stripe direction was perpendicular to QWR array to form a DFB cavity by using QWR array as an active grating. It was successfully operated at room temperature (20℃) under pulsed current injection. It showed lasing operation at threshold current density of 0.112[kA/cm^3] (threshold current of 84[mA]). The observation of lasing spectrum revealed that it worked as a DFB QWR laser with its lasing wavelength at 1535[nm] distant from the emission peak of QWRs at 1560[nm]. The operation of DFB QWR laser at room temperature, especially in long wavelength domain, was the first time in the world. Its threshold current (density) was the smallest even as a long wavelength QWR lasers.

■ Chapter 7

Conclusion

DFB lasers are undoubtedly one of the most important components in the future optoelectronic application. This research was devoted to the innovation of gain-coupled DFB lasers. We proposed to use a QWR array as an active region and grating in DFB lasers to achieve a gain coupling mechanism in lasers. Its structure is promising in the point that several drawbacks of DFB lasers compared with FP lasers are improved effectively. And it is also important that it is realized in gain-coupled DFB lasers.

Among fabrication methods ever reported, we concluded that the growth on V-grooved substrate was the best for the formation of active QWR grating in DFB lasers. It enables us to utilize a uniformly arrayed high quality QWRs with less defects during their fabrication process. It is helpful that their physical properties are studied better than the other methods.

Strained InGaAs QWRs were utilized to investigate how such a QWR array behaves in a DFB cavity. QWRs on a V-grooved substrate essentially have a disadvantage that they are accompanied by parasitic QWL structures. Because parasitic QWLs also work as an active part in a laser cavity, it causes a serious competition between the QWLs and QWRs. Normally the emission from a QWR array is expected to be suppressed under such a condition because QWL's emission is definitively more efficient due to its larger volume. And thus lasing occurs from QWLs in those lasers. When the Bragg wavelength was detuned from the QWR and QWL emission profile, those results were obtained just as had been predicted. But from EL spectra below threshold, the polarization dependence of the QWR emission was observed. It was a proof that 1 dimensional confinement was realized for those QWRs.

Next we fabricated DFB lasers with its Bragg wavelength matched to the QWR emission profile at low temperature. Lasing from QWRs was successfully achieved at about 905[nm] at 84[K]. By the observation of lasing spectra at various temperature, the oscillation as a DFB mode from QWR was confirmed. Among them, there exist anti-phase DFB operation and the singular temperature dependence of threshold current density. Though the achievement of lasing operation was only at low temperature below 145[K], it suggests sufficiently the possibility to make QWR DFB lasers operable at room temperature by the removal of parasitic QWLs and the improvement of regrowth quality. The confirmation of DFB operation from a QWR gating by the lasing spectra was for the first time.

Since it was clarified that the elimination of parasitic QWLs and the improvement of QWR quality inevitably leads to a better property of DFB lasers using a QWR array. For this purpose, we proposed a new fabrication technique to form QWRs without any parasitic structures on the V-grooves. It is the application of mass transport phenomenon on the nonplanar substrate. The formation of a QWR array by this method was carried out using InP substrates with excellent V-grooves on it. By applying it a fine structure of InAsP QWRs were successfully fabricated by controlling mass transport temperature, time, heating rate, and group V ambient pressure ratio in MOVPE reactor. It is important that the first 3 parameters which was neglected in the past mass transport process was proved to be essential to control the fabrication of such a small structure as QWRs. This method is also applicable to the formation of QDs as it is. The combination of these 3 parameters and the last one makes it possible to design QWR size and its emission peak wavelength independently.

The control of QWR size and composition were all achieved through the set of those parameters. In our experiment, QWR luminescence peak from 1200[nm] to 1580[nm] were demonstrated. The cross-sectional TEM observation of QWRs shows a good interface of InAsP and InP in spite of 2.5% strain estimated from their lattice constants. The triangular QWR's base side was 25[nm] and its thickness (or height) was 10[nm] for the observed sample. Much smaller QWRs were also realized by this method. No parasitic structures which can contribute to optical properties existed in these samples. The optical characteristics of those QWRs were not less excellent than the former QWRs grown on the V-grooves. It showed a strong photoluminescence even at room temperature. The anisotropy of PL intensity was also observed and it was stronger in the direction parallel to QWRs. Above all, they are the most excellent QWRs on V-grooves in the long wavelength domain. It was concluded that the excellent QWR array was fabricated by the improved mass transport method and, furthermore, that it has many improved properties in the device fabrication using QWRs.

Those QWRs were incorporated for the fabrication of new QWR DFB lasers. For the device fabrication, we developed the mass transport method so that QWRs were obtainable in the GaInAsP V-grooves for a better optical confinement factor and better carrier capturing into QWRs in laser cavities. The better growth quality tolerable for the operation of devices were achieved through these processes. The planarization technique of non-planar substrates after the formation of QWRs was also useful to improve the growth quality.

The DFB laser with a broad area stripe of 100[μm] and 750[μm] cavity length was fabricated and was successfully operated at room temperature under the pulsed current condition as a QWR DFB laser. The lasing wavelength was 1535[nm], and the peak emission wavelength was found separately at 1560[nm] which results the detuning of 25[nm] of the lasing mode. The threshold current density was about 0.112[kA/cm^2]. This value was the lowest as a long wavelength QWR lasers. The threshold current of 84[mA] was also the lowest as far as we know. The operation as a DFB laser using a QWR array as an active grating at room temperature was for the first time. Considering the low threshold current density of these lasers, it is also possible to expect a continuous wave operation of such lasers. In another aspect, all these facts proves the excellent quality of QWRs made by mass transport.

List of publications relevant to this research

Journals

[1] T.Toda, F.Reinhardt, E.Martinet, E.Kapon, and Y.Nakano, "Selective Lasing of InGaAs Quantum Wire Array on a V-Grooved GaAs Substrate by Distributed Optical Feedback", submitted to photonics technology letters.

International Conferences

[1]T.Toda, F.Reinhardt, E.Martinet, E.Kapon, and Y.Nakano, "Fabrication of InGaAs DFB Quantum Wire Lasers by Using V-grooved Substrates",Proc.of 10th International Conference on Indium Phosphide and Related Materials,WB1-5,Tsukuba,Ibaraki,May 1998.

[2] T.Toda and Y.Nakano, "Room Temperature Pulsed Operation of InAsP DFB Quantum Wirre Lasers Fabricated by Mass Transport Method", submitted to 11th International Conference on Indium Phosphide and Related Materials, MoA1-2,Davos,Switzerland,May 1999.

Workshops

[1]T.Toda, E.Kapon,Y.Nakano, and K.Tada, "Fabrication of InGaAs quantum wire DFB lasers by using MOVPE growth on V-grooved GaAs substrates",第 15 回半導体レーザシンポジウム,長津田,東工大,March 1998.

[2]T.Toda, and Y.Nakano, "Fabrication of 1.5μm DFB lasers with a mass transported InAsP quantum wire array as an active grating",第 16 回半導体レーザシンポジウム,長津田,東工大,March 1999.

[3]戸田知朗,中野義昭,"マストランスポートによるInAsP量子細線の作製と光学特性評価",電子情報通信学会技術研究報告,飯塚研究開発センター,福岡,1998 年 11 月.

[4] T.Toda, and Y.Nakano, "Room temperature oscillation of 1.5mm strained InAsP/InP quantum wire DFB lasers on V-grooved substrates", The 3rd symposium on Atomic-Scale Surface and Interface Dynamics",Fukuoka,March 1999.

国内大会論文

[1]戸田知朗,エリ．カポン,中野義昭,多田邦雄,"V溝基板を利用した分布帰還型 InGaAs 量子細線レーザの作製",第 45 回春季応用物理学会学術講演会予稿集,29p-ZH-6,1998 年 3 月.

[2]戸田知朗,中野義昭,"マストランスポートによる InPV 溝基板上への InAsP 量子細線の作製と評価",第 59 回秋季応用物理学会学術講演会予稿集,18a-ZH-3,1998 年 9 月.

[3]戸田知朗,中野義昭,"マストランスポートによる InP 基板上GaInAsP V 溝内への InAsP量子細線の作製と評価",第 46 回春季応用物理学会学術講演会予稿集,30a-ZL-5,1999 年 3 月.

[4]戸田知朗,中野義昭,"マストランスポート法で作製されたInAsP/InP分布帰還型歪み量子細線レーザの室温発振",第 46 回春季応用物理学会学術講演会予稿集,28p-B-9,1999 年 3 月.

[5]戸田知朗,中野義昭"Room temperature operation of 1.5μm mass-transported InAsP/InP strained quantum wire DFB lasers",電子情報通信学会 1999 年総合大会,C-4-4,1999 年 3 月.

Acknowledgment

I would like to express my gratitude to my research advisor Prof. Dr. Yoshiaki Nakano for his guidance and encouragement in this doctoral work. I am also thankful to Prof. Dr. Kunio Tada (professor emeritus of University of Tokyo ; Yokohama National University) for his advice in outlining this work. Especially, I appreciate both professors the opportunity to study abroad (in Switzerland) for one year during this work. And I must thank Prof. Dr. Yasuhiko Arakawa, Prof. Dr. Kazuro Kikuchi, Prof. Dr. Kazuhiko Hirakawa, Prof. Dr. Masahiro Tsuchiya, and Prof. Dr. Masaaki Tanaka for useful discussions for my final examination.

Je voudrais remercier à Prof. Dr. Eli Kapon (École Polytechnique Fédéral de Lausanne) pour sa aide gentile de commencer mon travail en Suisse. Presque tous les résultat de chapitre 4 a été faits dans son laboratoire. Je dis merci à mes collègues, Dr. Frank Reinhardt, Dr. Alok Rudra, et Dr. Eric Martinet pour leur coopération dans les croissances de la structure de laser et les mesures optiques de mon échantillon. Particulièrement, je voudrais m'experimer ma gratitude à Christophe Constantin. Ne pas seulement m'a-t-il aidé de preparer mon échantillon et discuté sur le résultat de ma expérience, mais il a aussi tourné mon séjour à EPFL agréable.

I owe to Masahiro Kito and Masato Ishino in Matsushita Electronics Co. for a useful information on the wet etching process and mass transport of InP. Their advice was very helpful to complete the QWR formation by mass transport for a short period.

Many thanks to Mr. Toru Murai, and secretaries for their help to keep things going smoothly in the laboratory. Mr. Naoki Futakuchi supported my MOVPE work. Mr. Keiichi Sano made his best for assisting my experimental work. And I am thankful to all the other members of Nakano laboratory. The discussions with them during lunch and dinner at the student restaurant was helpful for me to consider my research from multiple viewpoints.

Finally I wish to thank to my parents and brother, Saburo, Kazuko and Yosuke Toda with all my heart for their support and encouragement.

I would like thank in the rest of this page to all the art (my favorite novelist, poets and composers) for recreating me, and sometimes giving me an inspiration to overcome scientific problems in this work.